*Aust. J. Phys.*, 1989, **42**, 633–732

# A VLA Survey of Rich Clusters of Galaxies. I. Whole-cluster Maps, Source List and Source Statistics

*O. B. Slee,*[A] *R. A. Perley*[B] *and Betty C. Siegman*[A]

[A] Australia Telescope National Facility,* CSIRO, P.O. Box 76, Epping, N.S.W. 2121, Australia.
[B] National Radio Astronomy Observatory, P.O. Box 0, Socorro, NM 87801, U.S.A.

*Abstract*

We have surveyed 58 fields near rich clusters of galaxies with the Very Large Array using scaled arrays in the B/C and/or C/D configurations at 1·5 GHz and 4·9 GHz. The fields were centred on steep spectrum sources in or near clusters that were earlier surveyed with lower resolution telescopes. The whole-field maps at 1·5 GHz are given and a list of 940 sources with 1·5 GHz flux densities down to ~1 mJy is presented. Spectral indices of sources within 5′ of the field centres are given. Complete flux-limited samples of sources are used to establish a criterion for cluster membership. Sources with total 1·5 GHz flux density >20 mJy and closer to the cluster centre than 0·28 of the cluster radius (a total of 57 sources) are accepted as cluster members. We investigate statistical correlations between the radio parameters of cluster sources and between the radio properties of cluster sources and the optical properties of cluster richness and morphology. We find: (i) largest linear size and source area increase with radio power; (ii) total cluster radio power increases with cluster richness; (iii) spectral index is highest in clusters with central dominant galaxies; (iv) in resolved double sources, the component with the highest flux density also has the highest spectral index. Radio parameters of sources inside and outside clusters are compared. The more powerful component of a cluster double is longer but thinner than its counterpart outside a cluster.

## 1. Introduction

During the interval 1978–1981 we conducted surveys of many clusters of galaxies with the Culgoora Circular Array (CCA) at 80 MHz and 160 MHz (Slee and Siegman 1983) and with the Parkes 64 m telescope at 2·7 GHz (Slee *et al.* 1983). During these observations we detected many sources with steep radio spectra. Subsequently 58 cluster fields centred on sources with spectral indices $\alpha < -0{\cdot}90$ [$S(\nu) \propto \nu^{\alpha}$] were surveyed with the Very Large Array† (VLA) at 1·5 GHz and 4·9 GHz between 1981 and 1985.

The aims of the VLA survey included determination of: (i) the spectral indices of radio sources in clusters; (ii) their morphology; (iii) distribution of sources with respect to cluster centres; (iv) distribution of emitted radio power and how radio power varied with distance from the cluster centre; (v) linear polarisation and its distribution in the more resolved sources; (vi) optical identification of radio sources; (vii) relationship between radio power

* The Australia Telescope National Facility is operated in association with the Division of Radiophysics by CSIRO.

† The VLA is operated by the National Radio Astronomy Observatory for Associated Universities Inc., by co-operative agreement with the National Science Foundation.

0004-9506/89/060633$03.00

**Table 1. Parameters for observed clusters**

| Cluster | Angular Radius, $R_C$ (') | Redshift Z | Distance Class | Richness Class | B-M Class | Rood-Sastry Morphology |
|---|---|---|---|---|---|---|
| A 13 | 16.8 | 0.108 | 5 | 2 | II | L |
| 76* | 33.6 | 0.042 | 3 | 0 | II | L |
| 85 | 33.6 | 0.052 | 4 | 1 | I | cD |
| 86* | 24.6 | 0.074 | 4 | 0 | - | C |
| 115* | 14.6 | 0.197 | 6 | 3 | III | I |
| 133 | 26.9 | 0.060 | 4 | 0 | I | cD |
| 154* | 55.9 | 0.066 | 3 | 1 | II | B |
| 196 | 14.5 | 0.163 | 6 | 1 | III | I |
| 240* | 25.7 | 0.064 | 3 | 0 | II-III | B |
| 278 | 26.9 | 0.064 | 3 | 0 | III | I |
| 357* | 26.9 | 0.114 | 5 | 0 | - | C |
| 362 | 11.2 | 0.188 | 6 | 1 | II-III | C |
| 407 | 33.6 | 0.047 | 2 | 0 | I | I |
| 416* | 10.1 | 0.199 | 6 | 1 | III | F |
| 474 | 9.0 | 0.168 | 5 | 1 | III | I |
| 496 | 44.8 | 0.032 | 3 | 1 | I | cD |
| 514* | 33.6 | 0.054 | 3 | 1 | II-III | F |
| 519 | 23.5 | 0.126 | 5 | 0 | - | B |
| 531 | 17.9 | 0.141 | 5 | 1 | III | C |
| 658* | 14.5 | 0.122 | 5 | 1 | III | I |
| 912* | 24.6 | 0.074 | 4 | 0 | - | cD |
| 1142* | 33.6 | 0.035 | 3 | 0 | II-III | C |
| 1171* | 28.0 | 0.085 | 4 | 0 | - | I |
| 1189 | 24.6 | 0.126 | 5 | 0 | II-III | C |
| 1238 | 14.5 | 0.093 | 4 | 1 | III | C |
| 1273 | 11.2 | 0.172 | 6 | 1 | III | I |
| 1620* | 22.4 | 0.125 | 5 | 0 | III | I |
| 1631 | 28.0 | 0.051 | 3 | 0 | I | C |
| 3528 | 30.4 | 0.056 | 4 | 1 | II | |
| 1689 | 11.2 | 0.181 | 6 | 4 | II | C |
| 1772 | 13.4 | 0.138 | 5 | 1 | II-III | C |
| 1775 | 28.0 | 0.070 | 4 | 2 | I | B |
| 1791 | 25.7 | 0.126 | 5 | 1 | - | L |
| 1913 | 22.4 | 0.075 | 4 | 1 | III | I |
| 2009 | 11.2 | 0.153 | 5 | 1 | I-II | cD |
| 2029 | 22.4 | 0.077 | 4 | 2 | I | cD |
| 2052 | 22.4 | 0.035 | 3 | 0 | I-II | cD |
| ZW1518.8+0747 | 38.0 | 0.045 | 3 | 4 | II | |
| 2082* | 25.7 | 0.126 | 5 | 0 | - | C |
| 2091 | 8.9 | 0.183 | 6 | 1 | III | I |
| 2094 | 11.2 | 0.128 | 5 | 1 | III | I |
| 2103* | 25.7 | 0.133 | 5 | 0 | - | I |
| 2108* | 15.7 | 0.074 | 4 | 0 | III | C |
| 2151* | 28.0 | 0.037 | 1 | 2 | III | F |
| 2249 | 25.7 | 0.058 | 3 | 0 | III | C |
| 2354 | 11.2 | 0.154 | 5 | 2 | III | I |
| 2396 | 8.9 | 0.161 | 6 | 1 | I | cD |
| 2399* | 25.7 | 0.064 | 3 | 1 | III | I |
| 2443 | 12.3 | 0.108 | 5 | 2 | II | C |
| 2456 | 7.8 | 0.152 | 5 | 1 | I | B |
| 2457* | 25.7 | 0.070 | 4 | 1 | I-II | C |
| 2575 | 6.7 | 0.219 | 6 | 2 | I | I |
| 2593 | 28.0 | 0.047 | 3 | 0 | II | F |
| 2622 | 20.1 | 0.074 | 4 | 0 | II-III | cD |
| 2626 | 24.6 | 0.057 | 3 | 0 | I | cD |
| 2657* | 25.7 | 0.041 | 3 | 1 | III | F |
| 4038 | 63.3 | 0.028 | 2 | 2 | III | |
| 2670* | 22.4 | 0.074 | 4 | 3 | I-II | cD |

* VLA fields centred on steep spectrum sources displaced from the cluster centre by $>R_C/3$ (see Section 3).

and X-ray luminosity. This rather ambitious program has taken several years to complete but we are now in a position to derive some conclusions. Our first step is to publish the VLA maps and source lists derived from them in the belief that the data will be of use to others working in this field. We also include some basic statistical analyses aimed at establishing cluster membership and the relationships between different radio parameters and between radio and optical properties of clusters.

## 2. Observations and Reductions

We began our VLA programme in 1981/82 by observing with the B-Array at 1·5 GHz and the C-Array at 4·9 GHz. It soon became apparent, however, that we were failing to detect some of the extended cluster sources with very steep spectra because their radio brightness fell below our sensitivity limit.

To correct for this, from mid-1982 to late 1985 the remaining observing sessions were made with the C-Array at 1·5 GHz and D-Array at 4·9 GHz. Both the B/C and C/D combinations form scaled arrays, which are very useful for accurate determinations of spectral indices. The clusters were observed in the 'snapshot' mode with some 10,000–30,000 visibilities available on each field. The UV data were calibrated at the VLA and brought back to Sydney on 'Export' format tapes. Subsequent mapping and cleaning were done with a VAX 750 and Convex computers using the AIPS software.

Much of the long processing interval (some six years) was required to obtain the best possible cleaning solutions. This is particularly important at 1·5 GHz, where the large primary beam of the VLA antennae (30′ FHPW) may contain several strong sources, whose side-lobes (if not reduced by a large factor) will determine the rms noise level over the map and distort source morphology.

Thus in order to confirm the presence of weak sources and to establish the reliability of the weaker features of extended sources we used two or three mapping and cleaning windows on each field and varied the number of clean iterations to obtain the lowest rms deviation over the cleaned map. Generally, the best cleaning solutions were obtained with 1024×1024 pixel areas at 1·5 GHz and 512×512 pixel areas at 4·9 GHz. The pixel sizes were $1''\cdot5\times1''\cdot5$ in the B/C combination and $4''\cdot5\times4''\cdot5$ in the C/D combination. The angular resolution achieved was ~4″ in the B/C scaled arrays and ~14″ in the C/D scaled arrays. Our final maps possessed rms noise levels of typically 80 μJy/beam at 1·5 GHz and 40 μJy/beam at 4·9 GHz.

## 3. The Cluster Maps

The fields surveyed are listed in Table 1 together with some of the more useful parameters of the associated clusters. Cluster name (column 1), distance

**Figs 1–71.** The cleaned VLA maps of the 58 fields observed in this experiment. The majority of the maps were obtained in the C-Array at 1·5 GHz and are the inner 512×512 pixels of 1024×1024 pixel cleaned areas. Most of the essential information is given at the top and bottom of each map. The FHPW beam shape is not shown but approximates the shape of the most compact source near the map centre; beam widths are ~14″ in the scaled C/D configurations and ~4″ in the scaled B/C configurations. The epoch of the coordinates is 1950·0. See further explanation in Section 3 of the text.

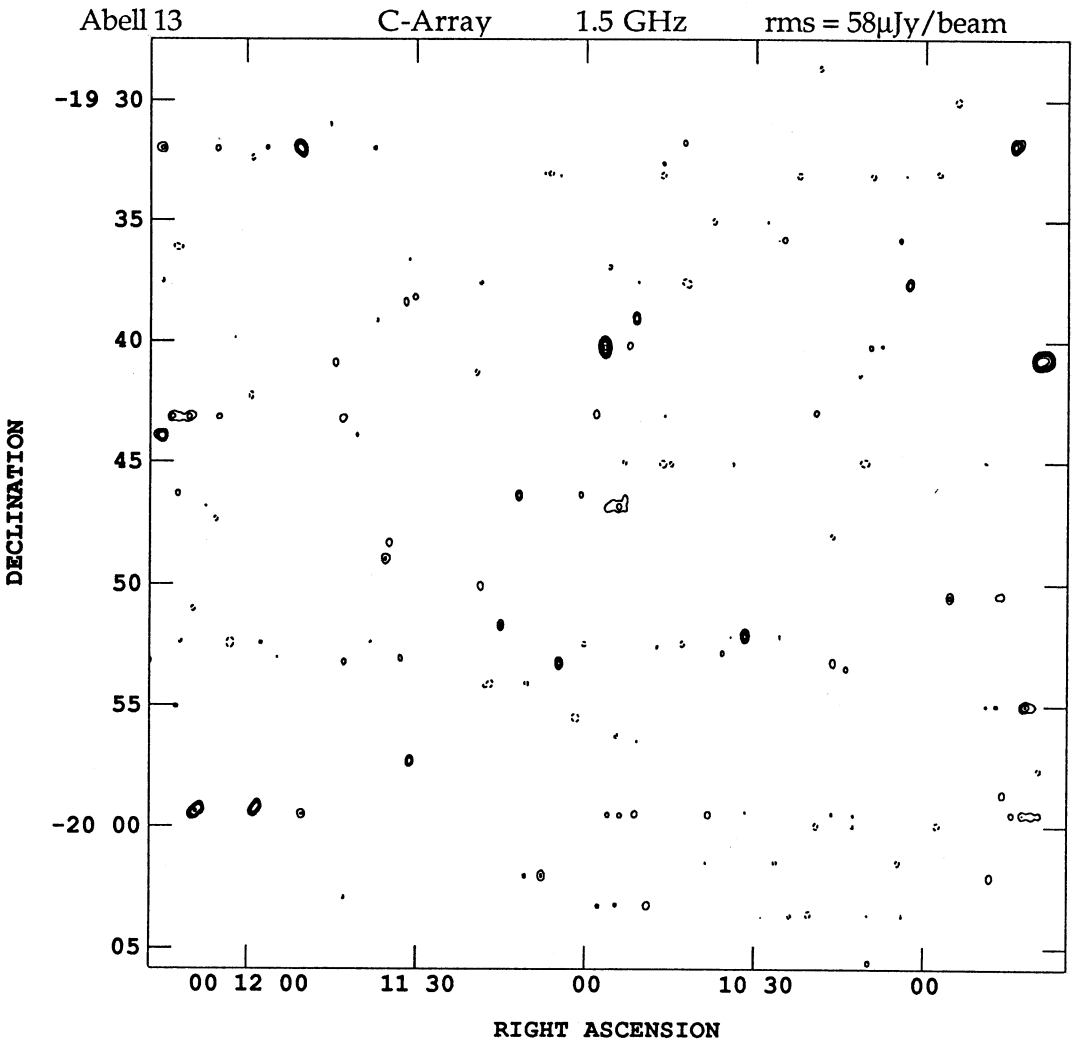


Contour levels: -2,2,4,6,,10,20,40,80 percent of peak of 15.5mJy/beam

**Figure 1**

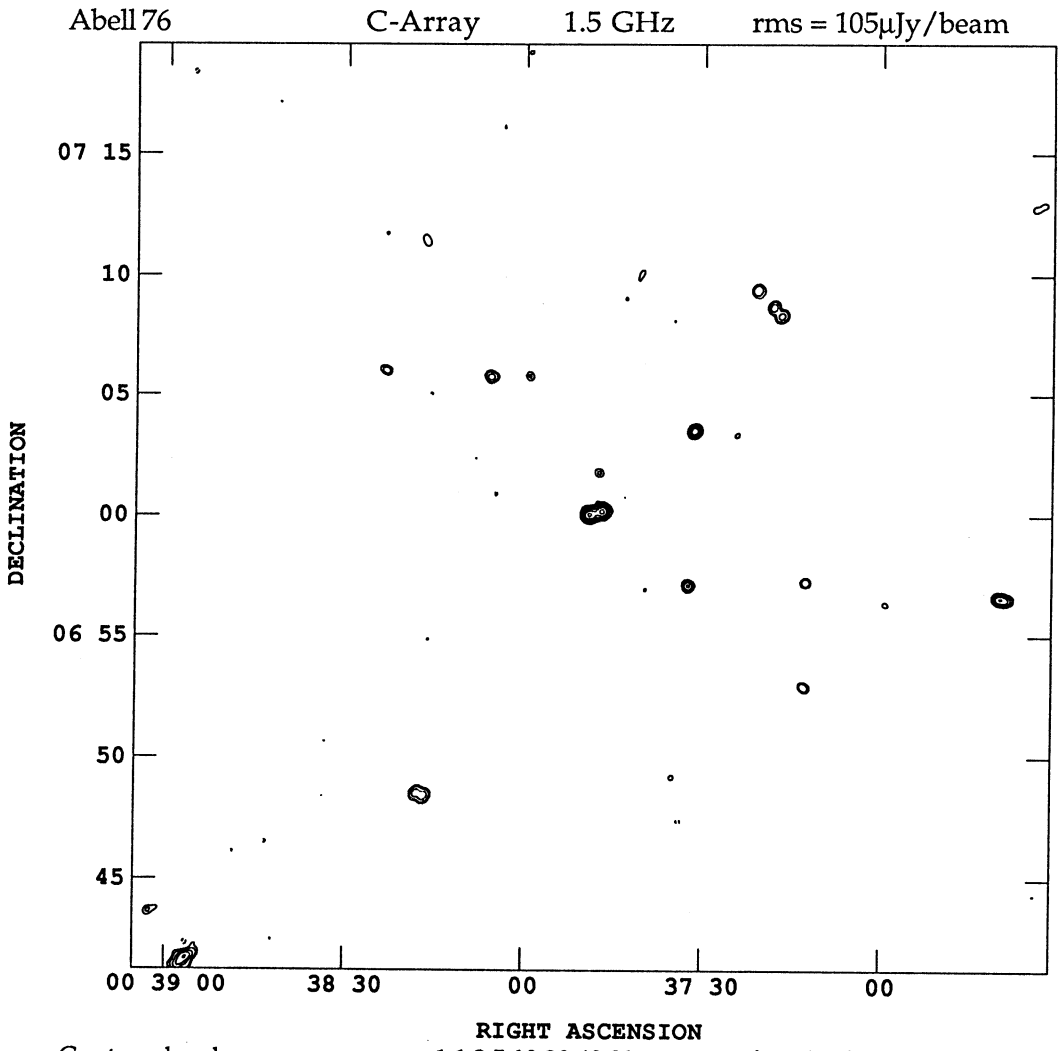


Contour levels: -1,1,2,5,10,20,40,80 percent of peak of 58.2mJy/beam

**Figure 2**

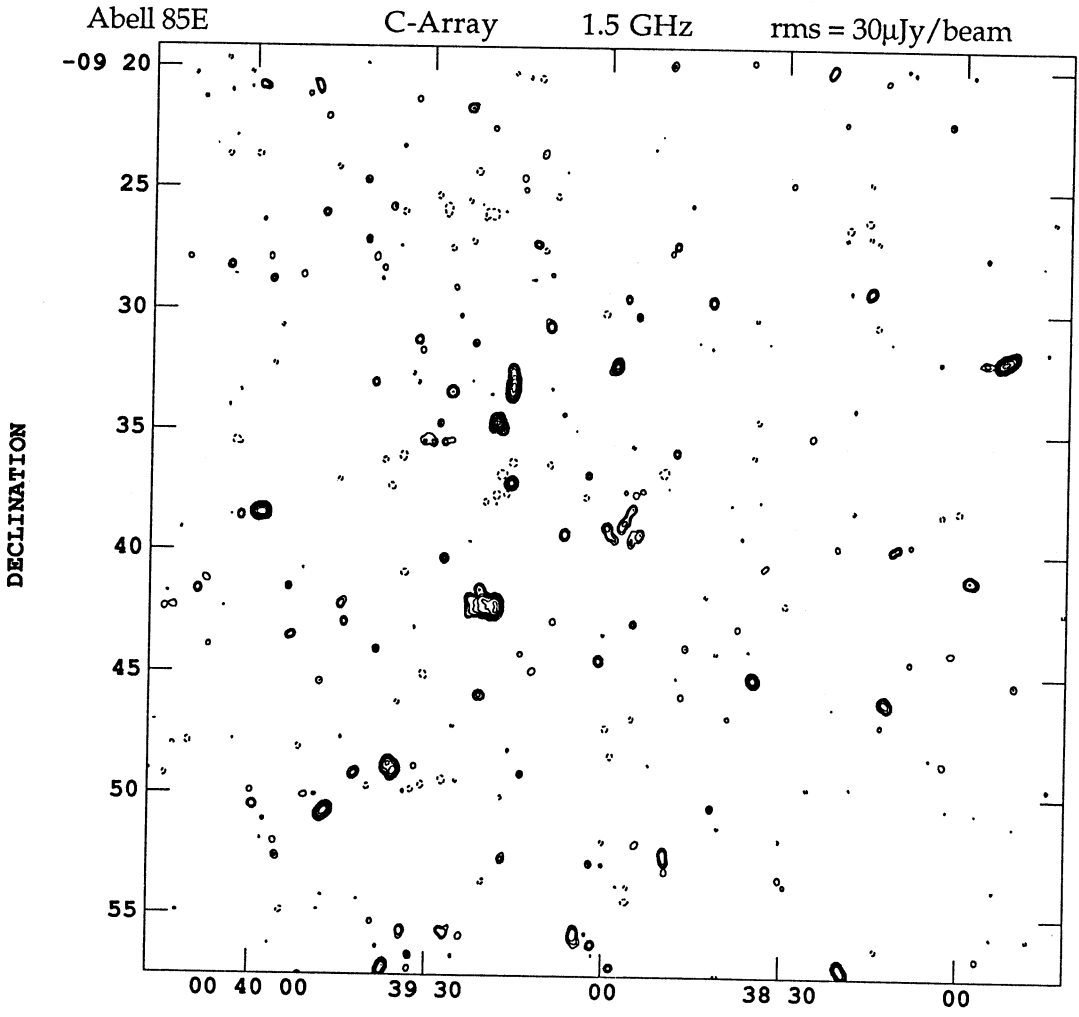


Contour levels: -0.5,0.5,1,2,5,10,20,40,80 percent of peak of 31.4mJy/beam

**Figure 3**

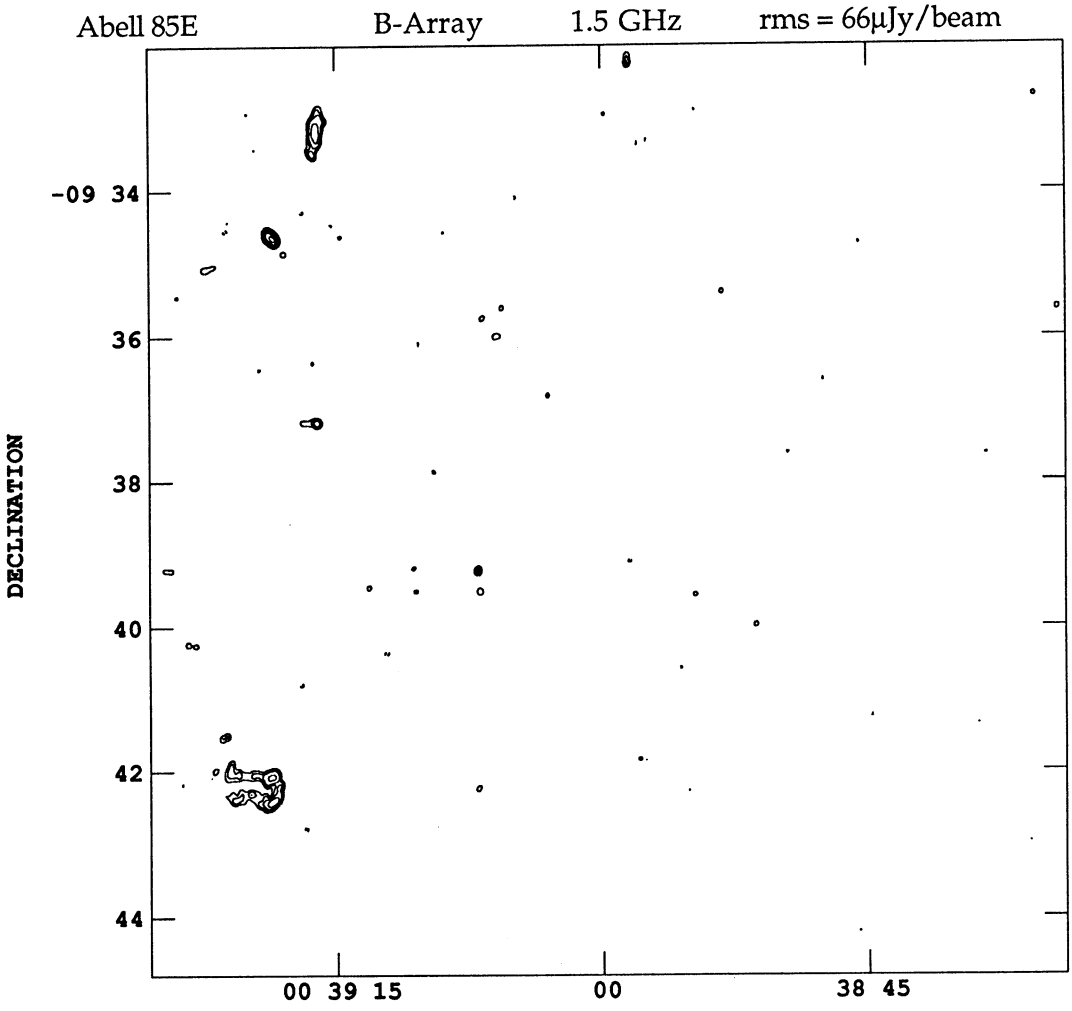


Contour levels: -3,3,6,10,20,40,80 percent of peak of 13.7mJy/beam

**Figure 4**

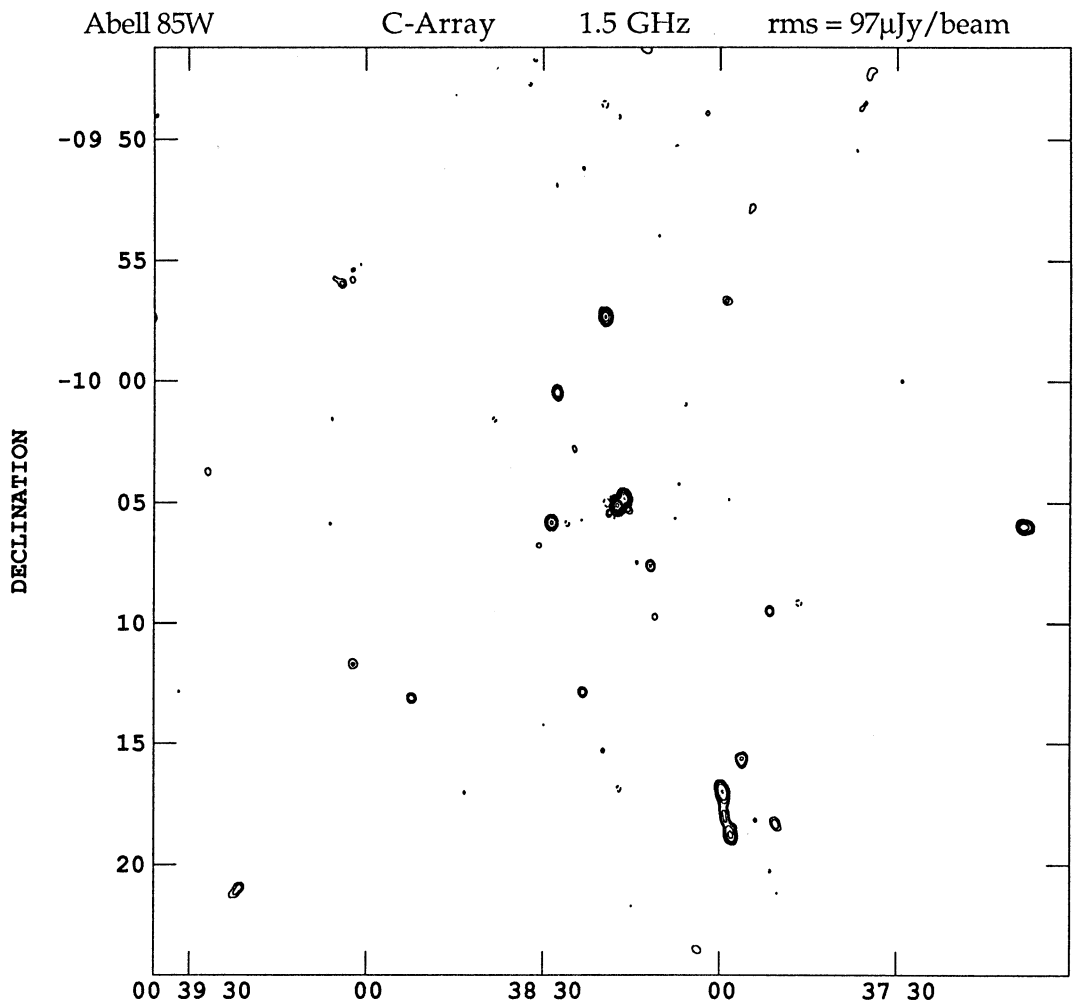


Contour levels: -0.25,0.25,0.5,1,2,5,10,20,40,80 percent of peak of 260mJy/beam

**Figure 5**

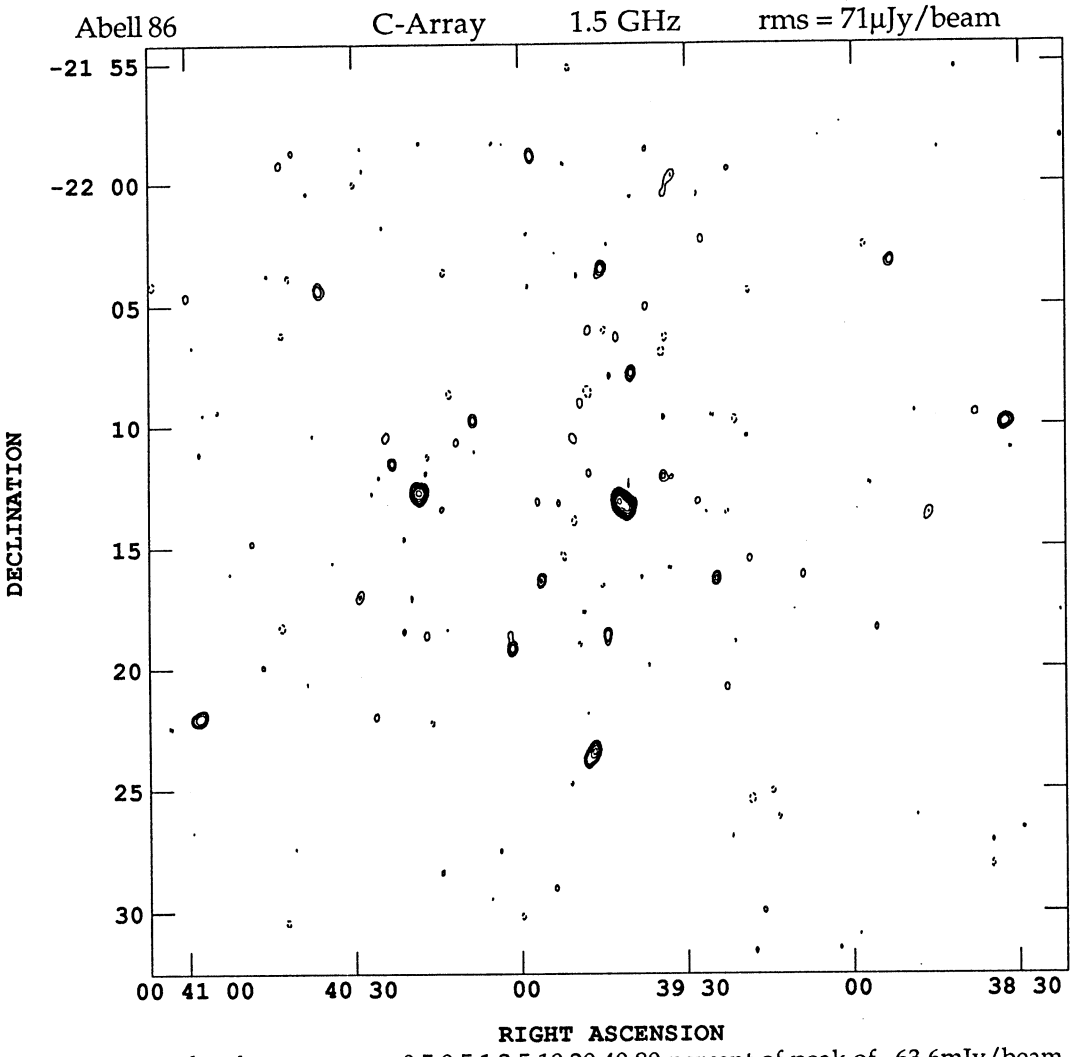


Contour levels: -0.5,0.5,1,2,5,10,20,40,80 percent of peak of 63.6mJy/beam

**Figure 6**

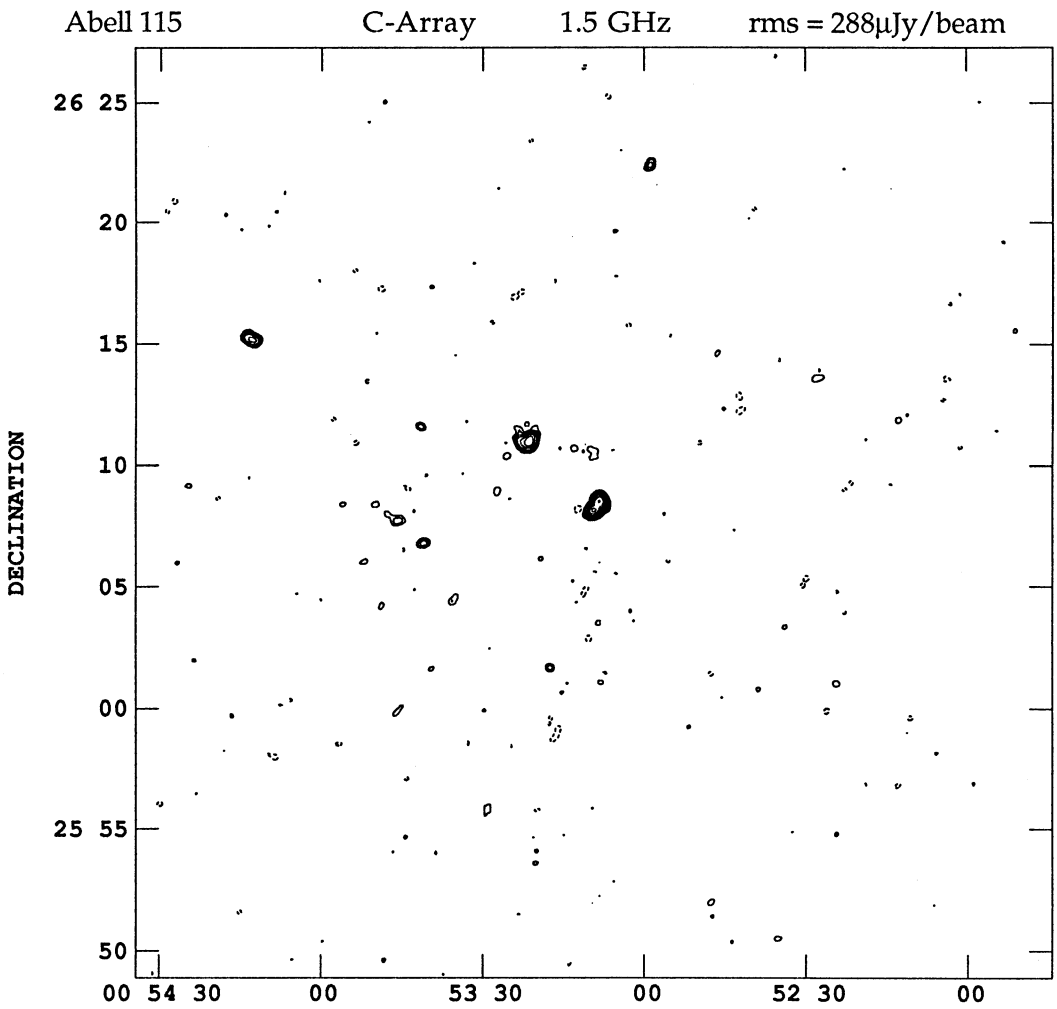


Contour levels: -0.25,0.25,0.5,1,2,5,10,20,40,80 percent of peak of 459mJy/beam

**Figure 7**

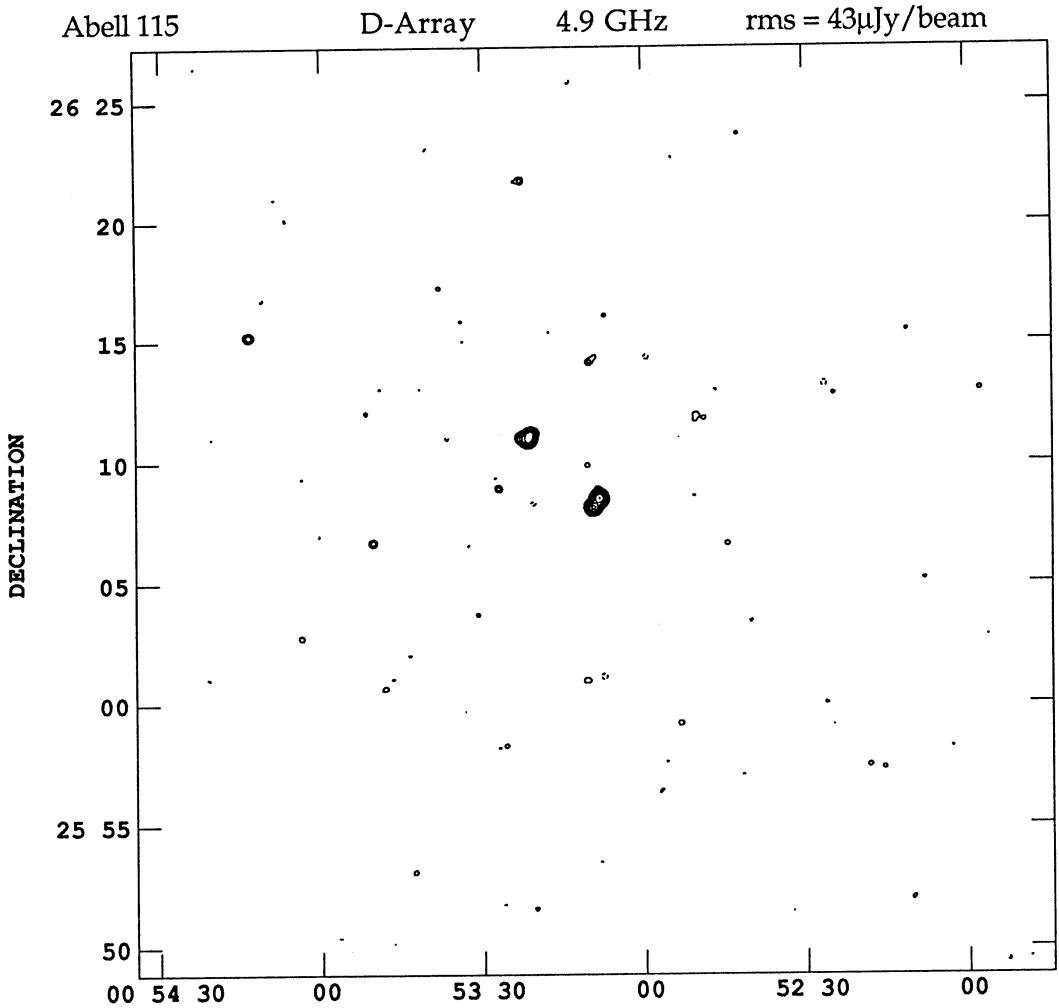


Contour levels: -0.5,0.5,1,2,5,10,20,40,80 percent of peak of 51.7mJy/beam

**Figure 8**

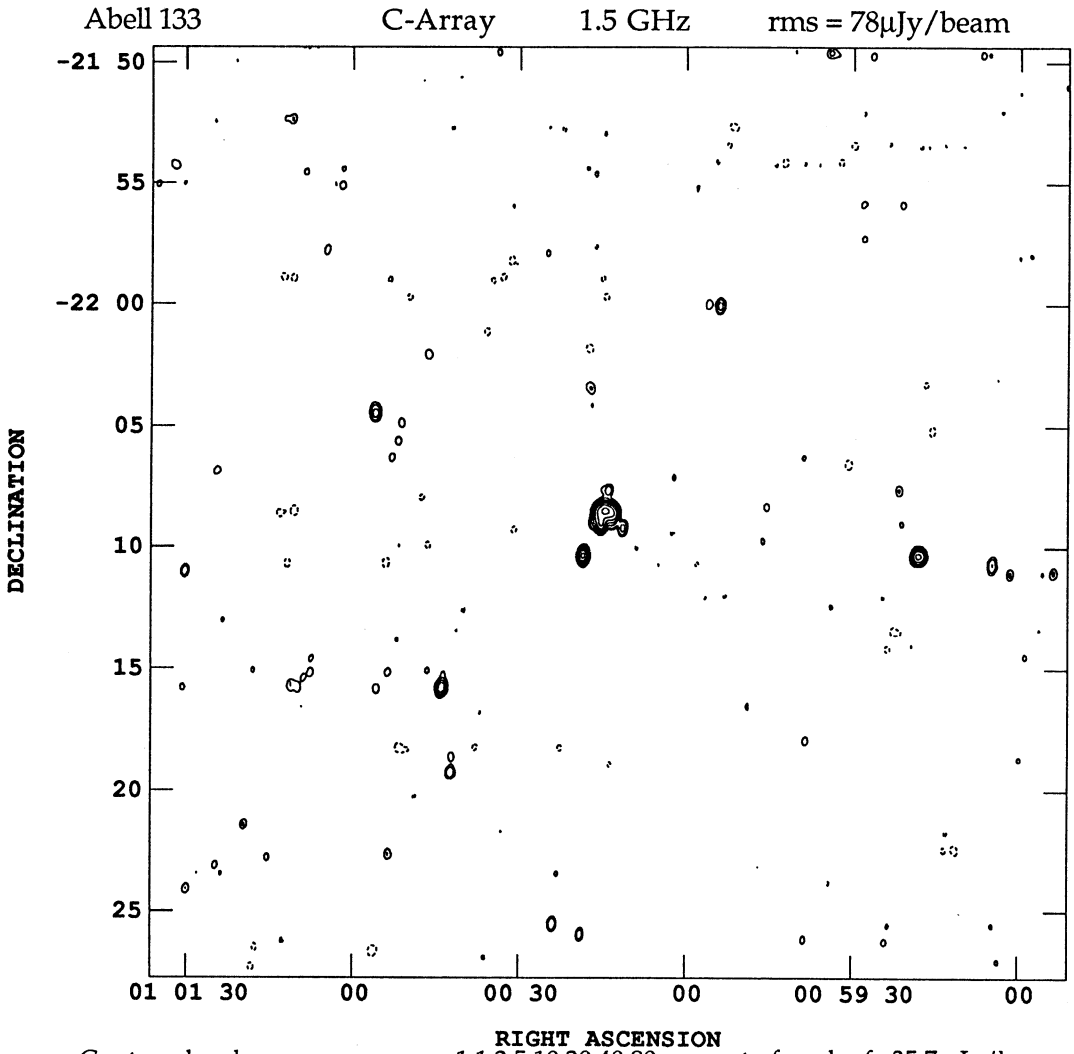


Contour levels: -1,1,2,5,10,20,40,80 percent of peak of 35.7mJy/beam

**Figure 9**

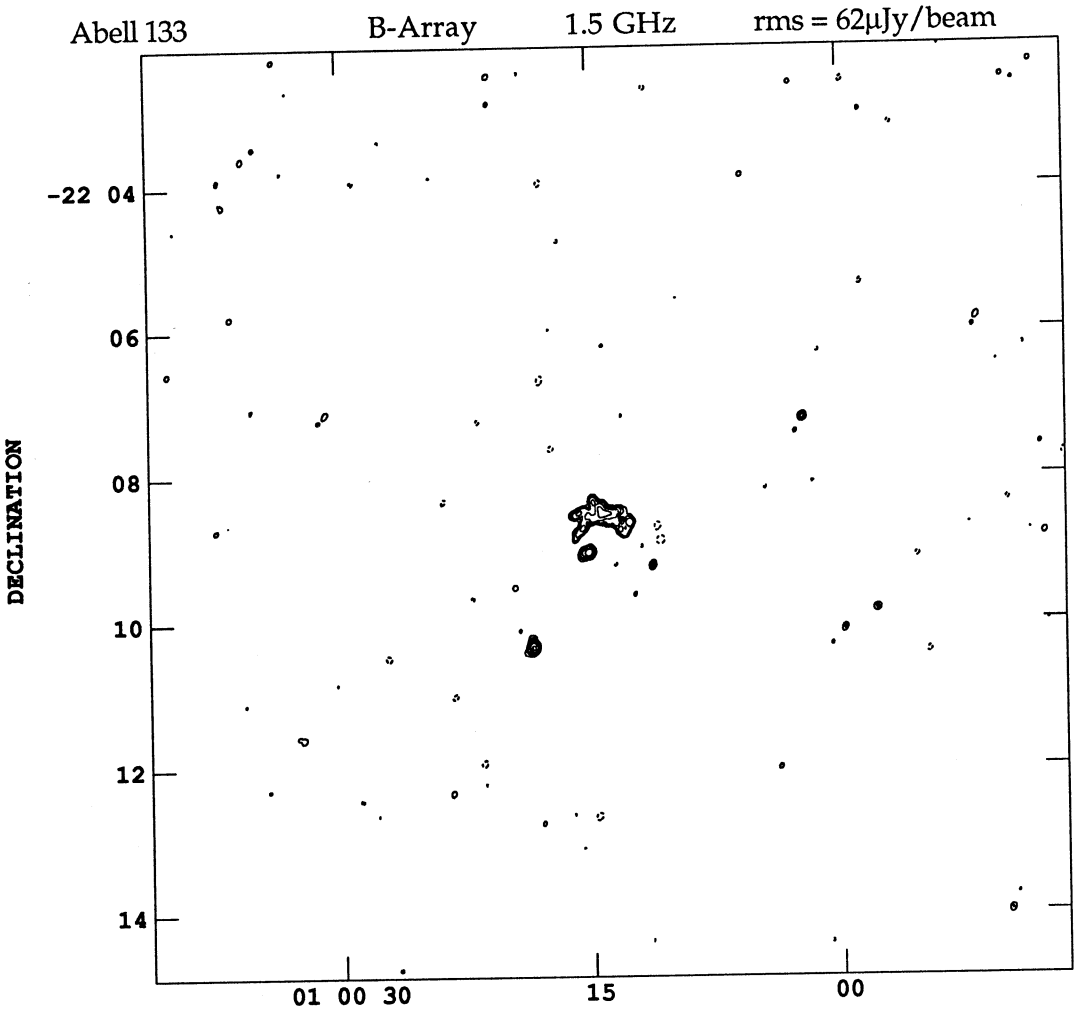


Contour levels: -3,3,6,10,20,40,80 percent of peak of 9.4mJy/beam

**Figure 10**

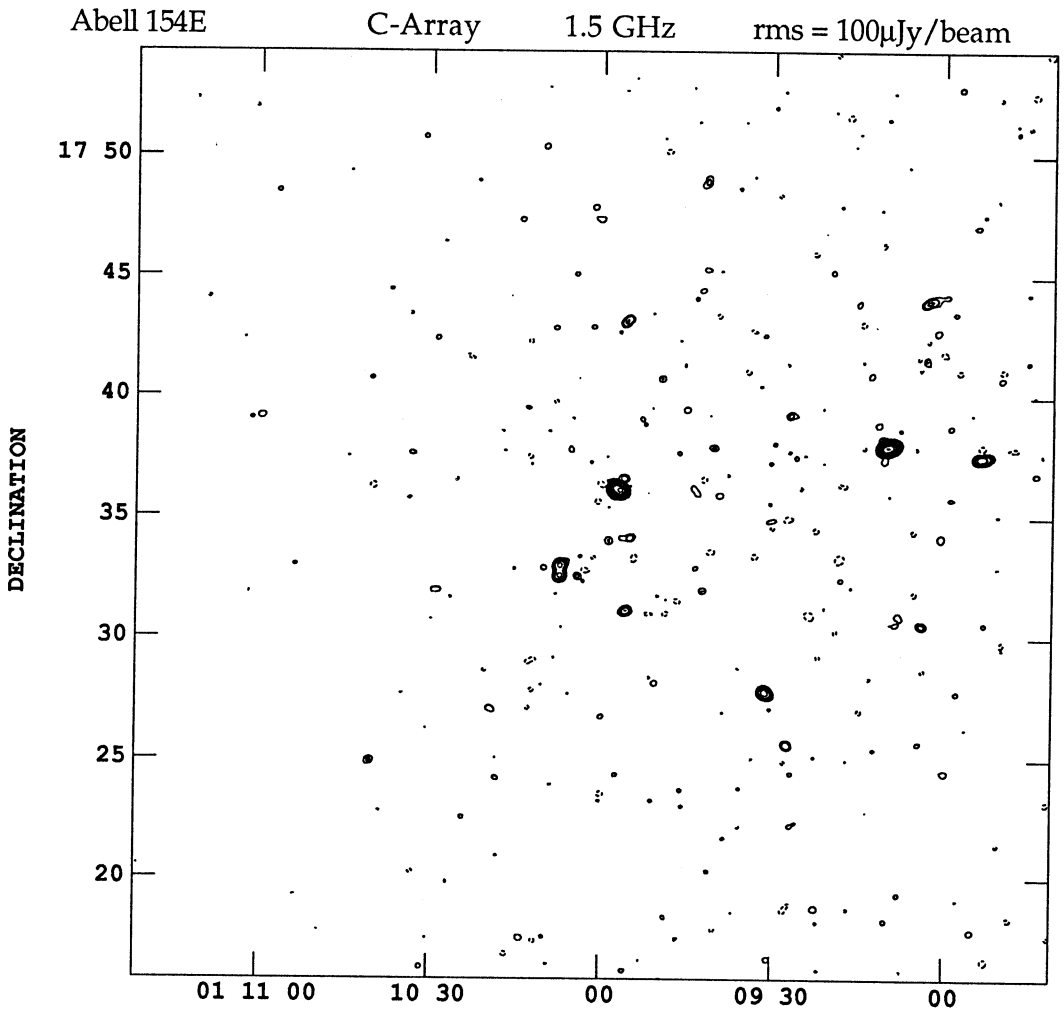


Contour levels: -0.25,0.25,0.5,1,2,5,10,20,40,80 percent of peak of 192mJy/beam

**Figure 11**

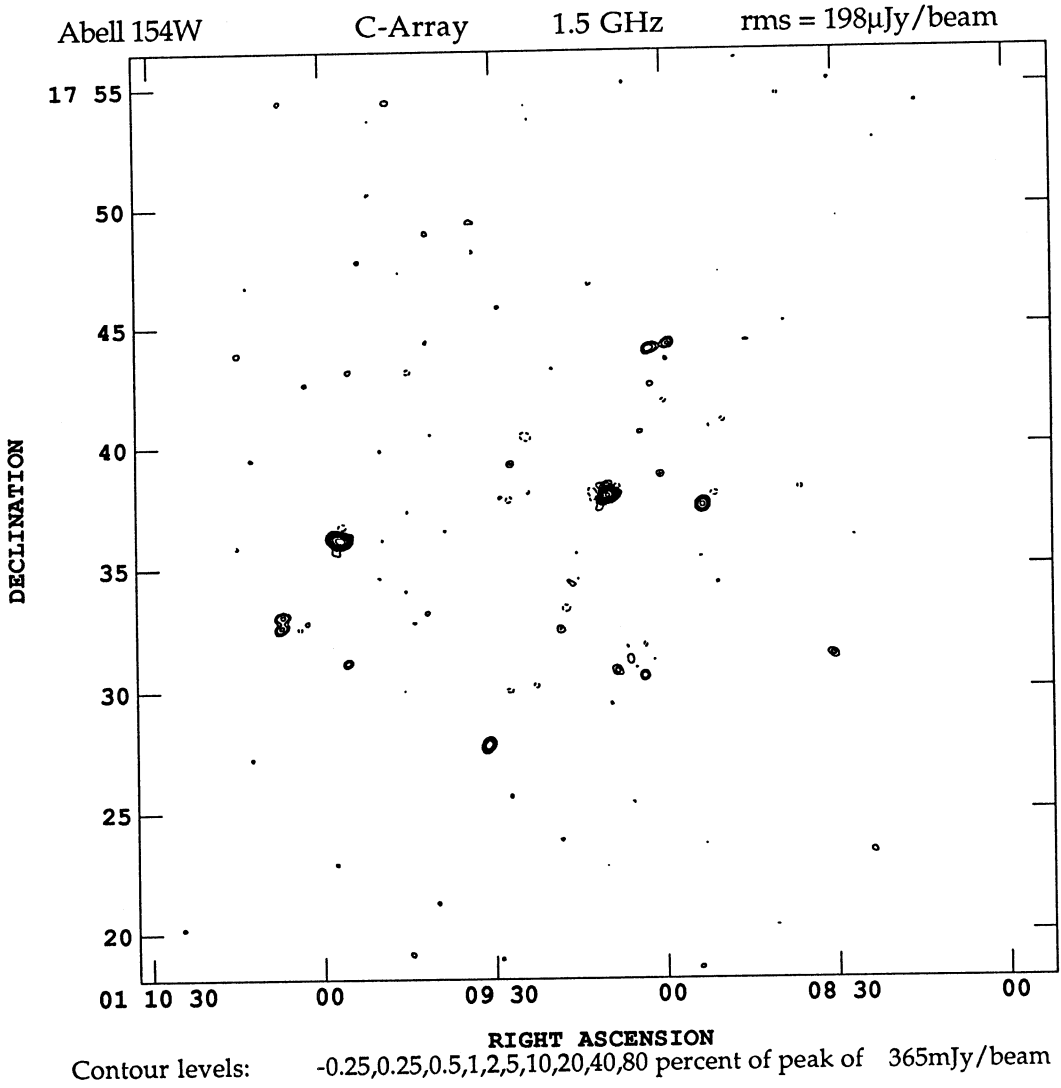
Abell 154W
C-Array
1.5 GHz
rms = 198μJy/beam
17 55
50
45
40
35
30
25
20
DECLINATION
01 10 30
00
09 30
00
08 30
00
RIGHT ASCENSION
Contour levels: -0.25,0.25,0.5,1,2,5,10,20,40,80 percent of peak of 365mJy/beam

**Figure 12**

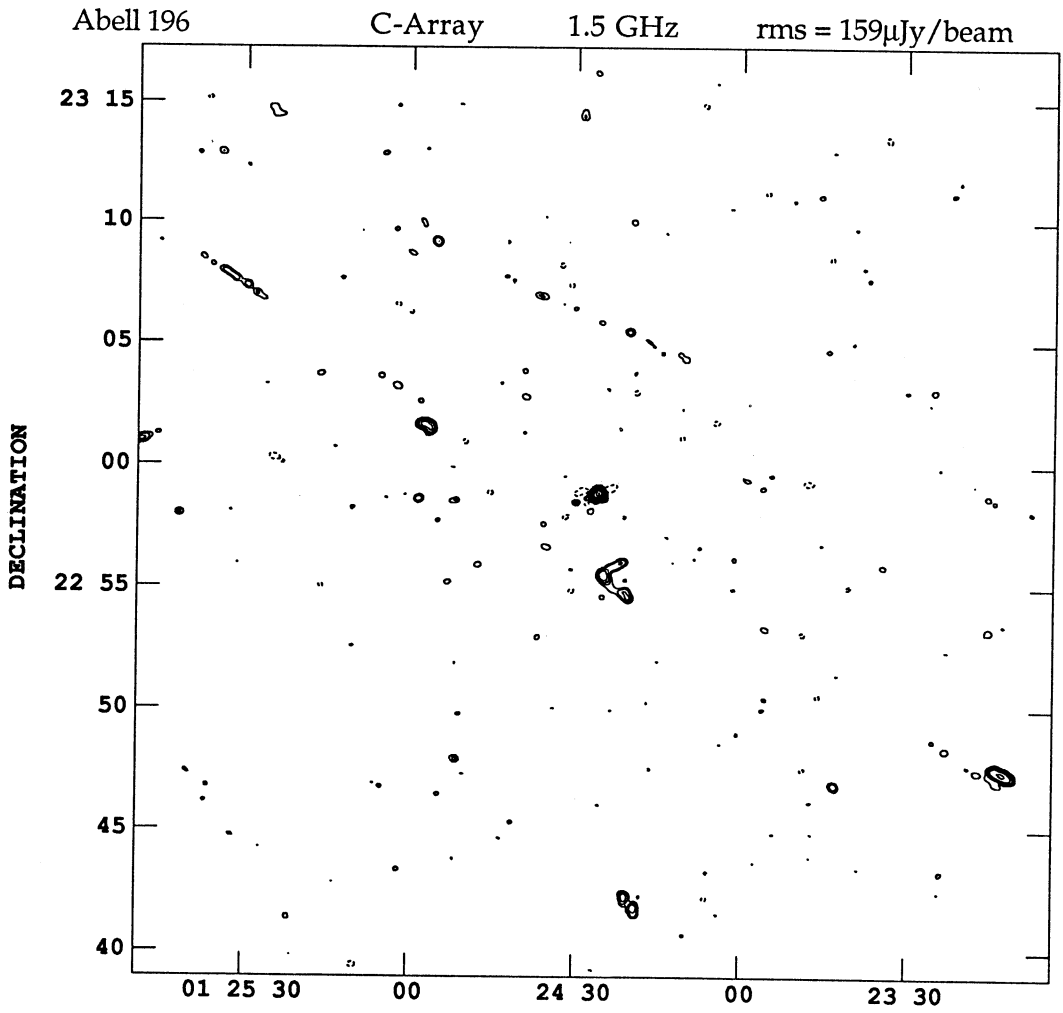


Contour levels: -0.25,0.25,0.5,1,2,5,10,20,40,80 percent of peak of 290mJy/beam

**Figure 13**

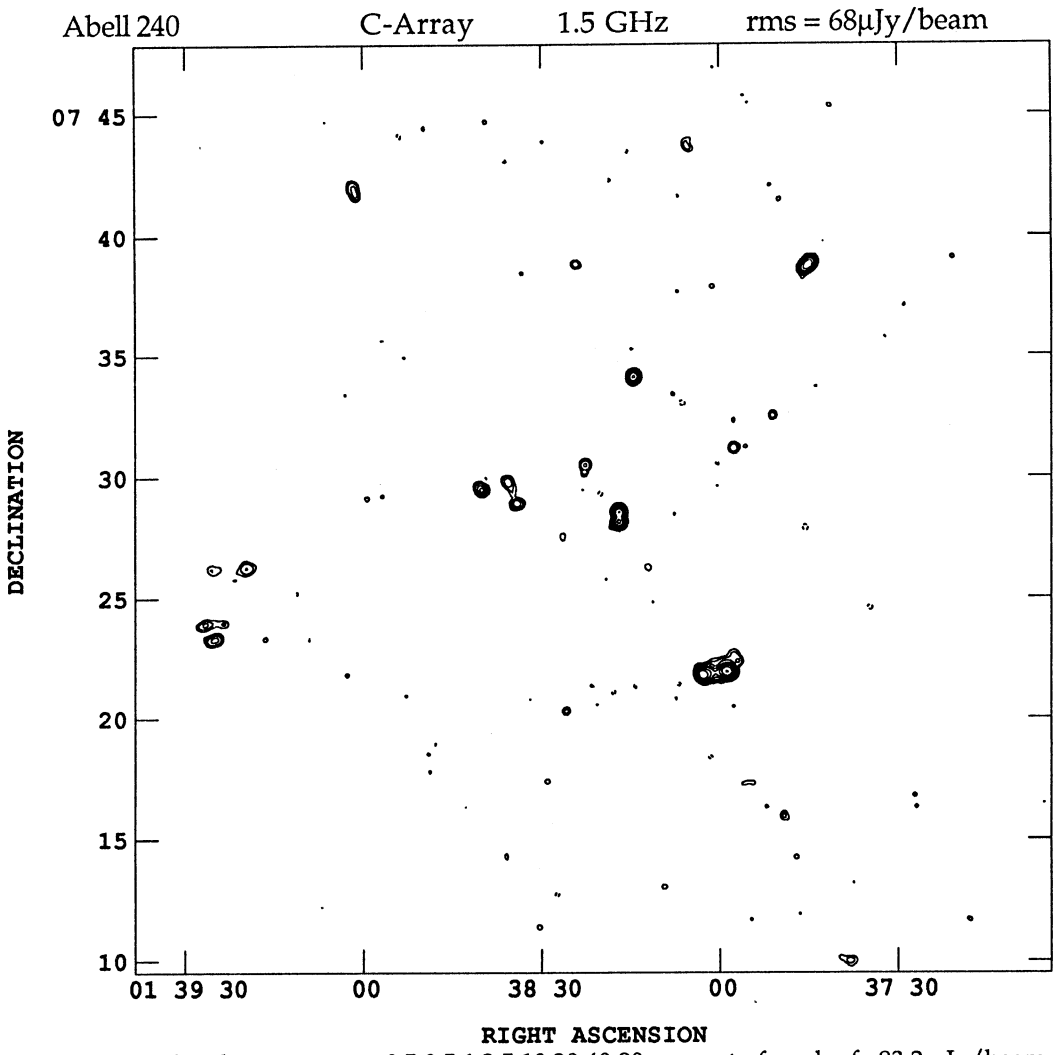


Contour levels: -0.5,0.5,1,2,5,10,20,40,80 percent of peak of 83.2mJy/beam

**Figure 14**

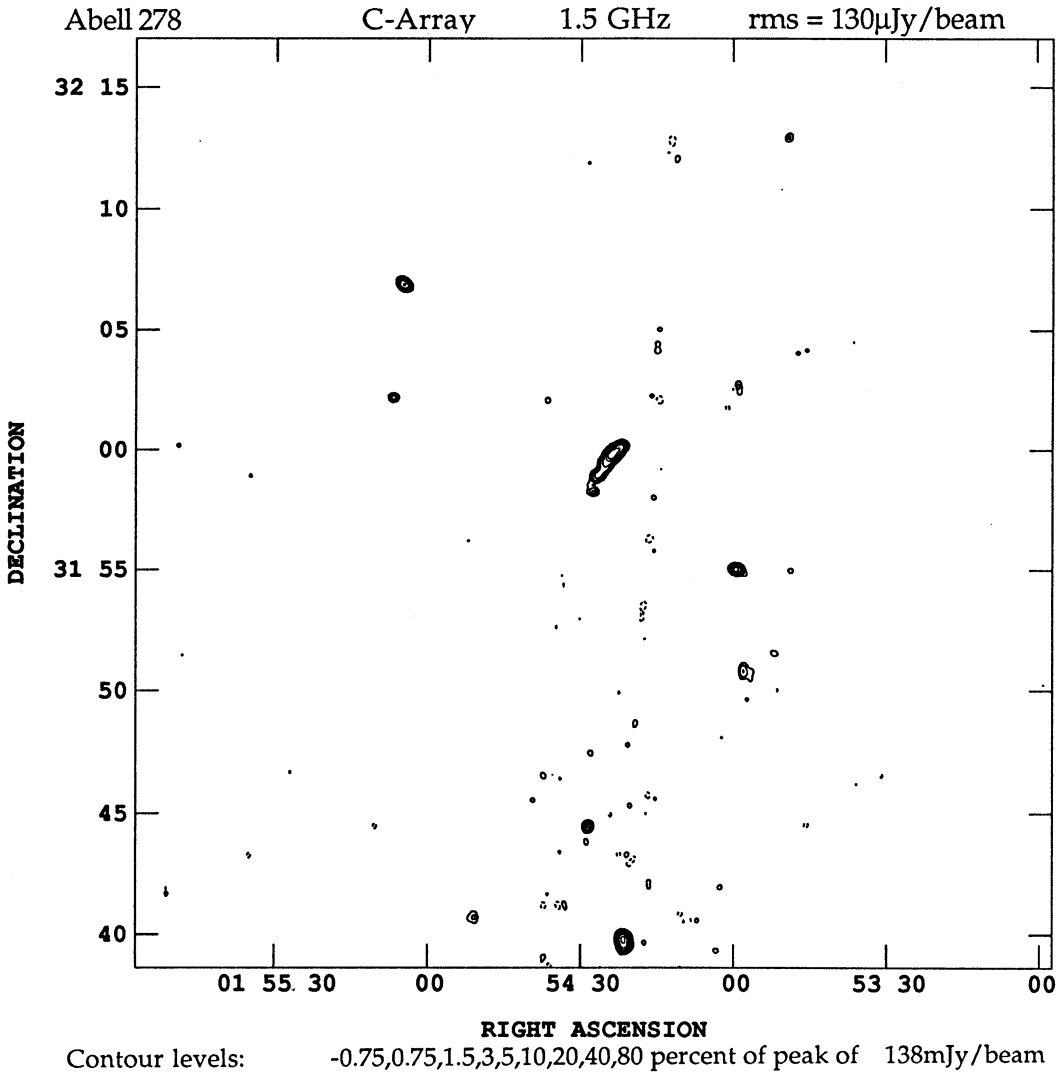
Abell 278
C-Array
1.5 GHz
rms = 130μJy/beam
32 15
10
05
00
31 55
50
45
40
DECLINATION
01 55 30
00
54 30
00
53 30
00
RIGHT ASCENSION
Contour levels: -0.75,0.75,1.5,3,5,10,20,40,80 percent of peak of 138mJy/beam

**Figure 15**

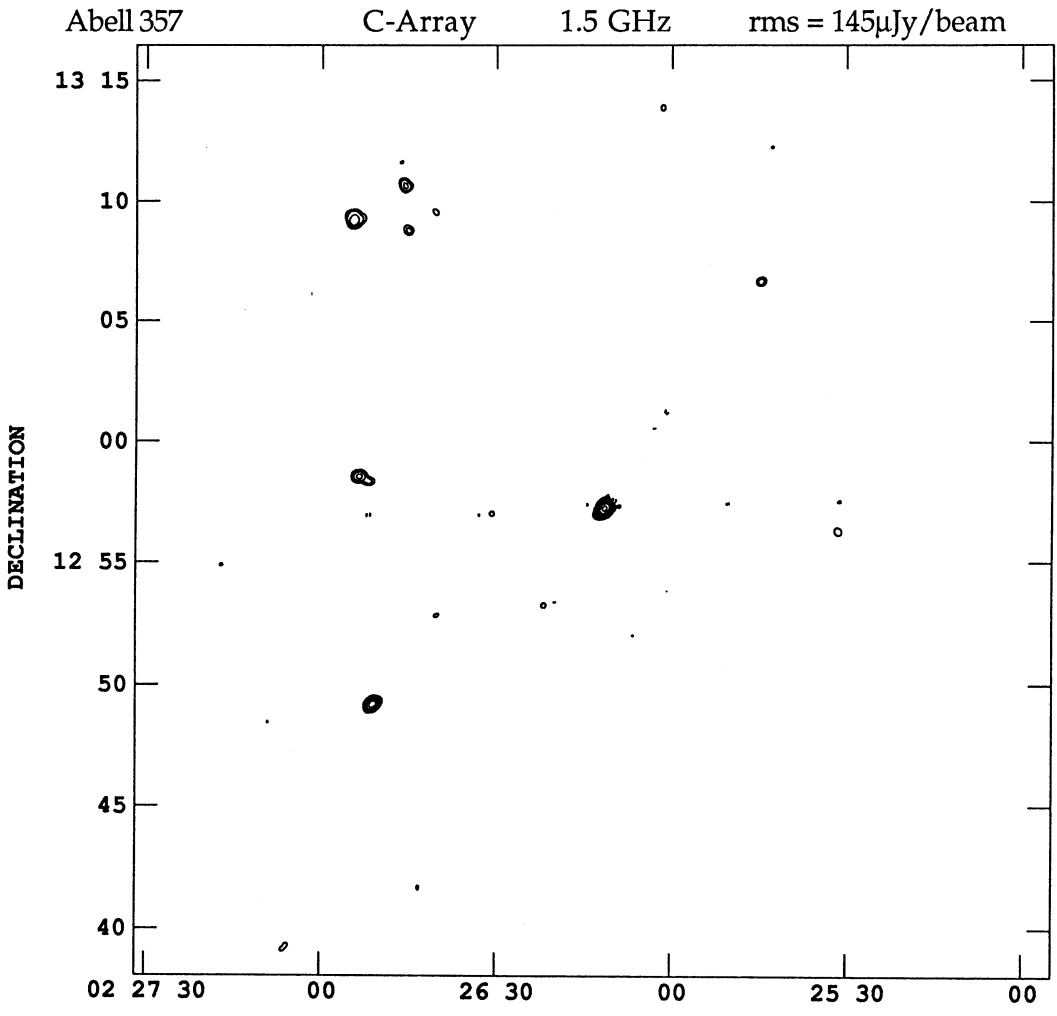


Contour levels: -0.5,0.5,1,2,5,10,20,40,80 percent of peak of 217mJy/beam

**Figure 16**

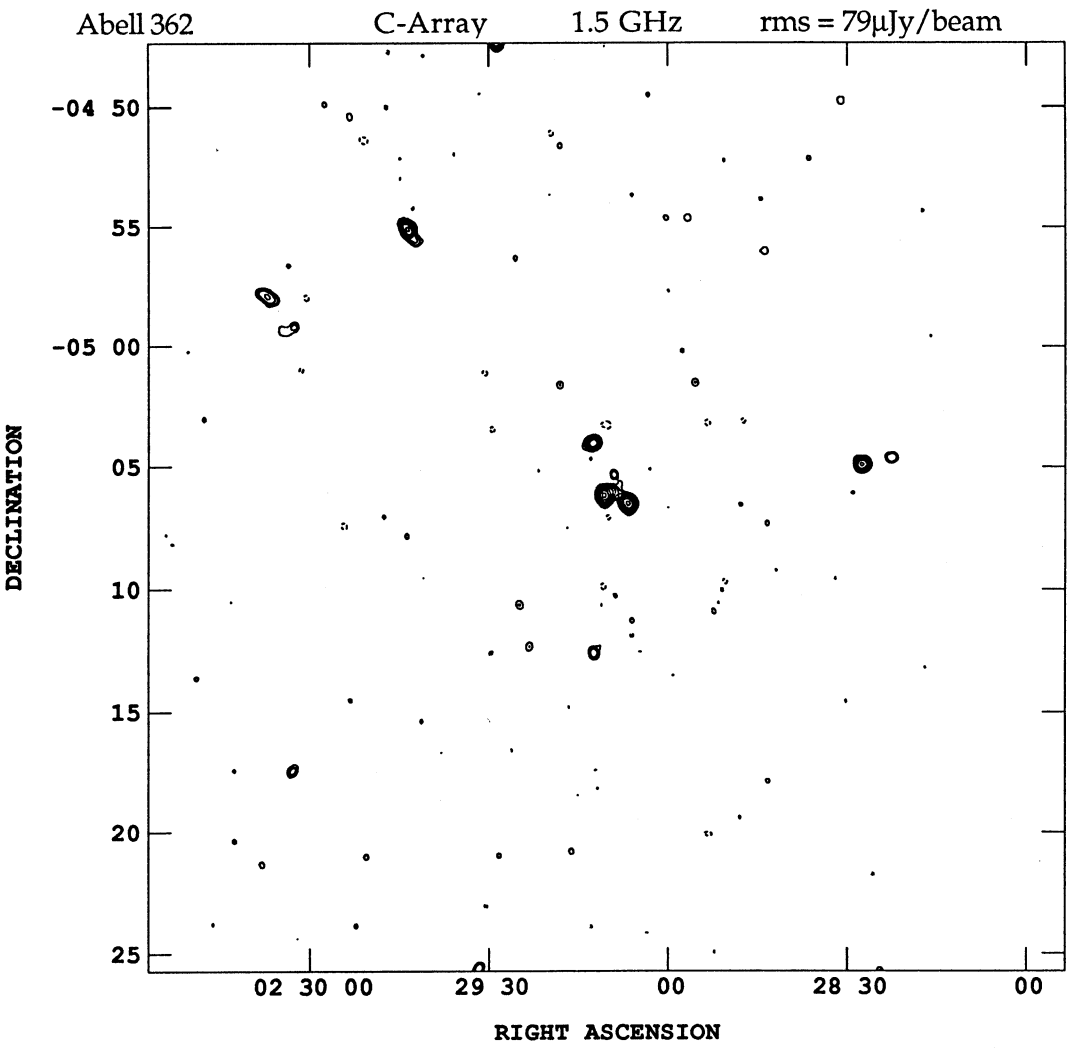


Contour levels: -0.5,0.5,1,2,5,10,20,40,80 percent of peak of 86.1mJy/beam

**Figure 17**

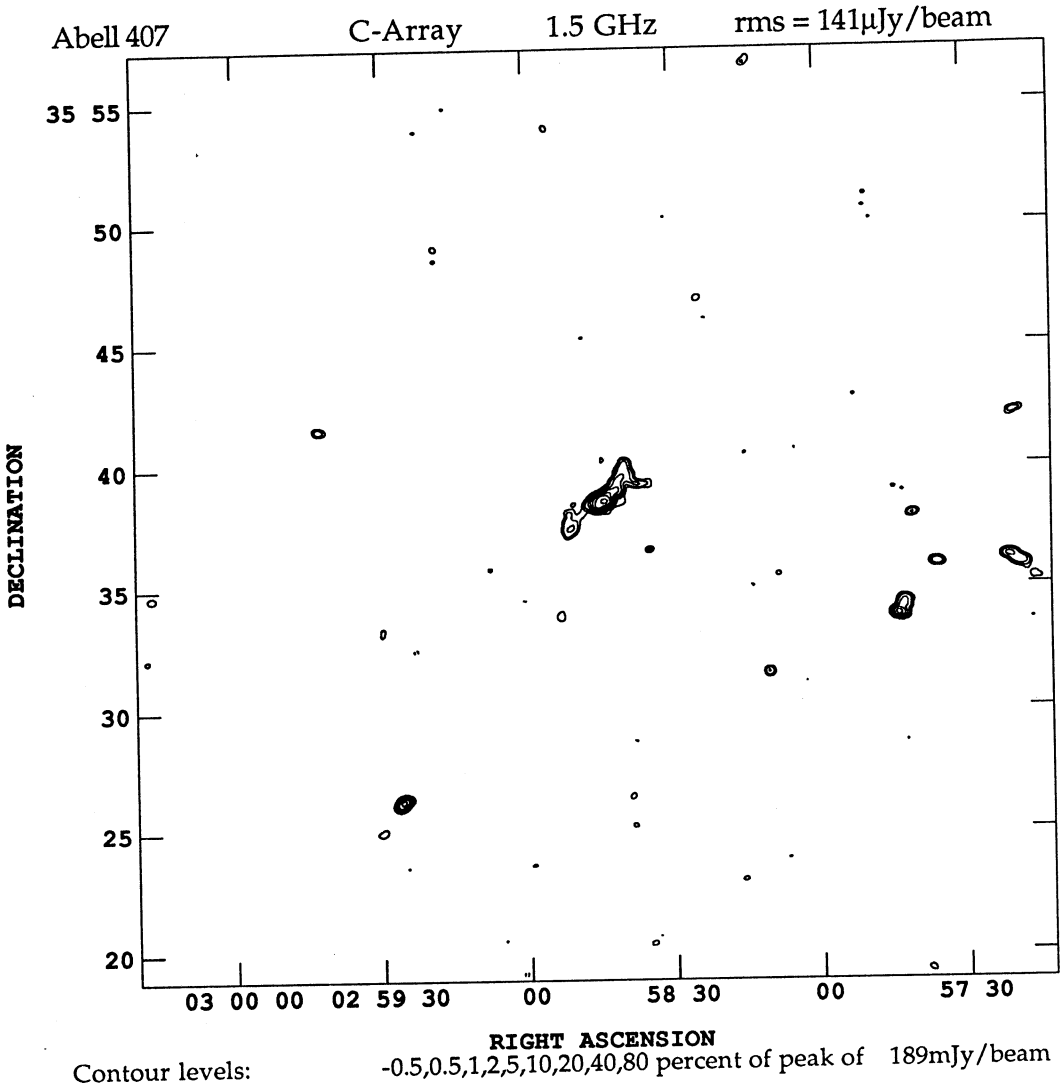


Contour levels: -0.5,0.5,1,2,5,10,20,40,80 percent of peak of 189mJy/beam

**Figure 18**

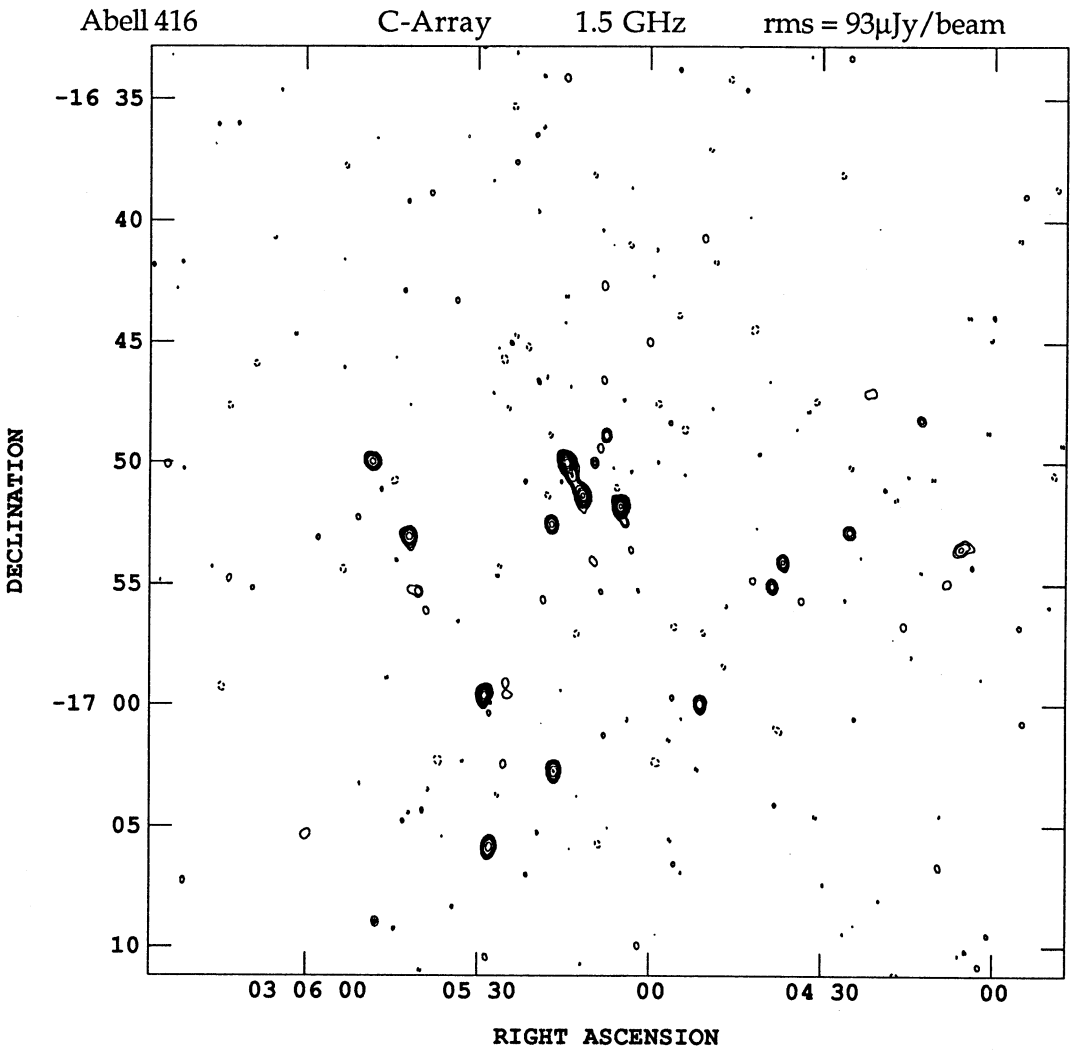


Contour levels: -0.25,0.25,0.5,1,2,5,10,20,40,80 percent of peak of 161mJy/beam

**Figure 19**

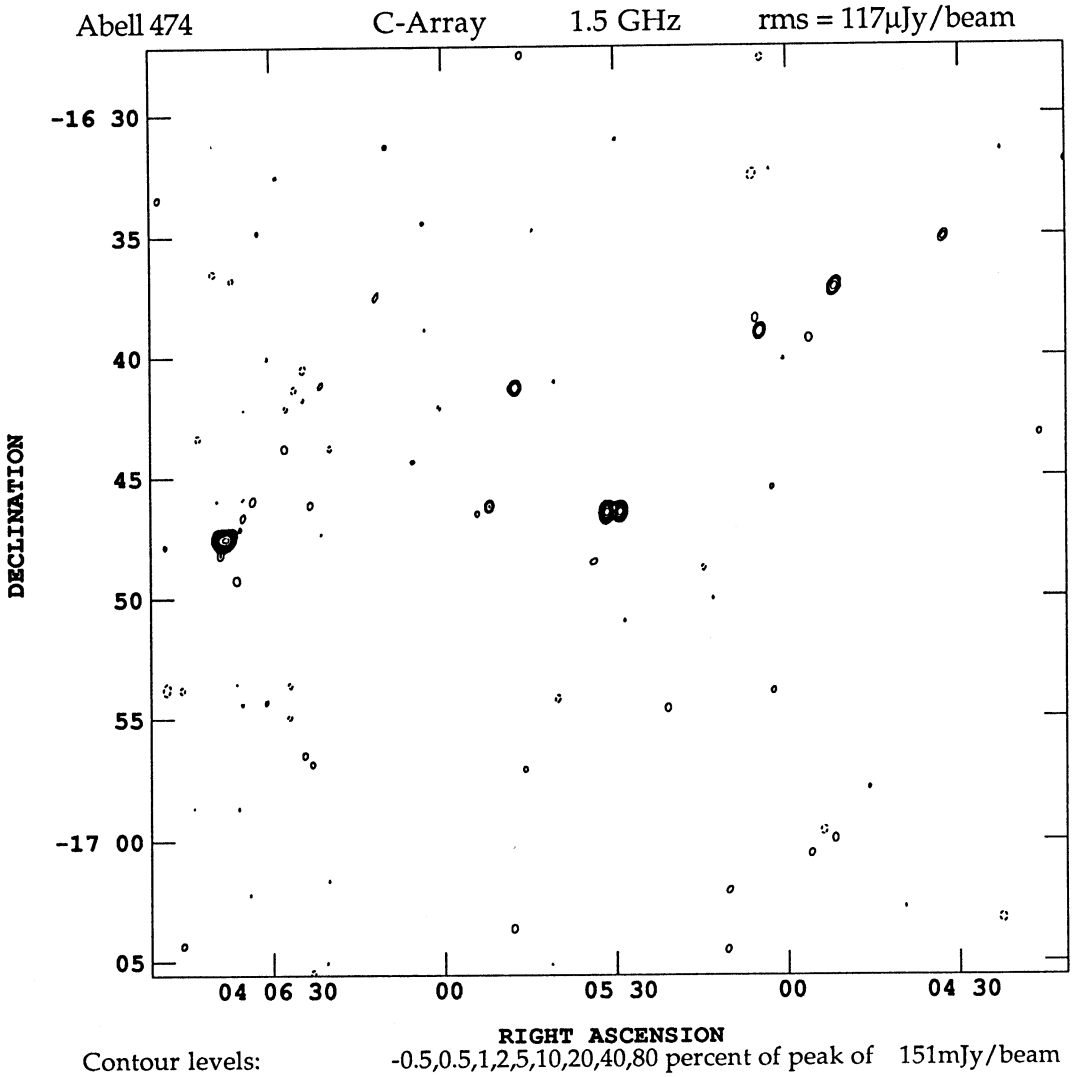


Contour levels: -0.5,0.5,1,2,5,10,20,40,80 percent of peak of 151mJy/beam

**Figure 20**

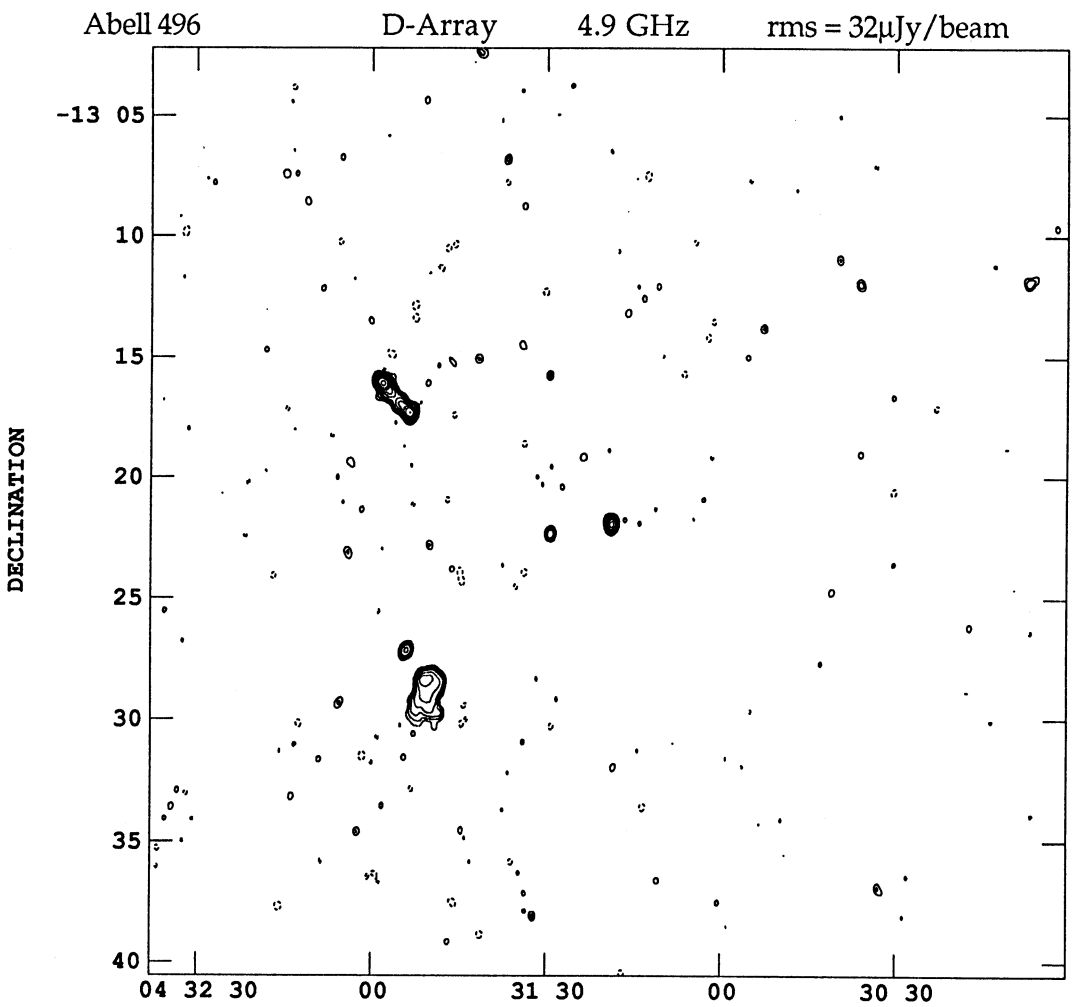


Contour levels: -0.25,0.25,0.5,1,2,5,10,20,40,80 percent of peak of 335mJy/beam

**Figure 21**

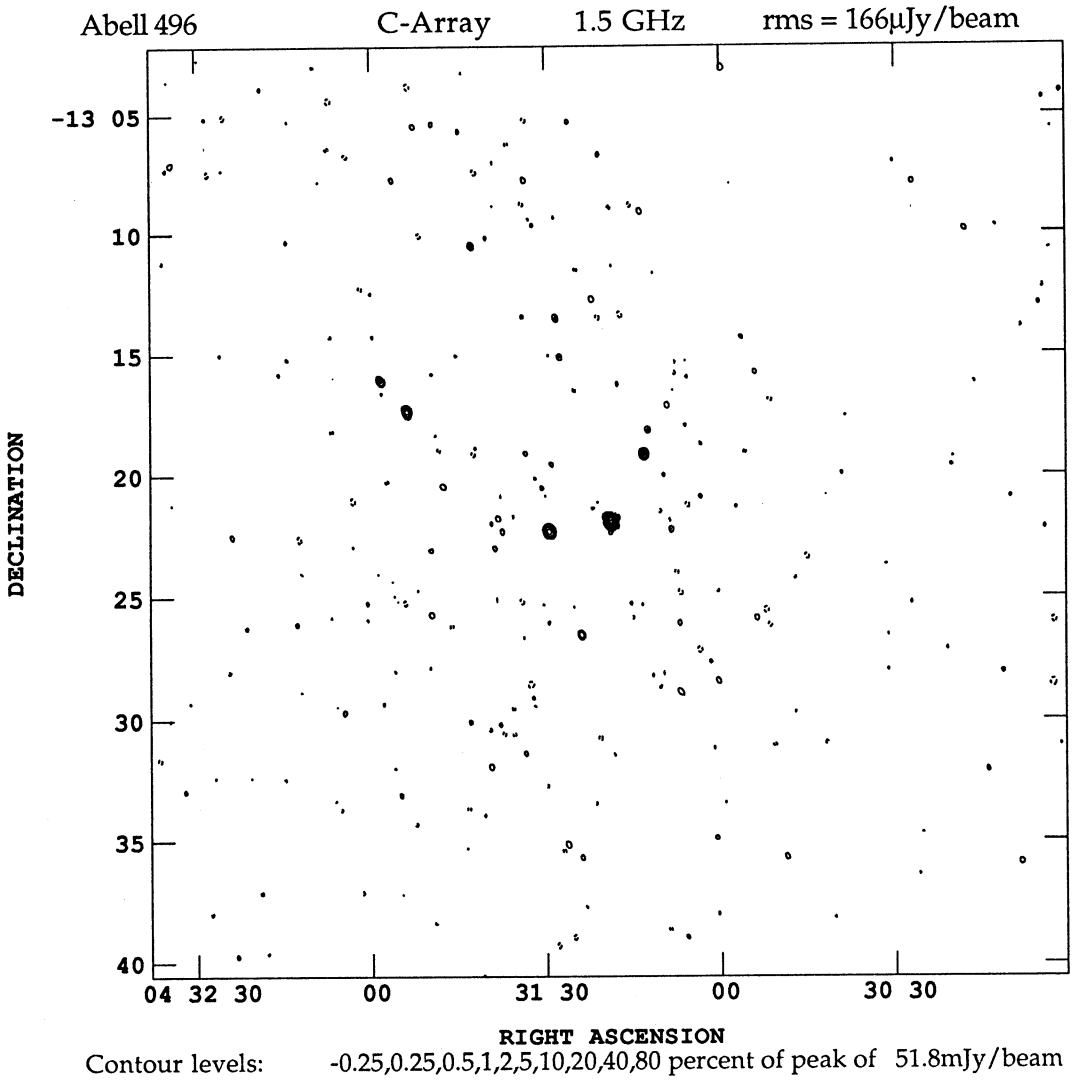


Contour levels: -0.25,0.25,0.5,1,2,5,10,20,40,80 percent of peak of 51.8mJy/beam

**Figure 22**

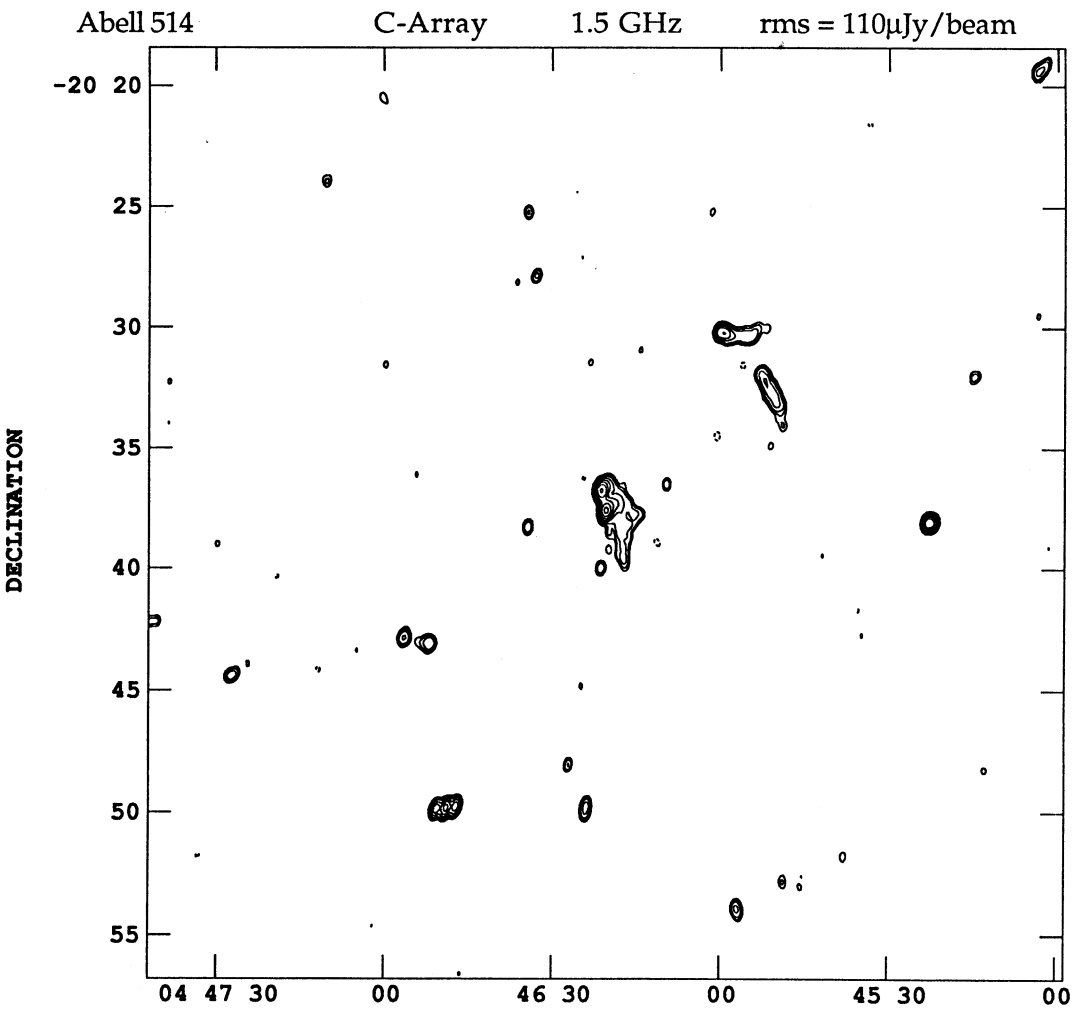


Contour levels: -0.5,0.5,1,2,5,10,20,40,80 percent of peak of 135mJy/beam

**Figure 23**

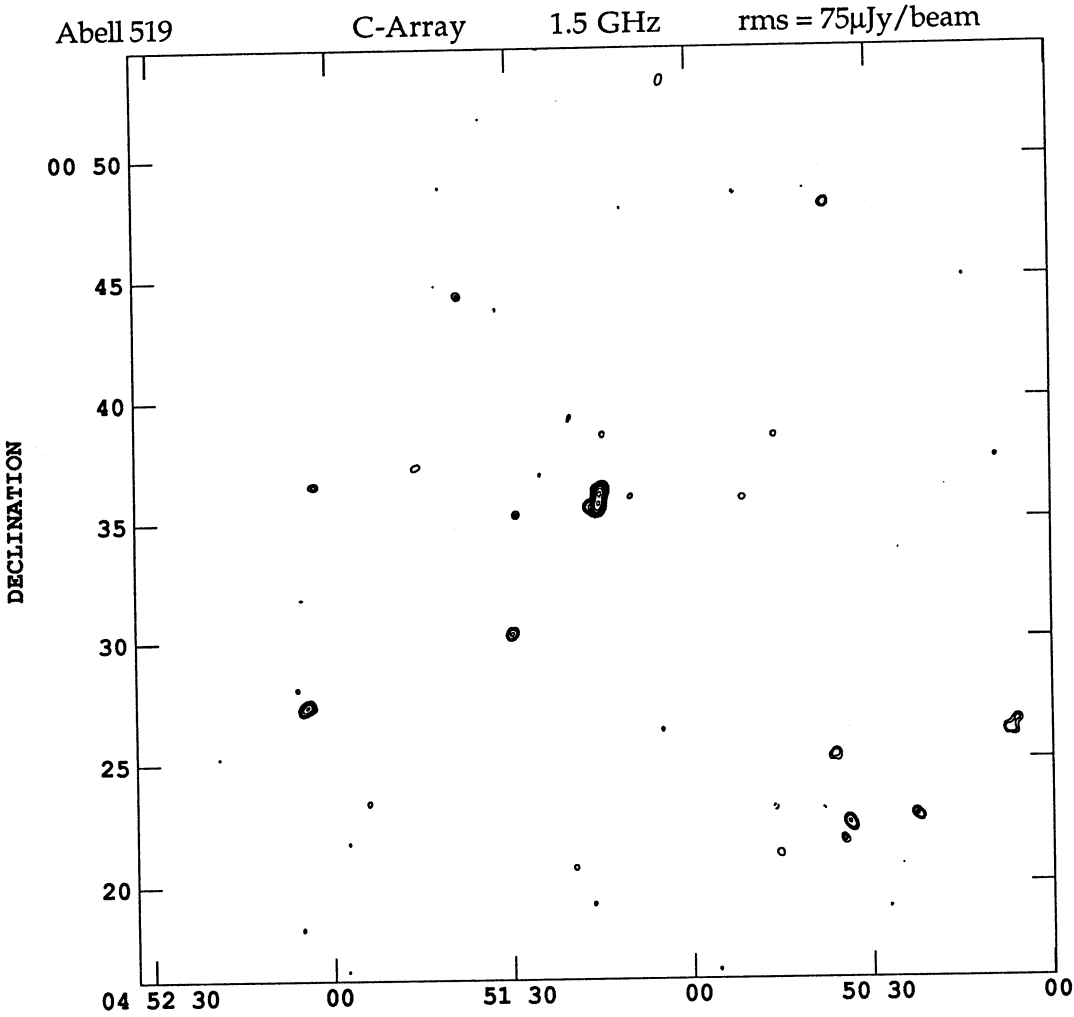


Contour levels: -0.5,0.5,1,2,5,10,20,40,80 percent of peak of 102mJy/beam

**Figure 24**

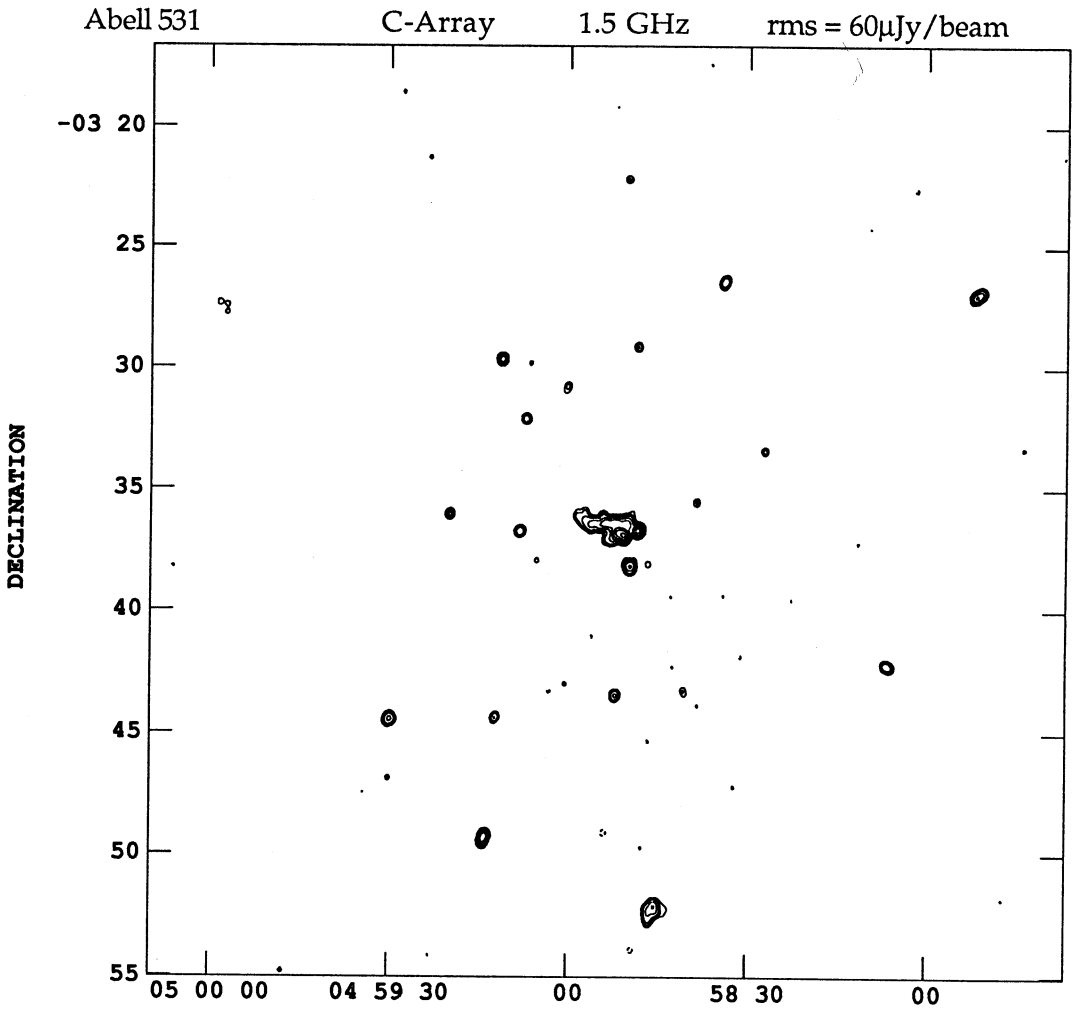


Contour levels: -0.5,0.5,1,2,5,10,20,40,80 percent of peak of 78.2mJy/beam

**Figure 25**

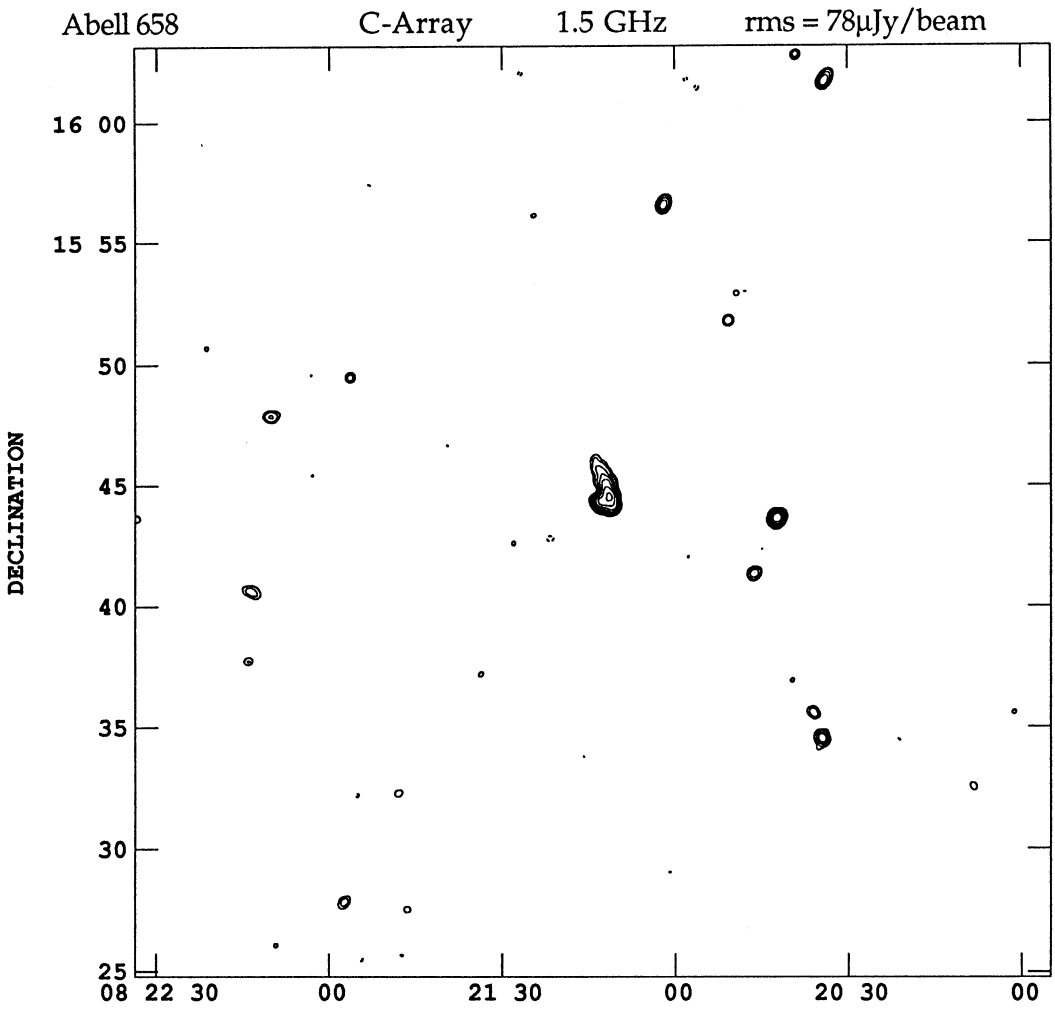


Contour levels: -1,1,2,5,10,20,40,80 percent of peak of 51.8mJy/beam

**Figure 26**

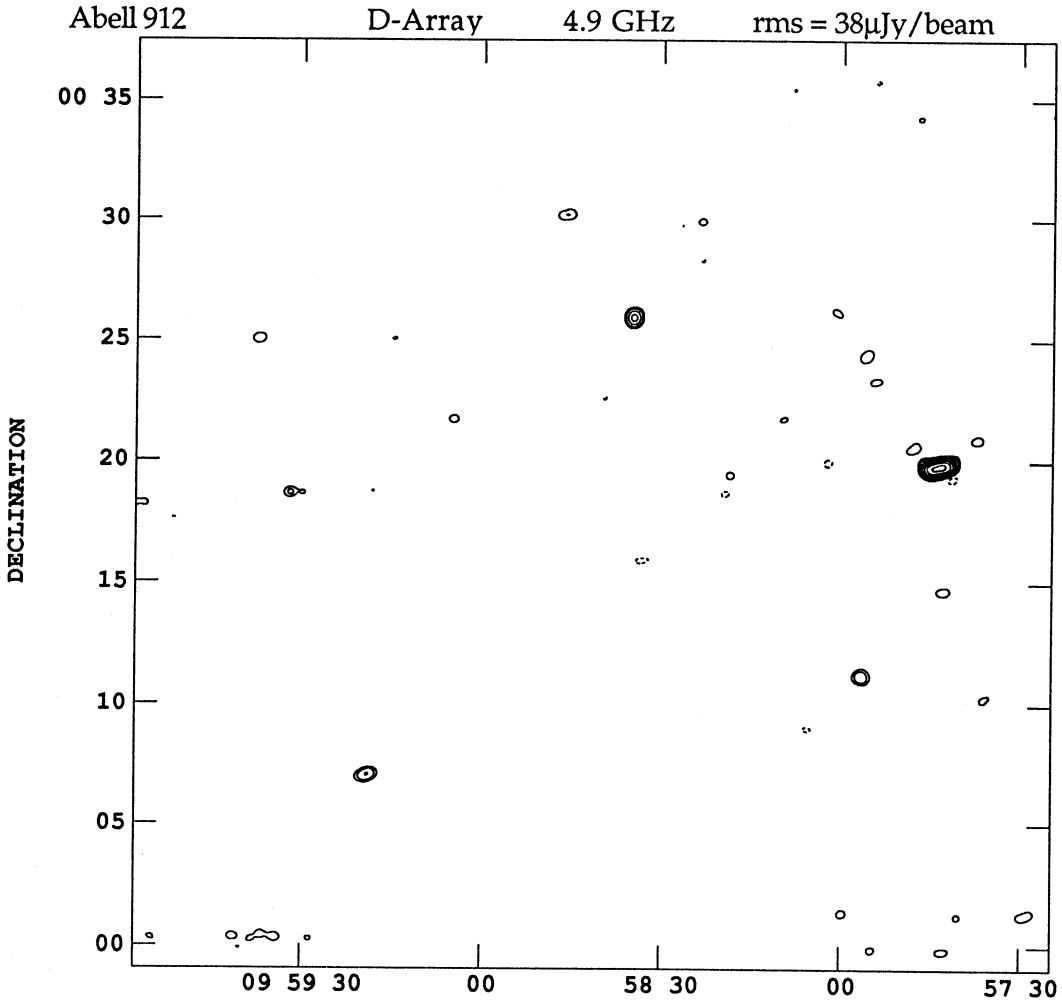


Contour levels: -1,1,2,5,10,20,40,80 percent of peak of 203mJy/beam

**Figure 27**

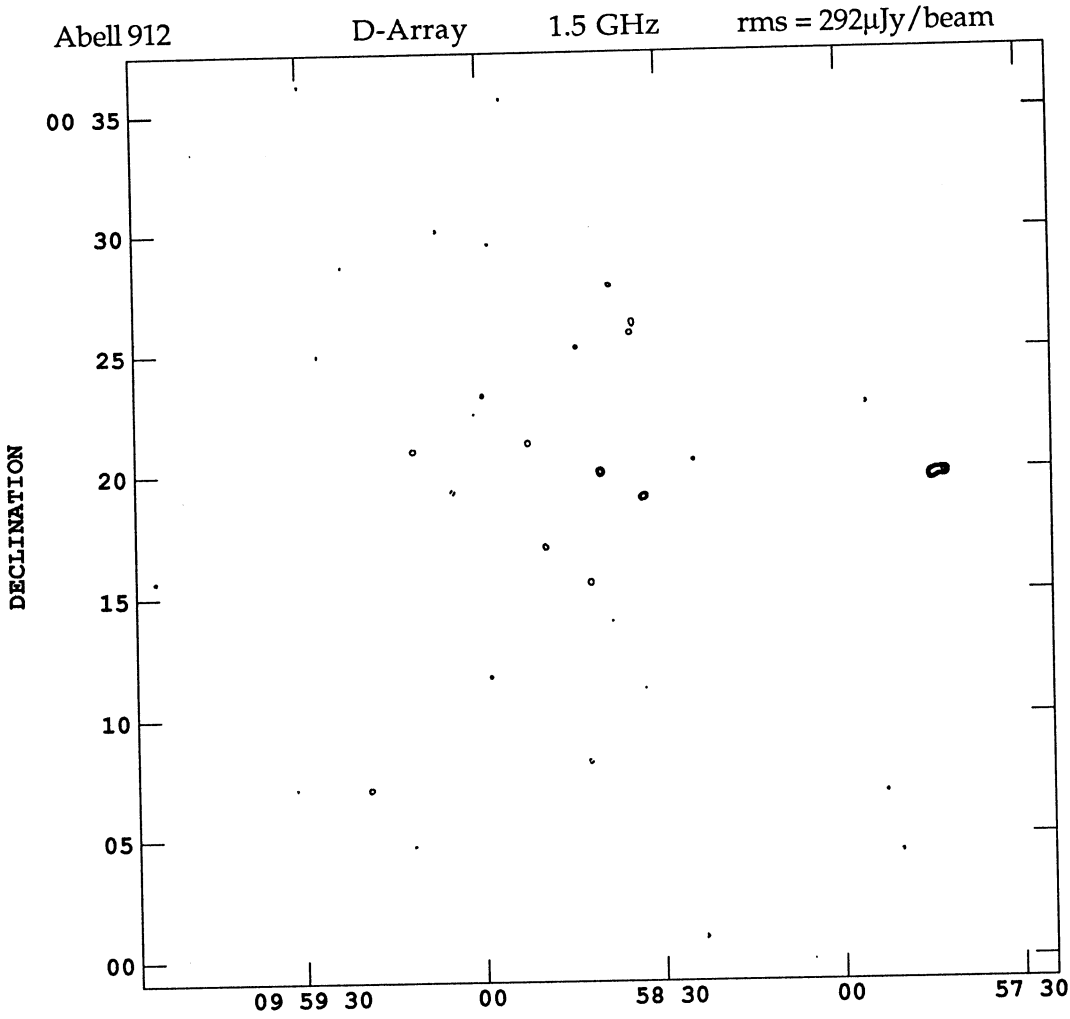


Contour levels: -10,10,20,30,50,80 percent of peak of 2.2mJy/beam

**Figure 28**

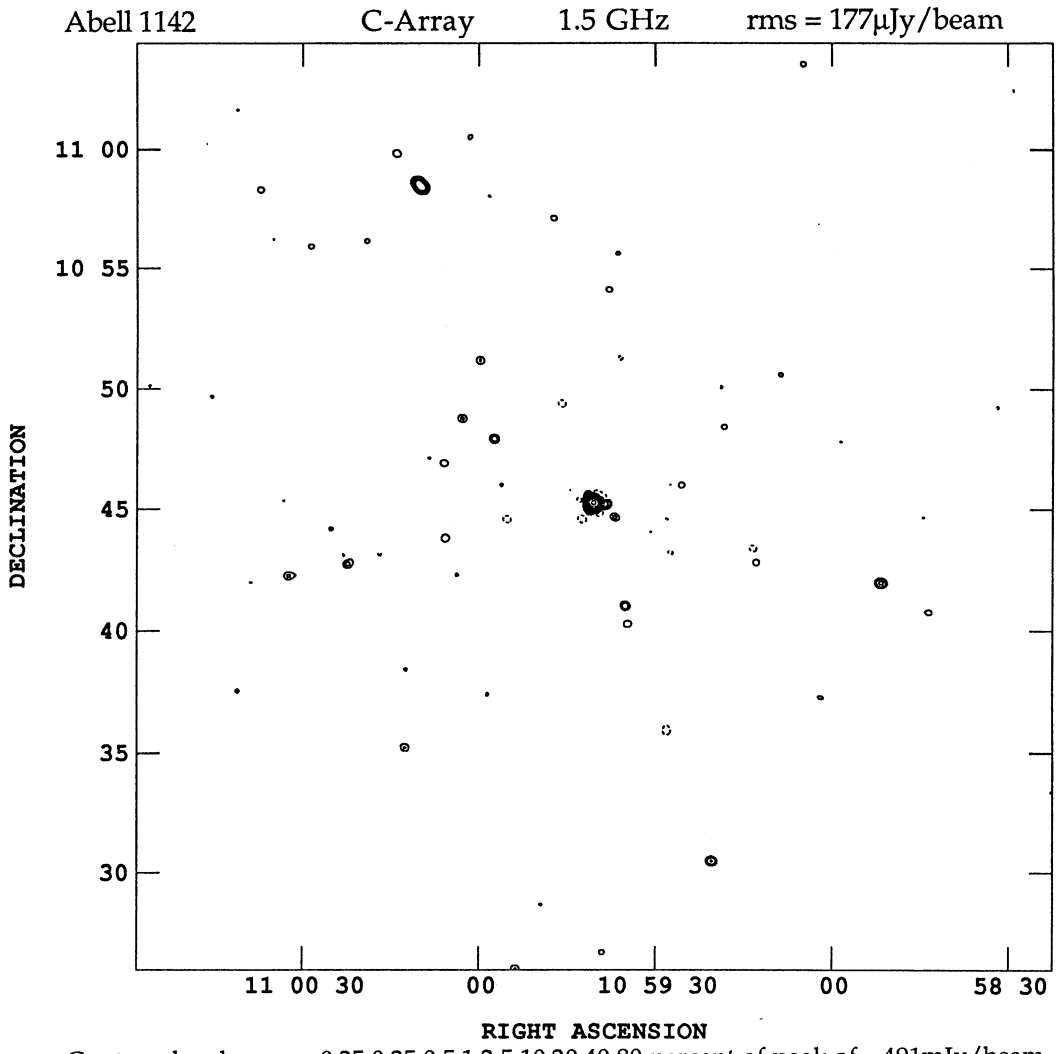


Contour levels: -0.25,0.25,0.5,1,2,5,10,20,40,80 percent of peak of 491mJy/beam

**Figure 29**

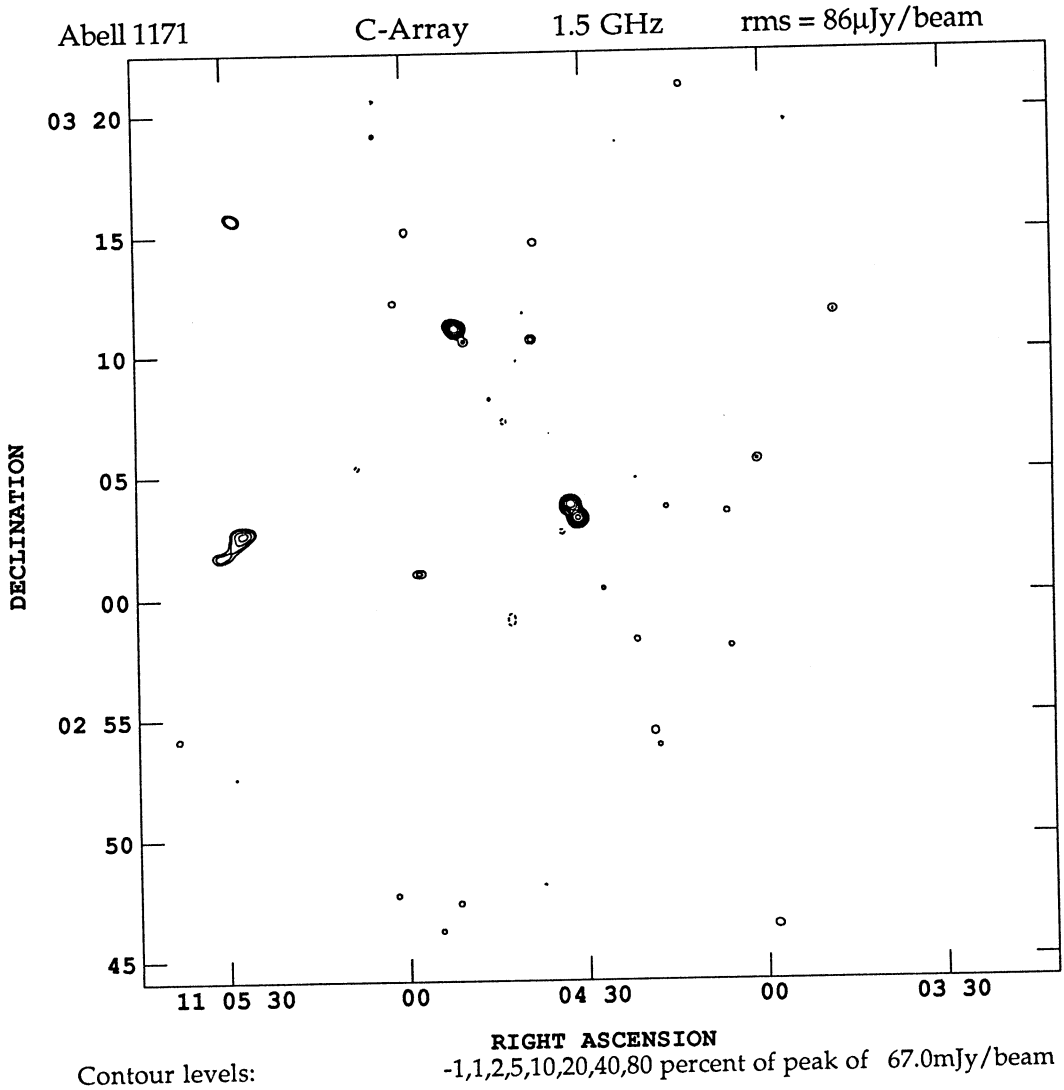


Contour levels: -1,1,2,5,10,20,40,80 percent of peak of 67.0mJy/beam

**Figure 30**

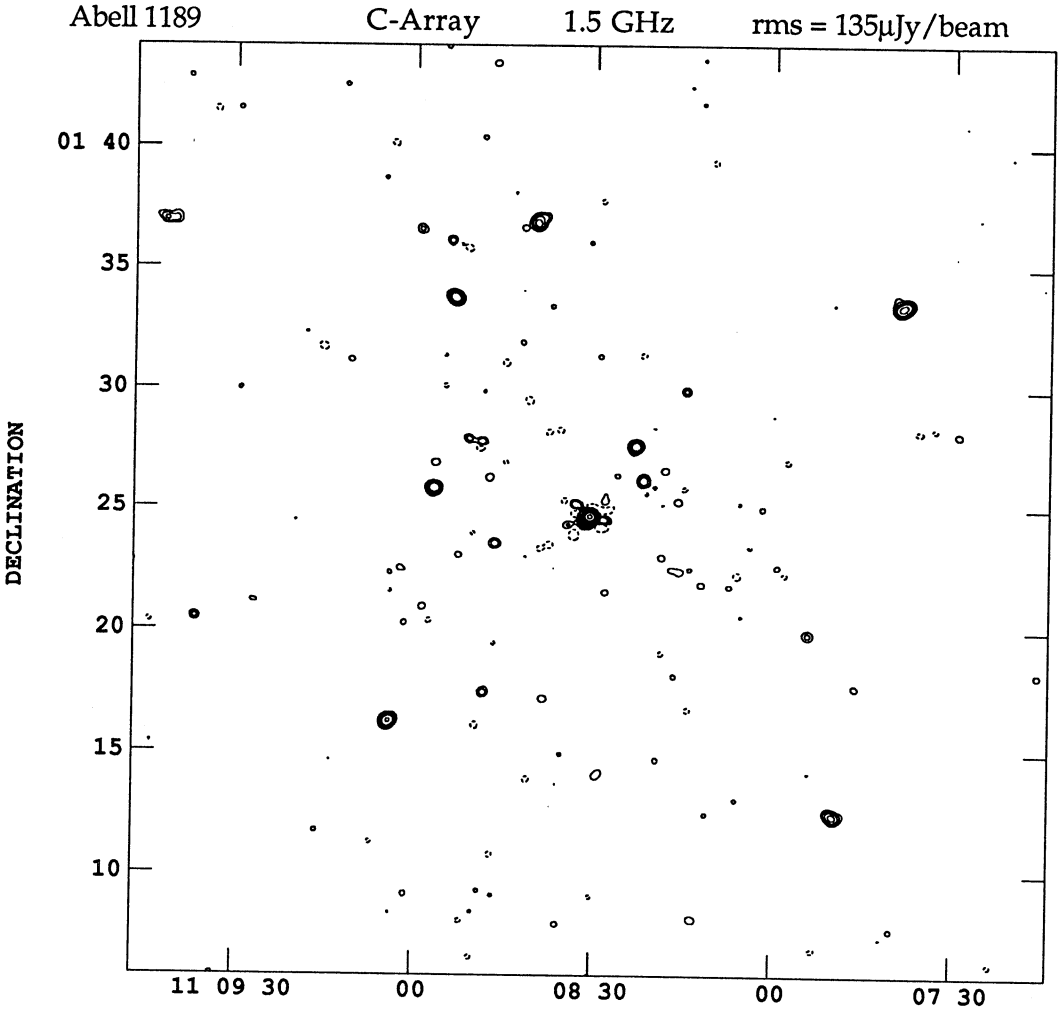


Contour levels: -0.25,0.25,0.5,1,2,5,10,20,40,80 percent of peak of 260mJy/beam

**Figure 31**

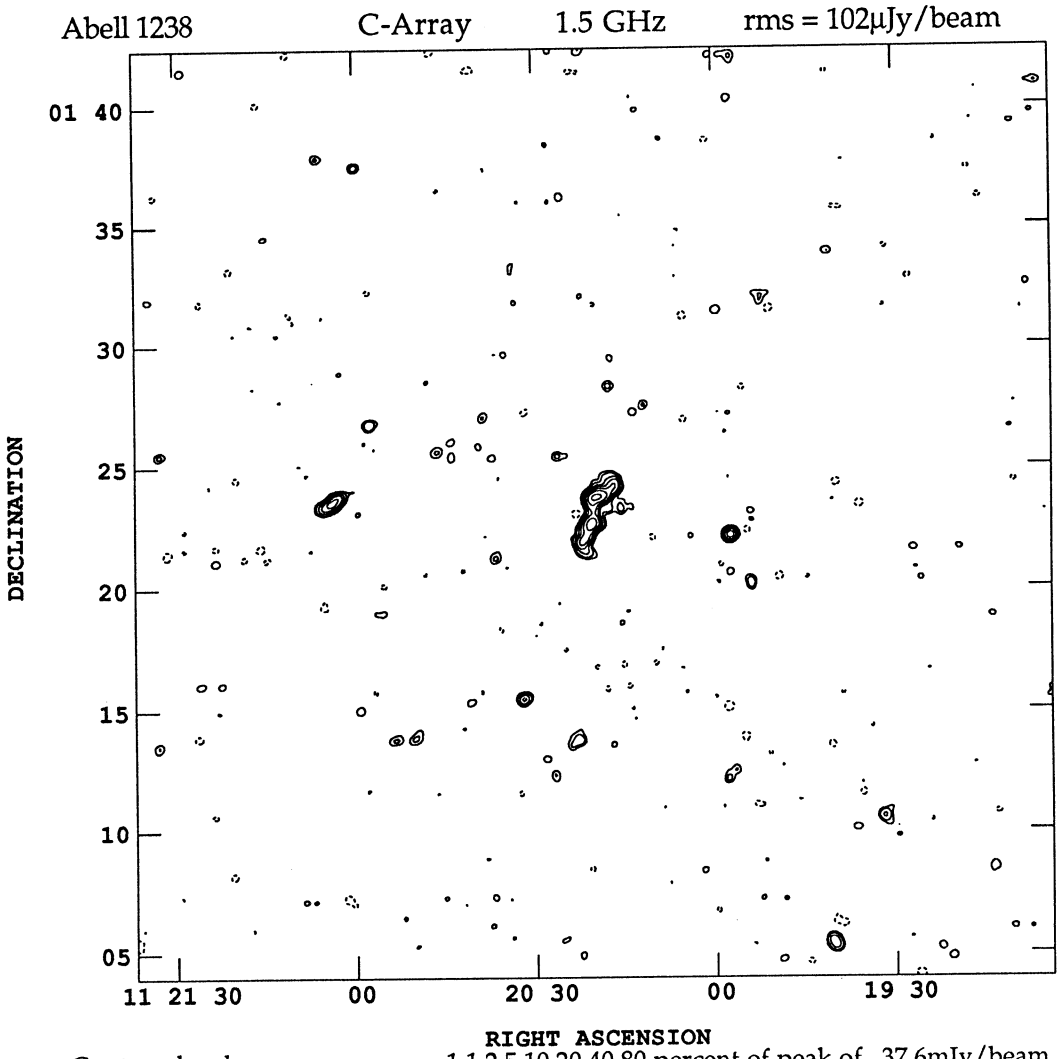


Contour levels: -1,1,2,5,10,20,40,80 percent of peak of 37.6mJy/beam

**Figure 32**

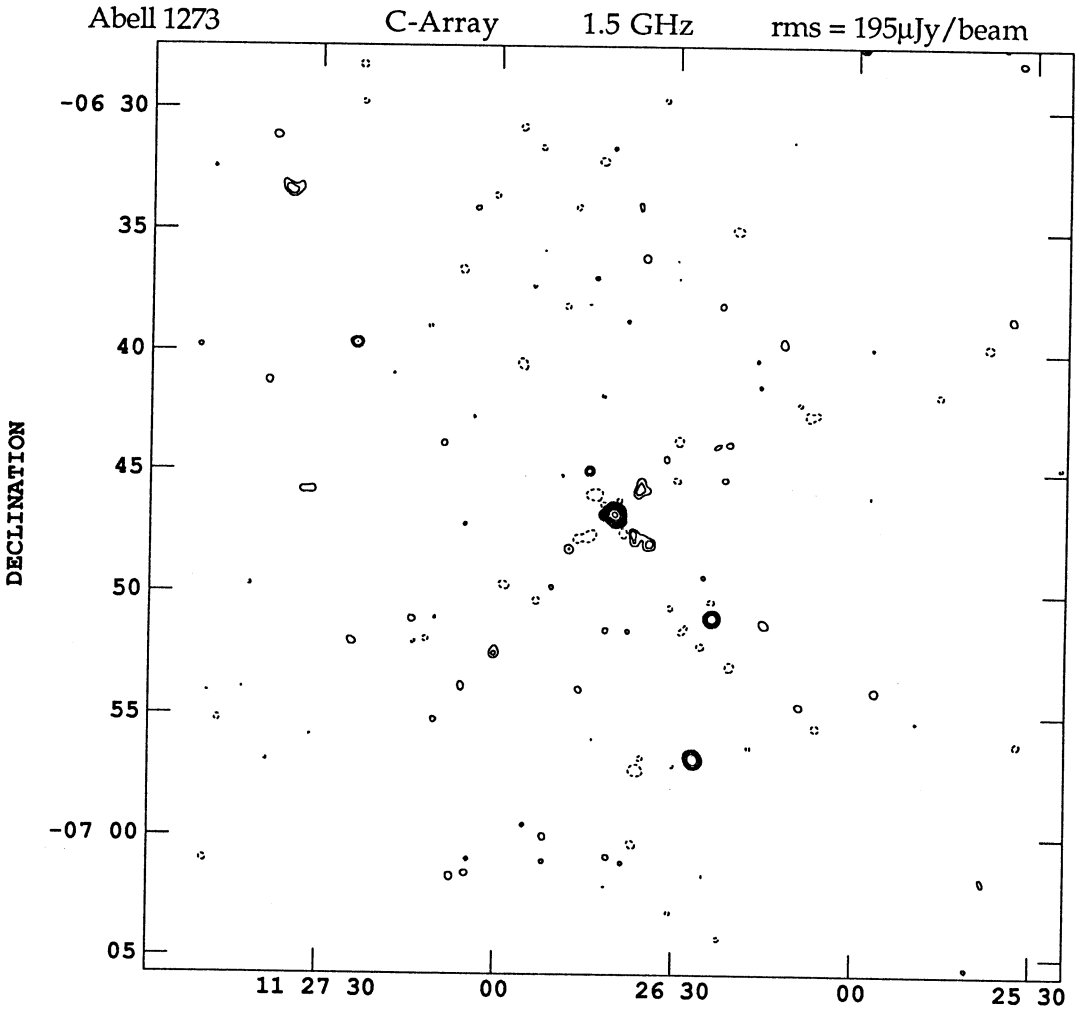


Contour levels: -0.25,0.25,0.5,1,2,5,10,20,40,80 percent of peak of 392mJy/beam

**Figure 33**

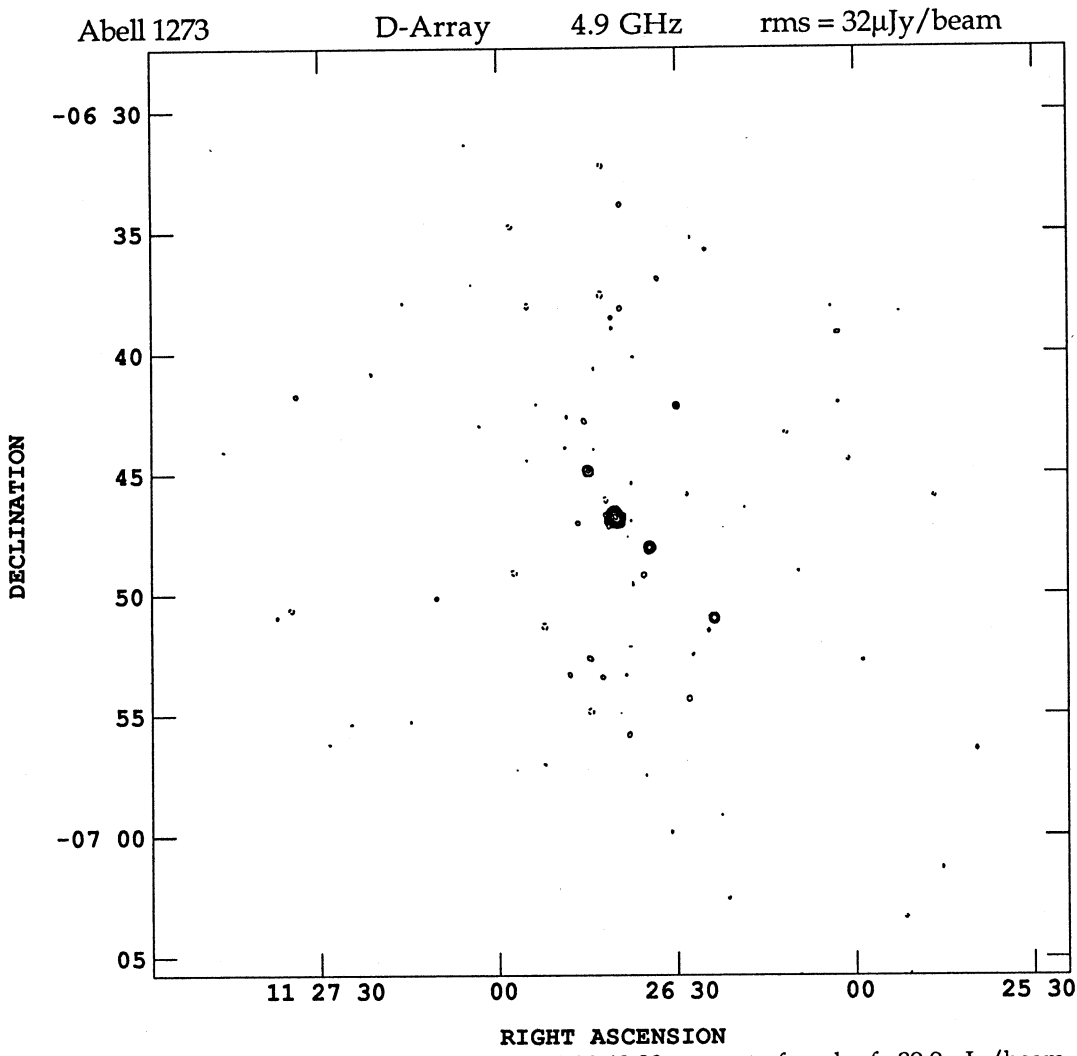


Contour levels: -0.25,0.25,0.5,1,2,5,10,20,40,80 percent of peak of 89.9mJy/beam

**Figure 34**

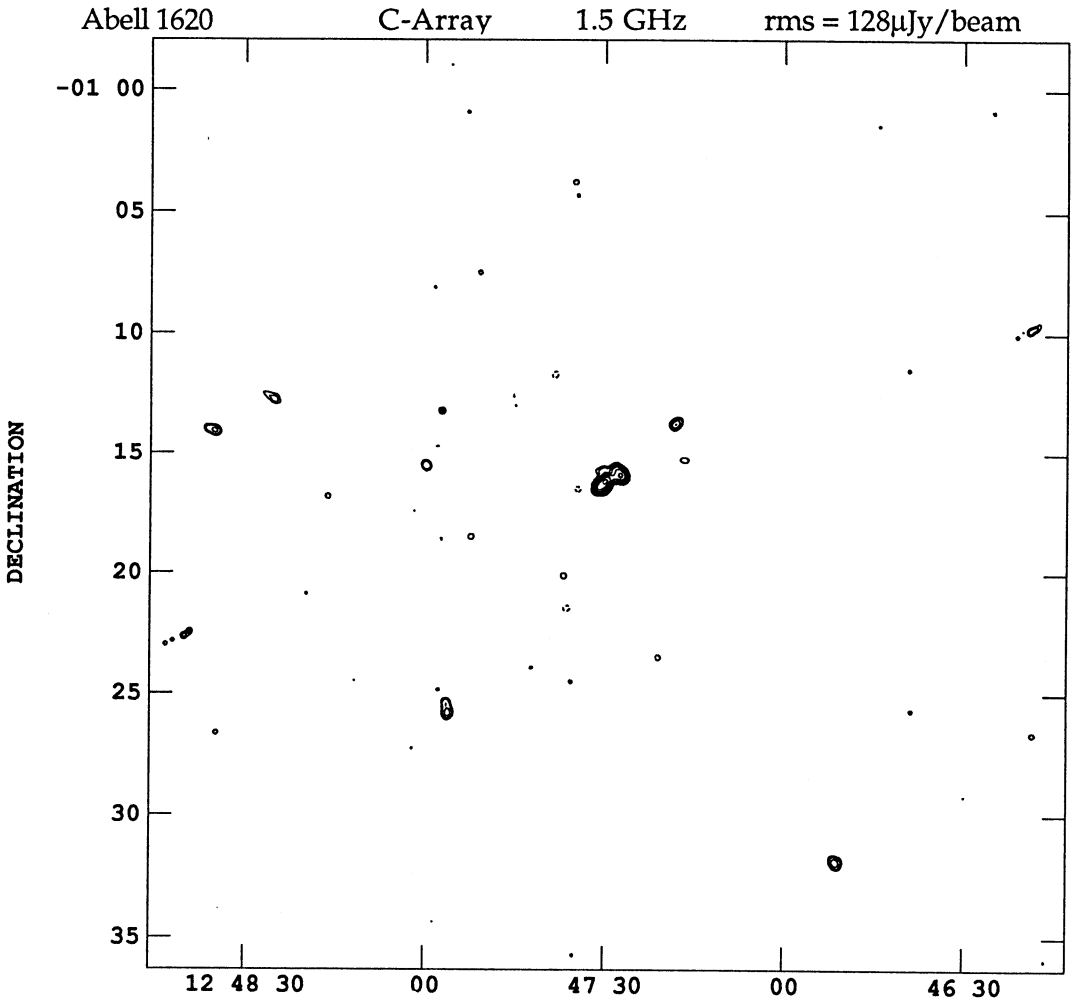


Contour levels: -1,1,2,5,10,20,40,80 percent of peak of 89.0mJy/beam

**Figure 35**

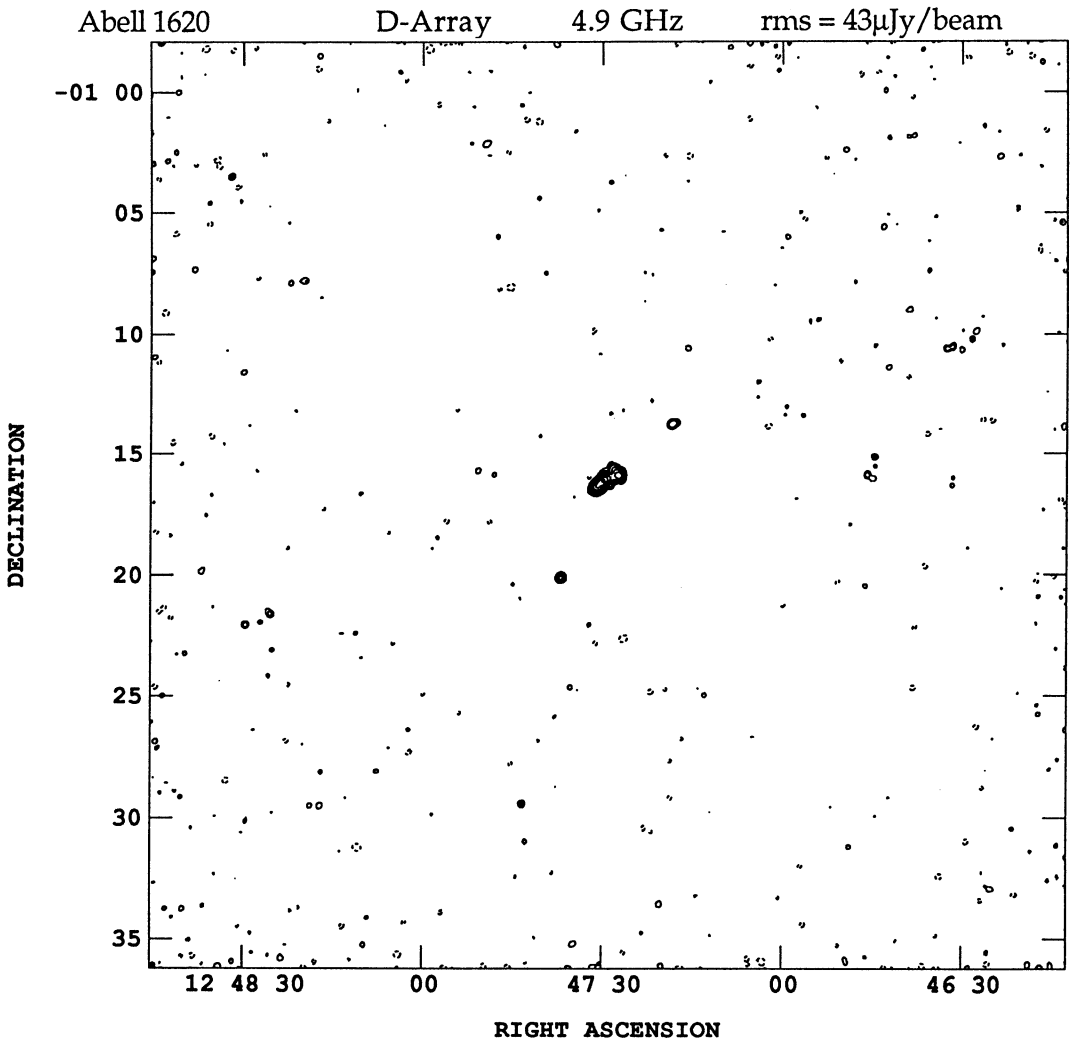


Contour levels: -0.5,0.5,1,2,5,10,20,40,80 percent of peak of 41.8mJy/beam

**Figure 36**

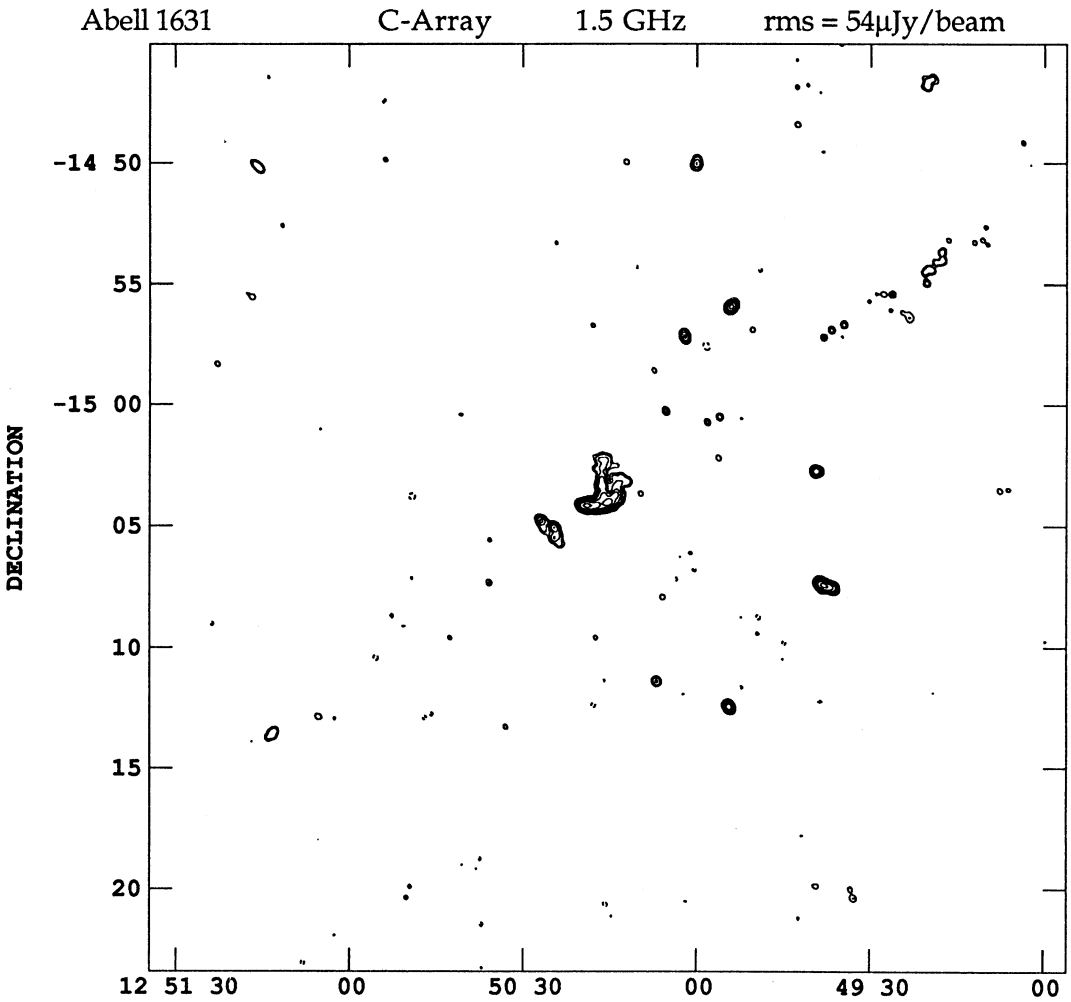


Contour levels: -1,1,2,5,10,20,40,80 percent of peak of 39.0mJy/beam

**Figure 37**

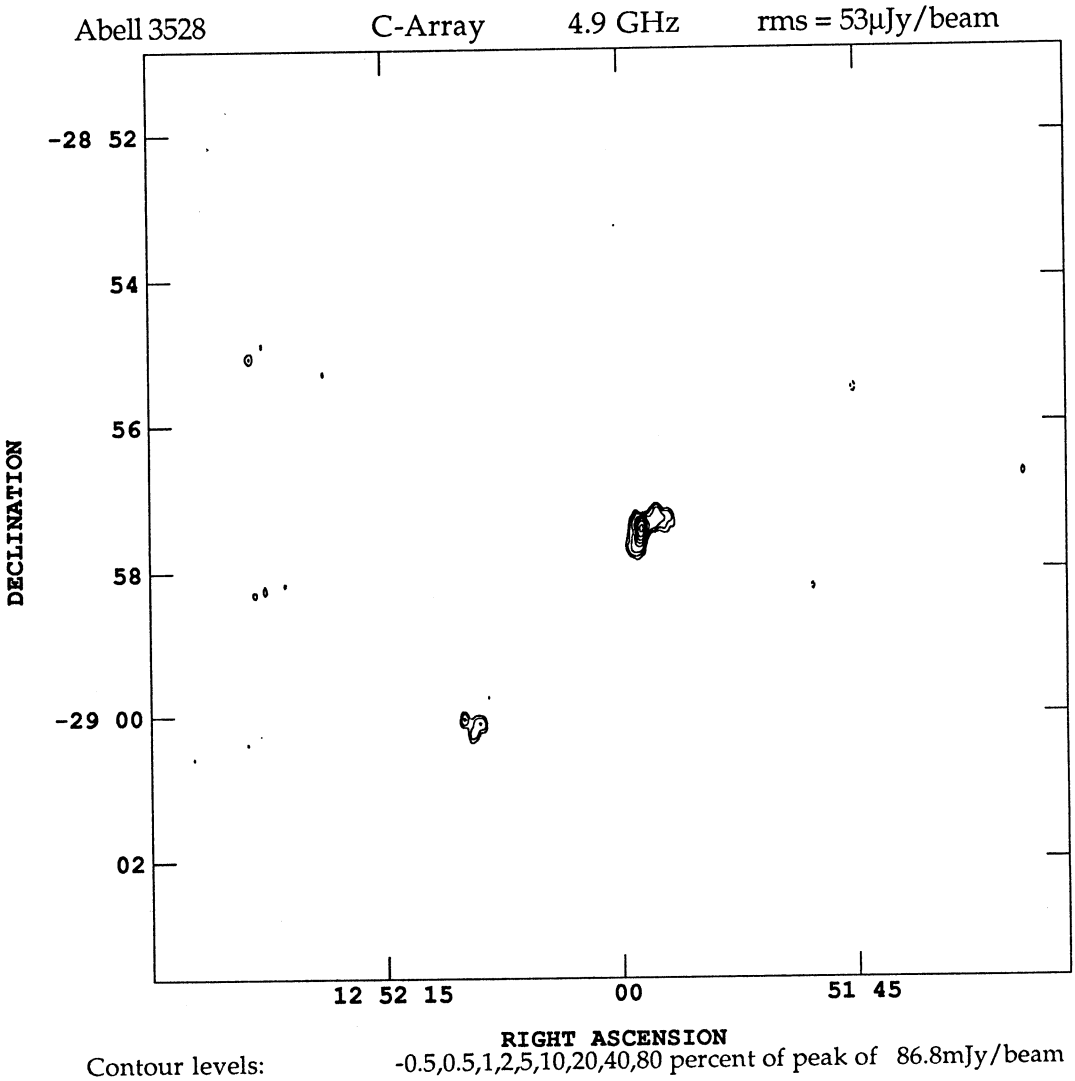


Contour levels: -0.5,0.5,1,2,5,10,20,40,80 percent of peak of 86.8mJy/beam

**Figure 38**

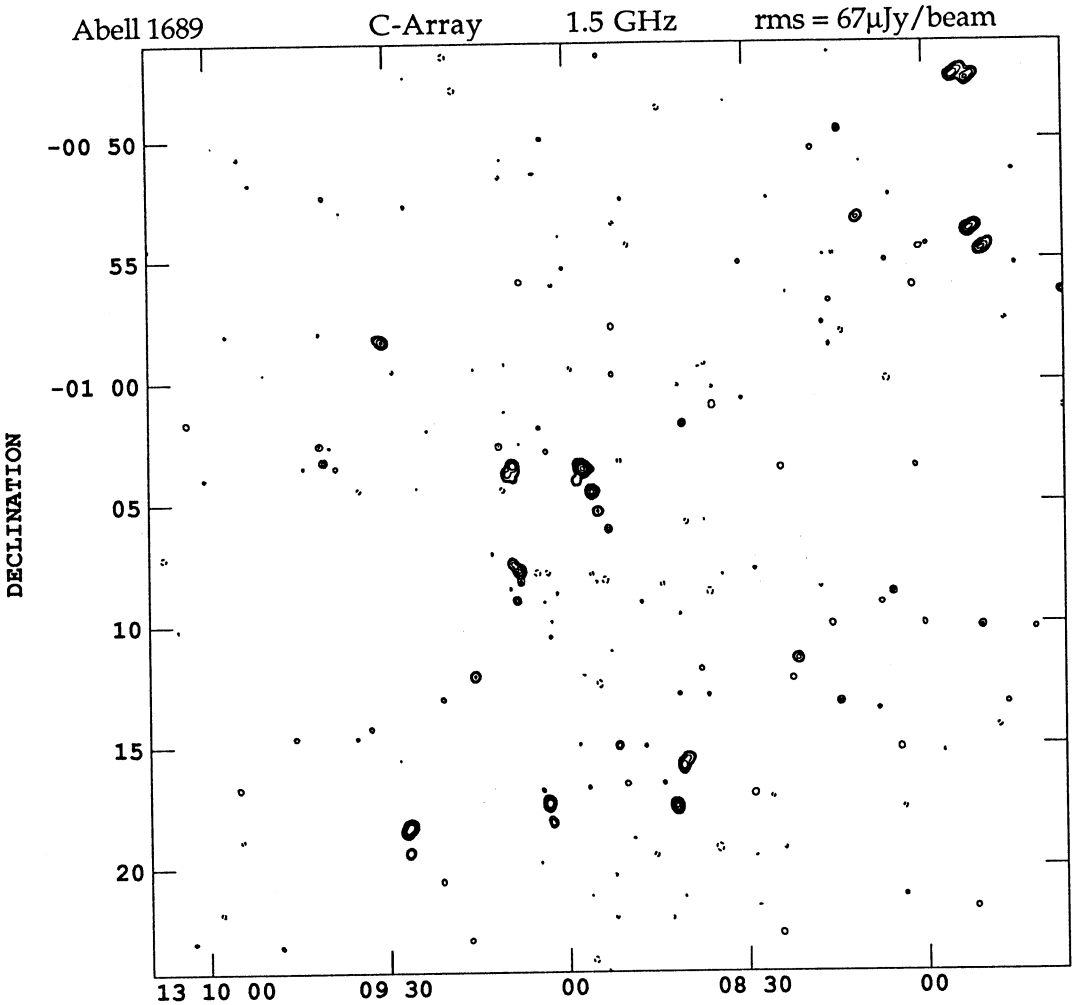


Contour levels: -1,1,2,5,10,20,40,80 percent of peak of 29.1mJy/beam

**Figure 39**

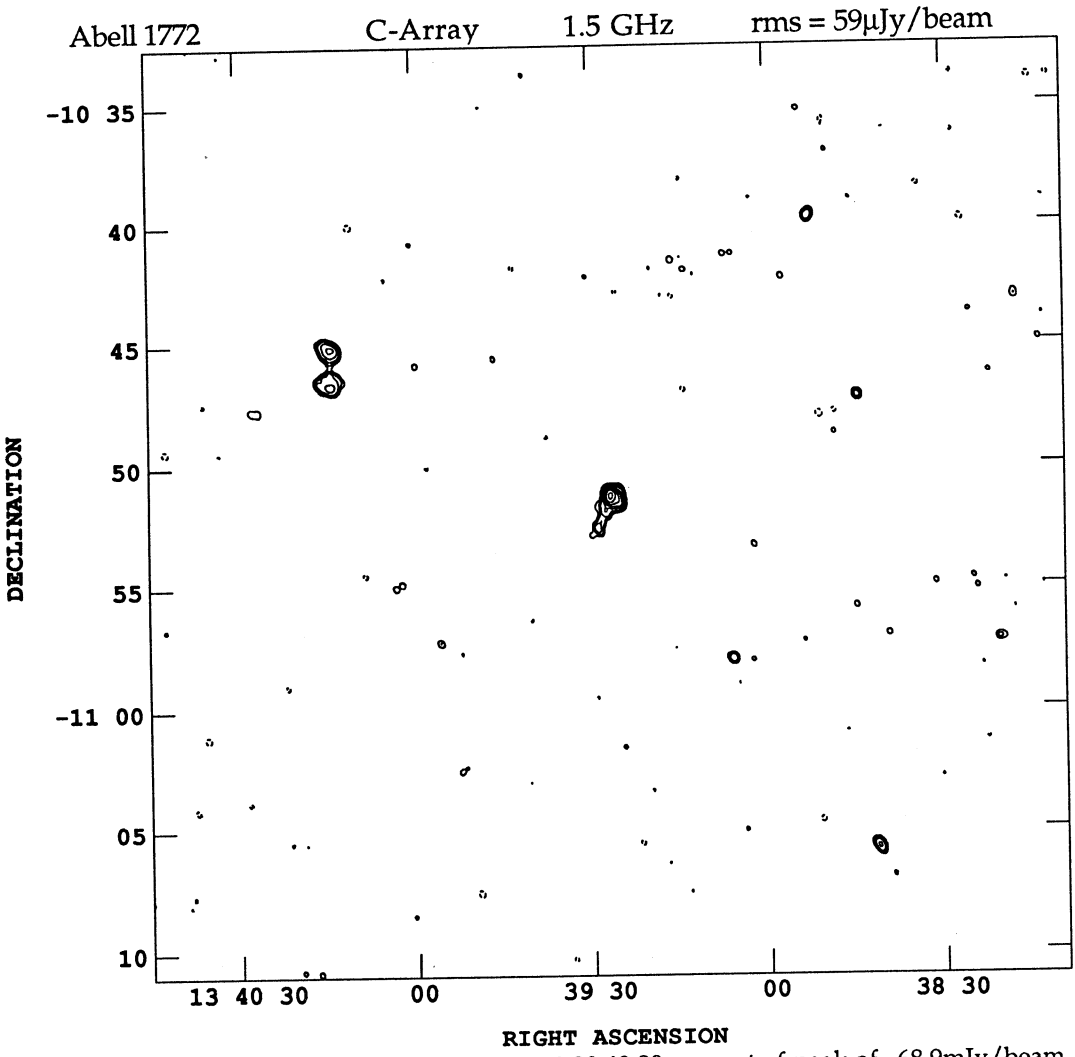


Contour levels: -0.5,0.5,1,2,5,10,20,40,80 percent of peak of 68.9mJy/beam

**Figure 40**

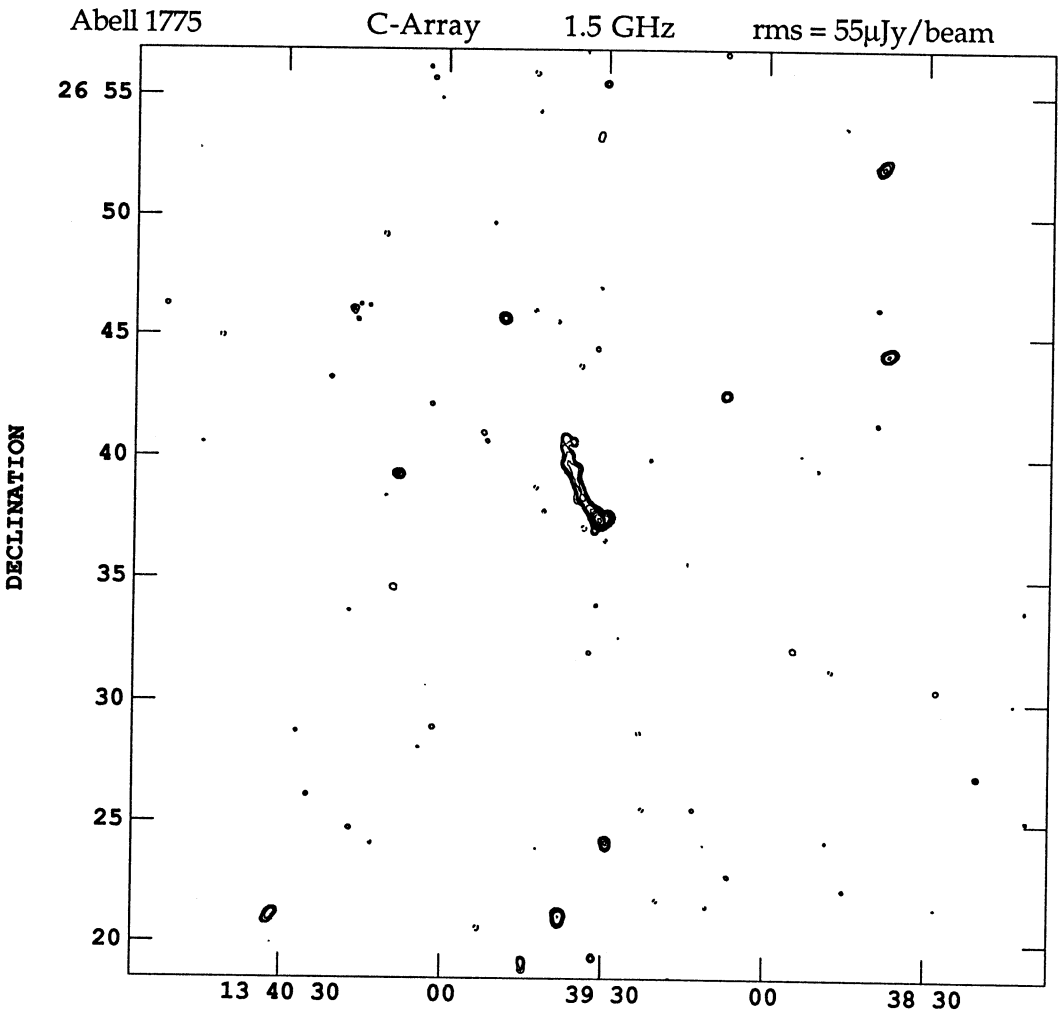


Contour levels: -0.25,0.25,0.5,1,2,5,10,20,40,80 percent of peak of 148mJy/beam

**Figure 41**

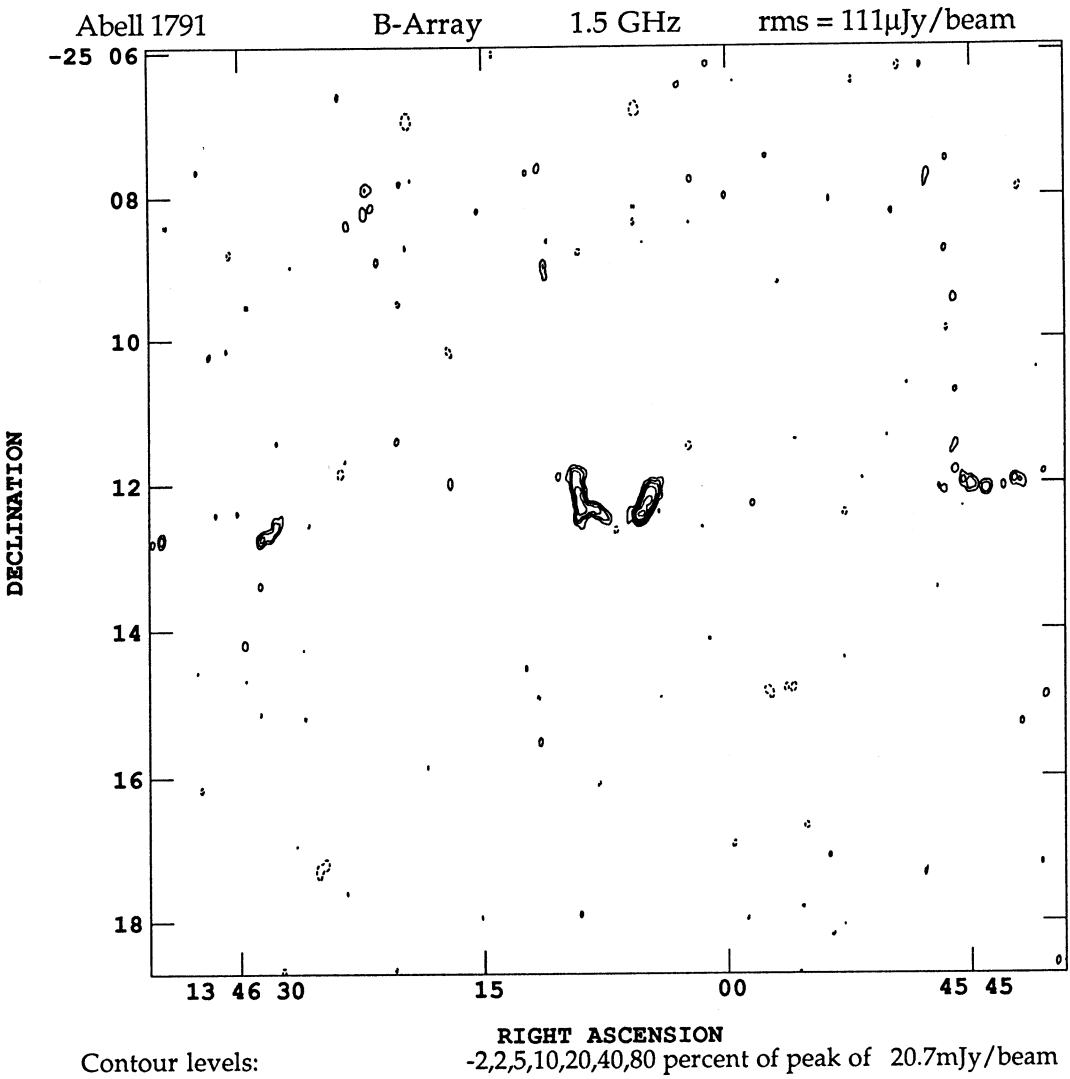


Contour levels: -2,2,5,10,20,40,80 percent of peak of 20.7mJy/beam

**Figure 42**

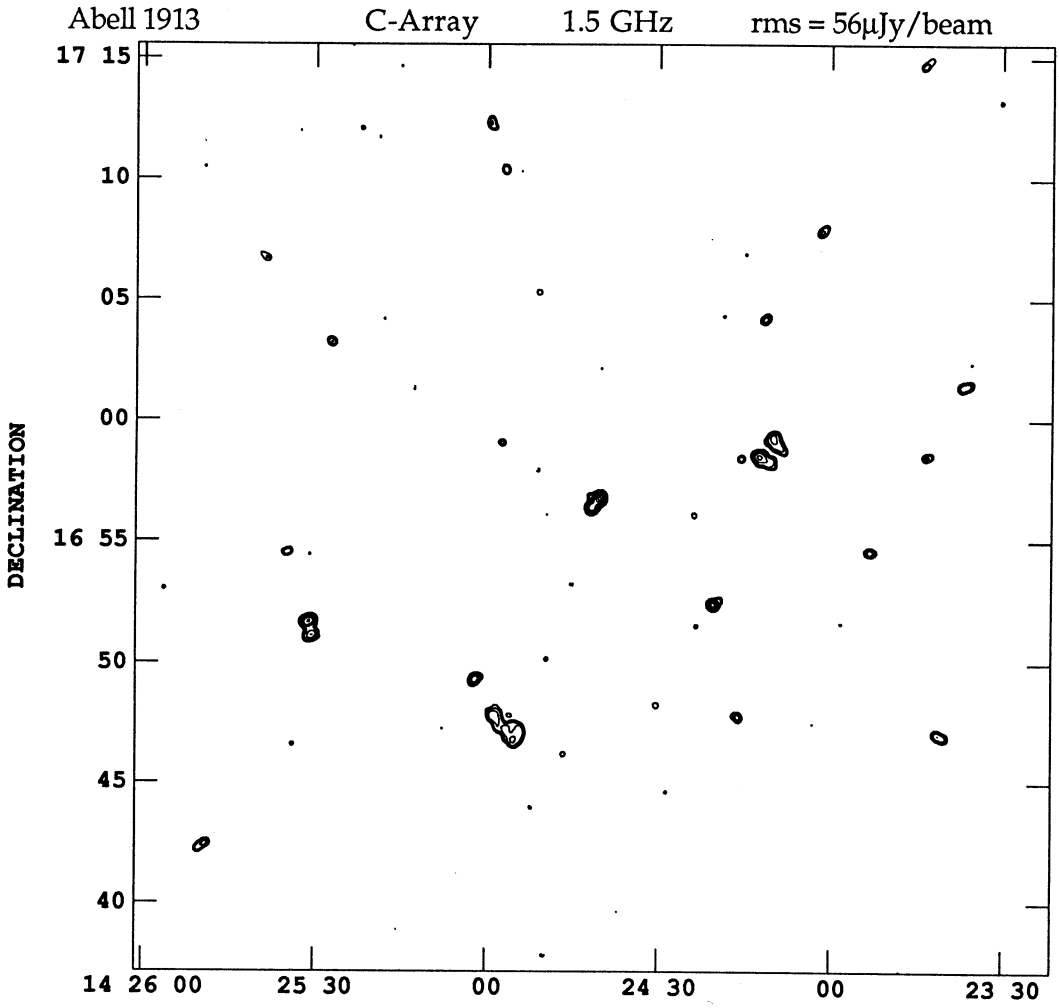


Contour levels: -0.5,0.5,1,2,5,10,20,40,80 percent of peak of 78.9mJy/beam

**Figure 43**

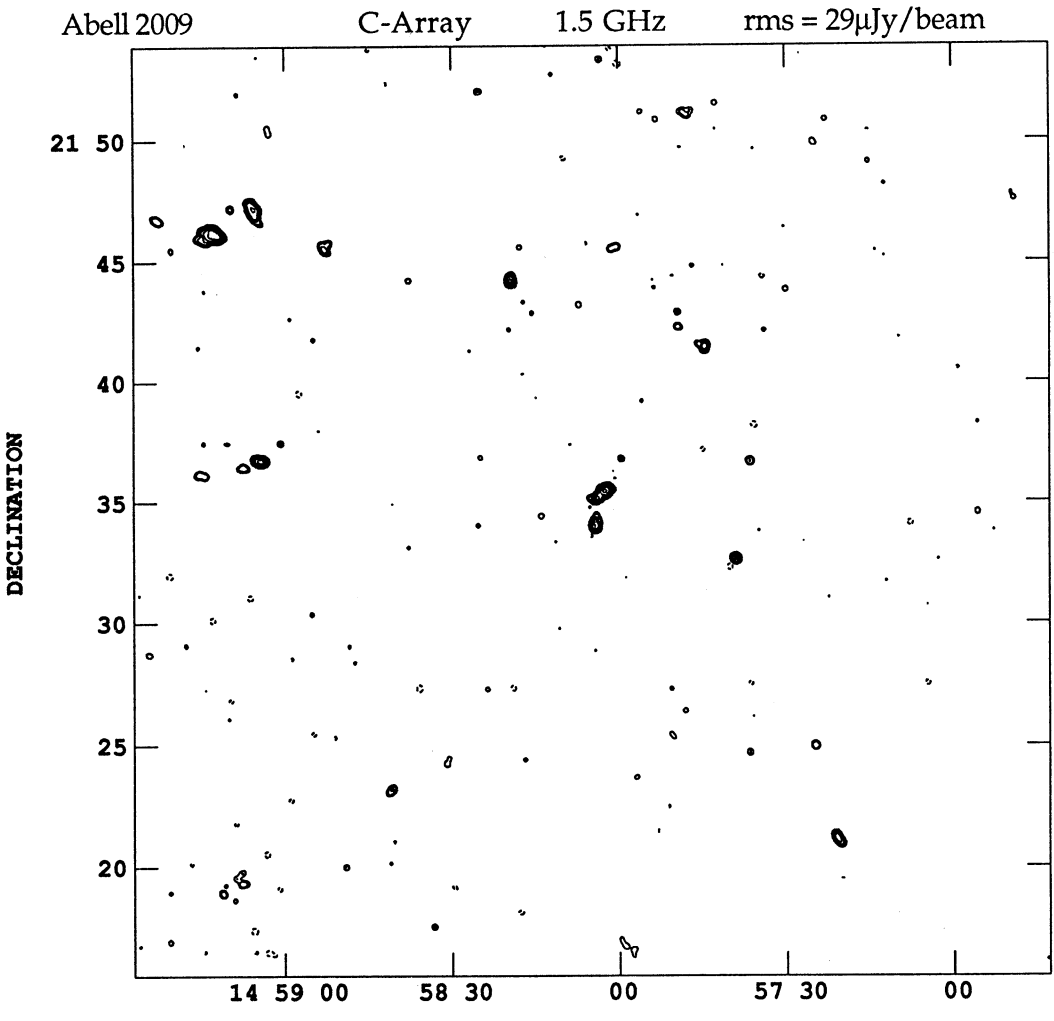


Contour levels: -1,1,2,5,10,20,40,80 percent of peak of 17.2mJy/beam

**Figure 44**

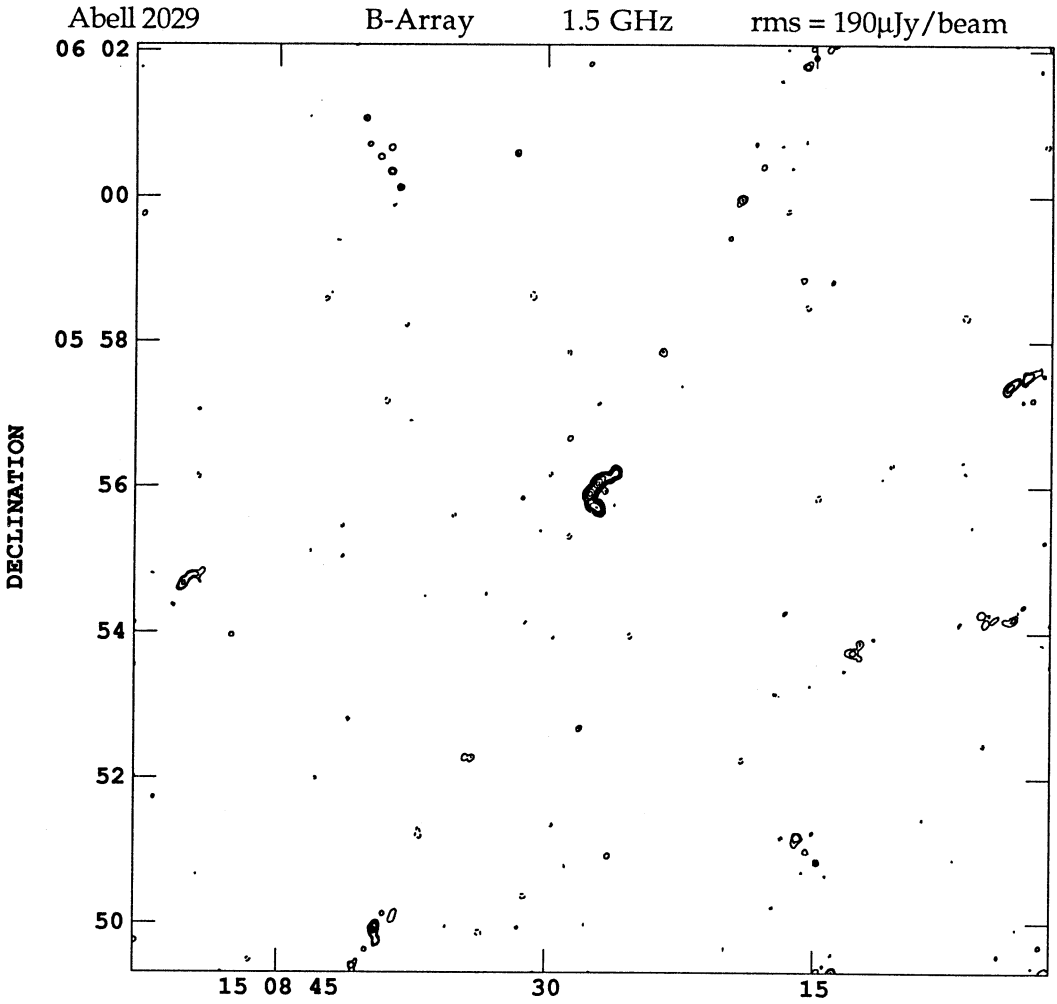


Contour levels: -1,1,2,5,10,20,40,80 percent of peak of 80.7mJy/beam

**Figure 45**

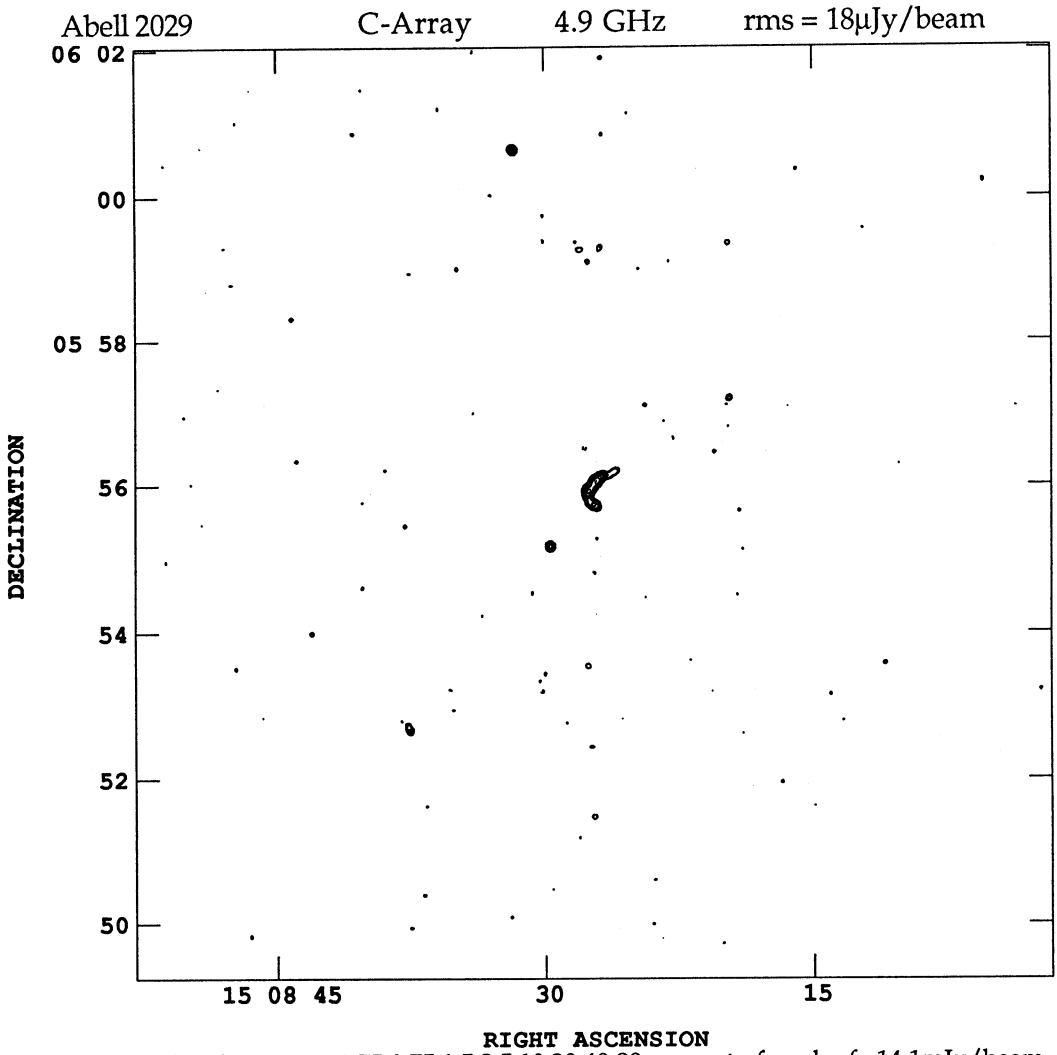


Contour levels: -0.75,0.75,1.5,3,5,10,20,40,80 percent of peak of 14.1mJy/beam

**Figure 46**

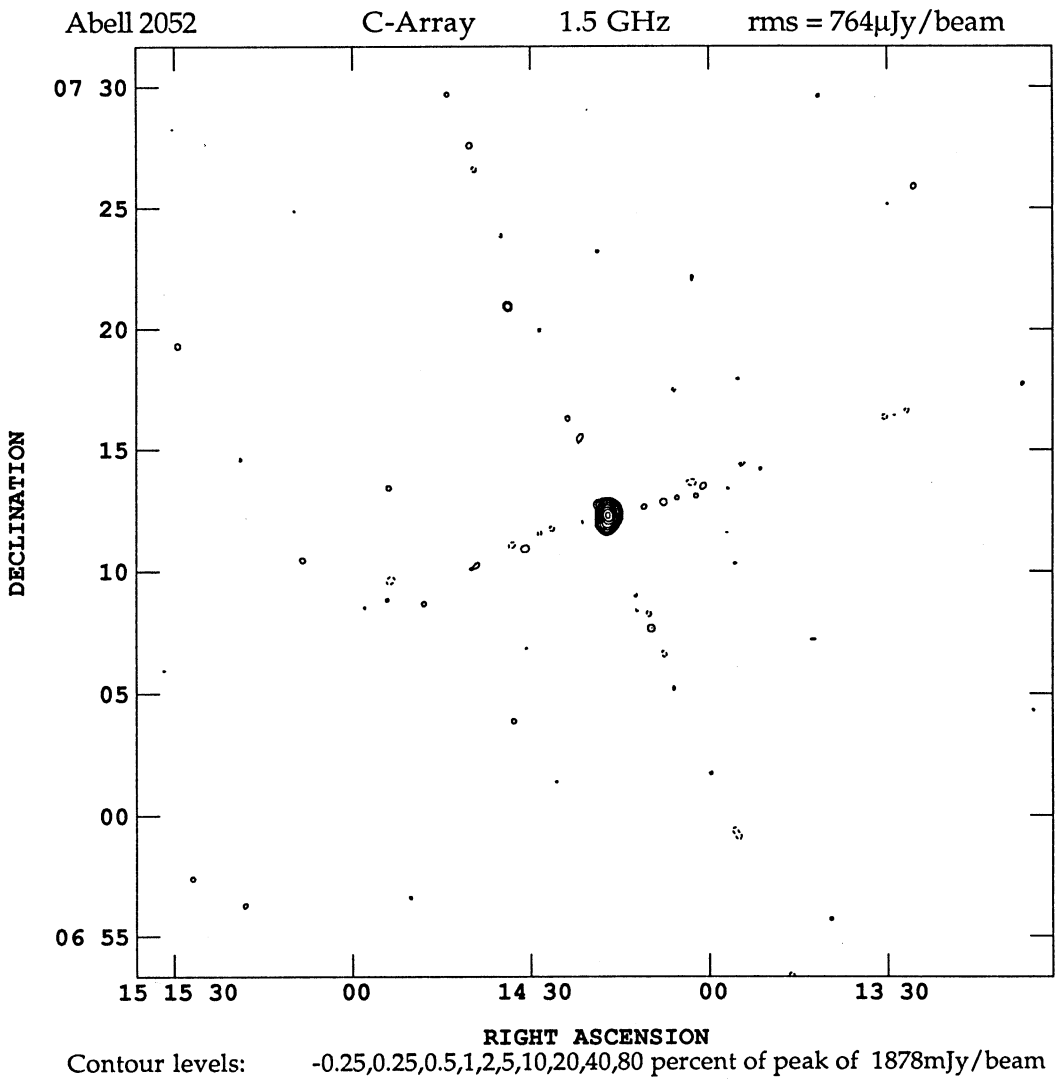
Abell 2052
C-Array
1.5 GHz
rms = 764μJy/beam
07 30
25
20
15
10
05
00
06 55
DECLINATION
15 15 30
00
14 30
00
13 30
RIGHT ASCENSION
Contour levels: -0.25,0.25,0.5,1,2,5,10,20,40,80 percent of peak of 1878mJy/beam

**Figure 47**

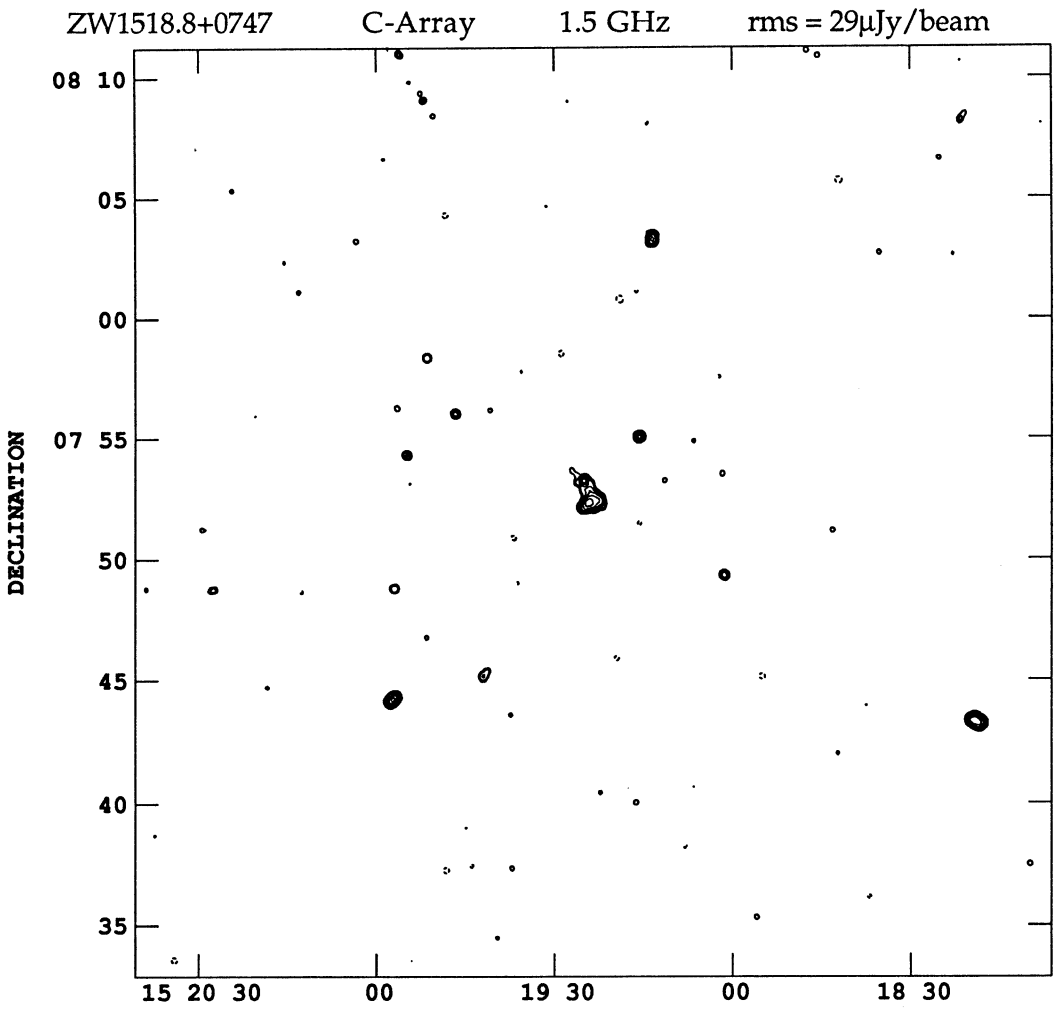


Contour levels: -1,1,2,5,10,20,40,80 percent of peak of 25.2mJy/beam

**Figure 48**

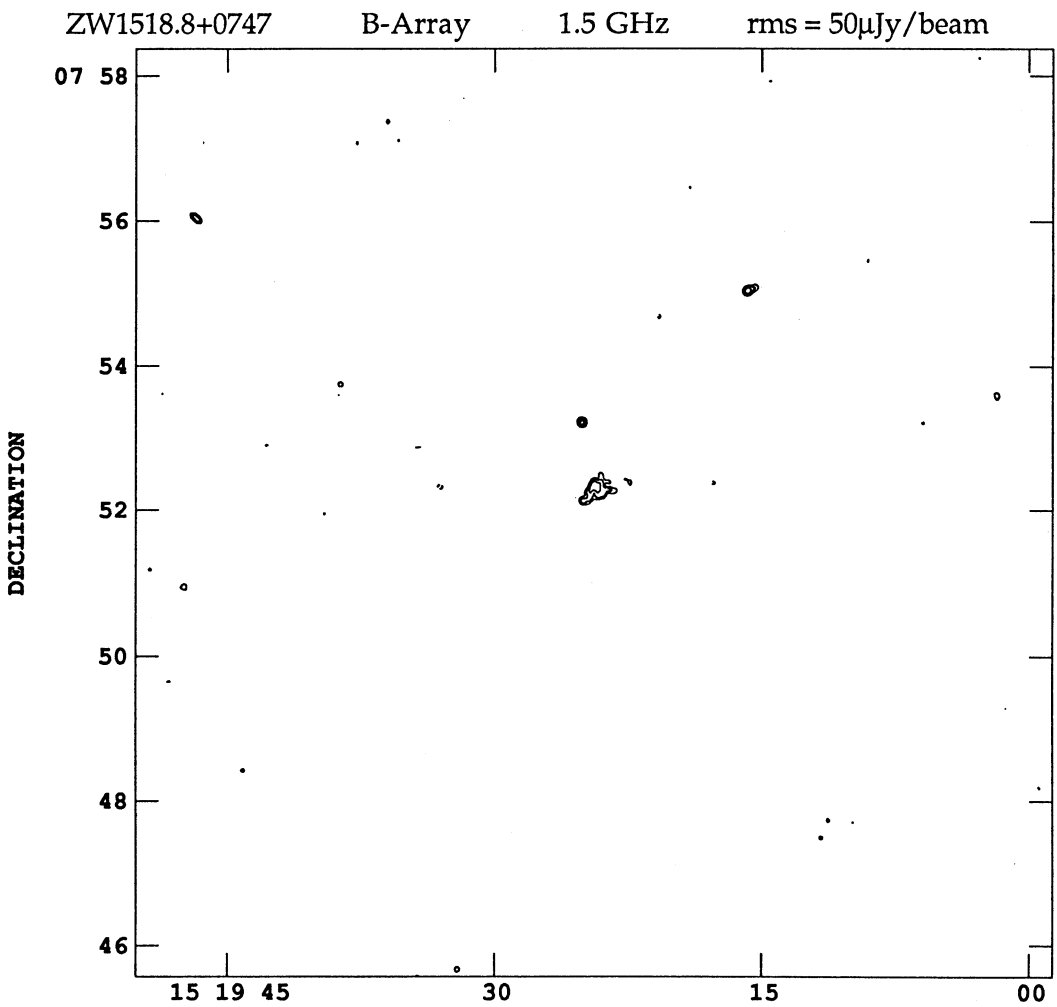


Contour levels: -5,5,10,20,40,80 percent of peak of 7.3mJy/beam

**Figure 49**

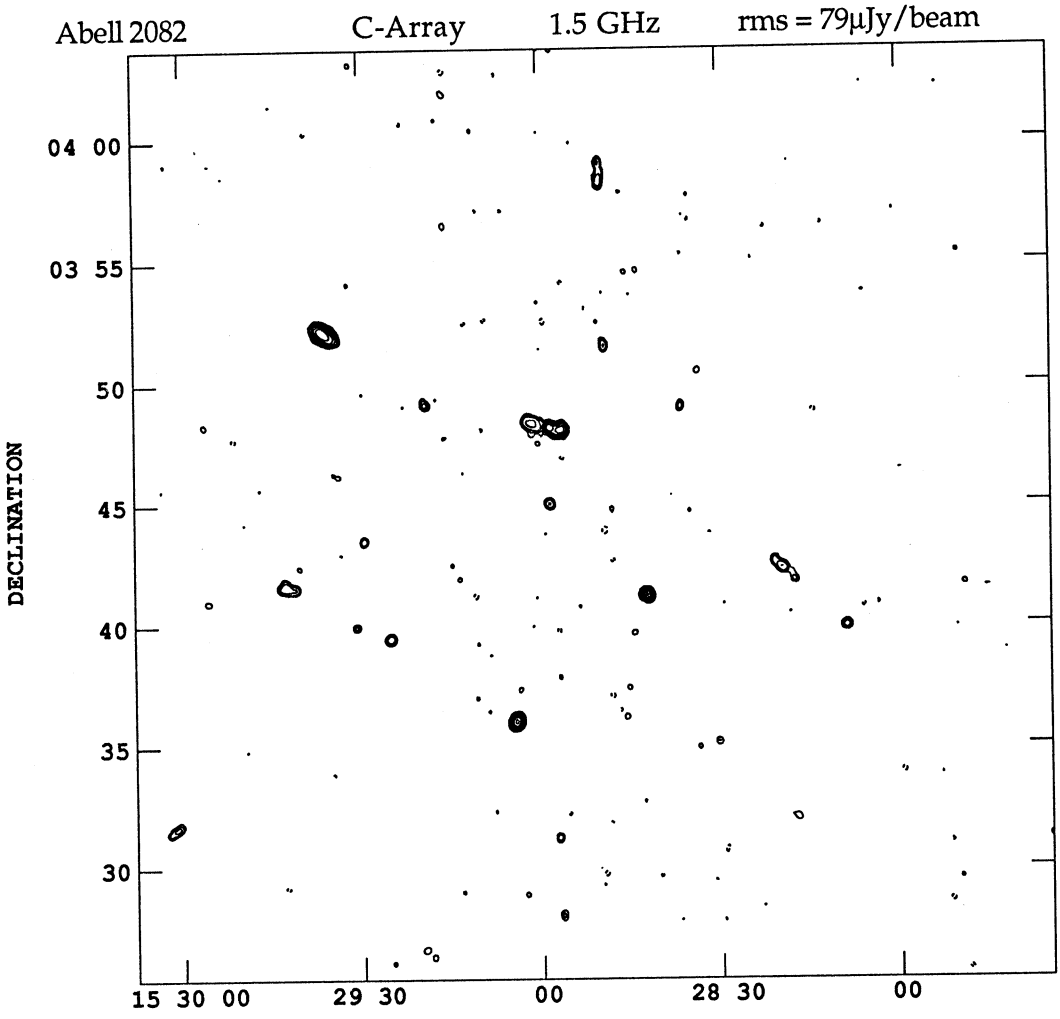


Contour levels: -0.5,0.5,1,2,5,10,20,40,80 percent of peak of 83.2mJy/beam

**Figure 50**

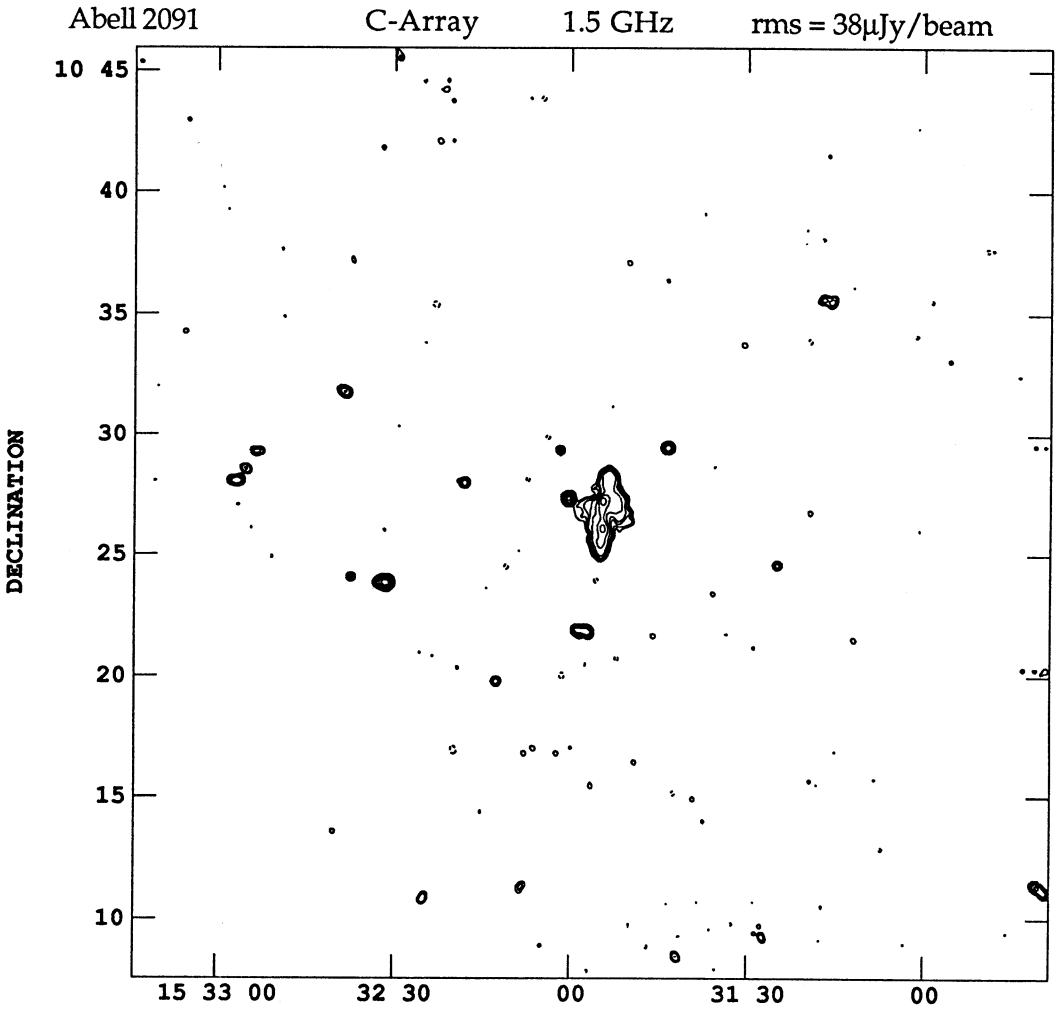


Contour levels: -0.75,0.75,1.5,3,5,10,20,40,80 percent of peak of 32.8mJy/beam

**Figure 51**

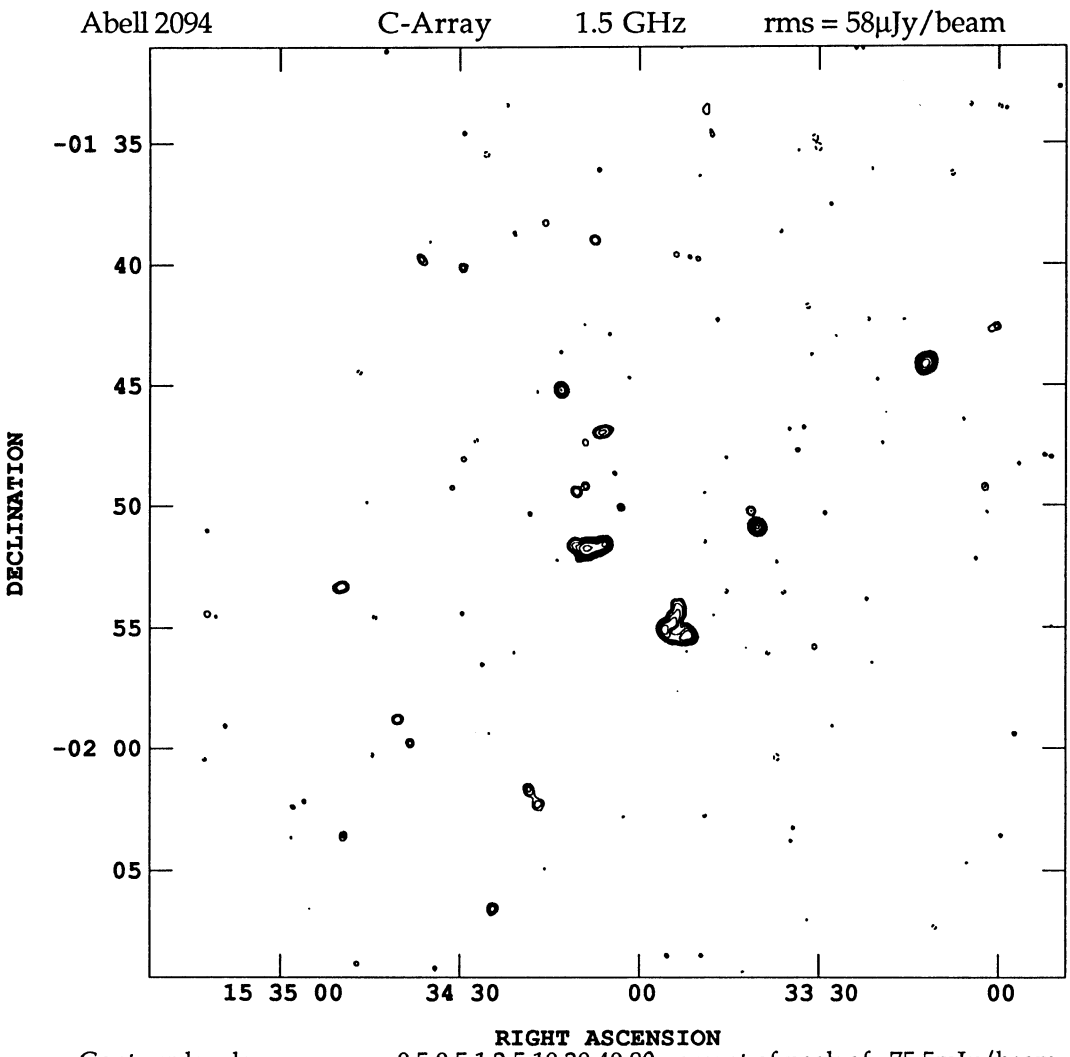


Contour levels: -0.5,0.5,1,2,5,10,20,40,80 percent of peak of 75.5mJy/beam

**Figure 52**

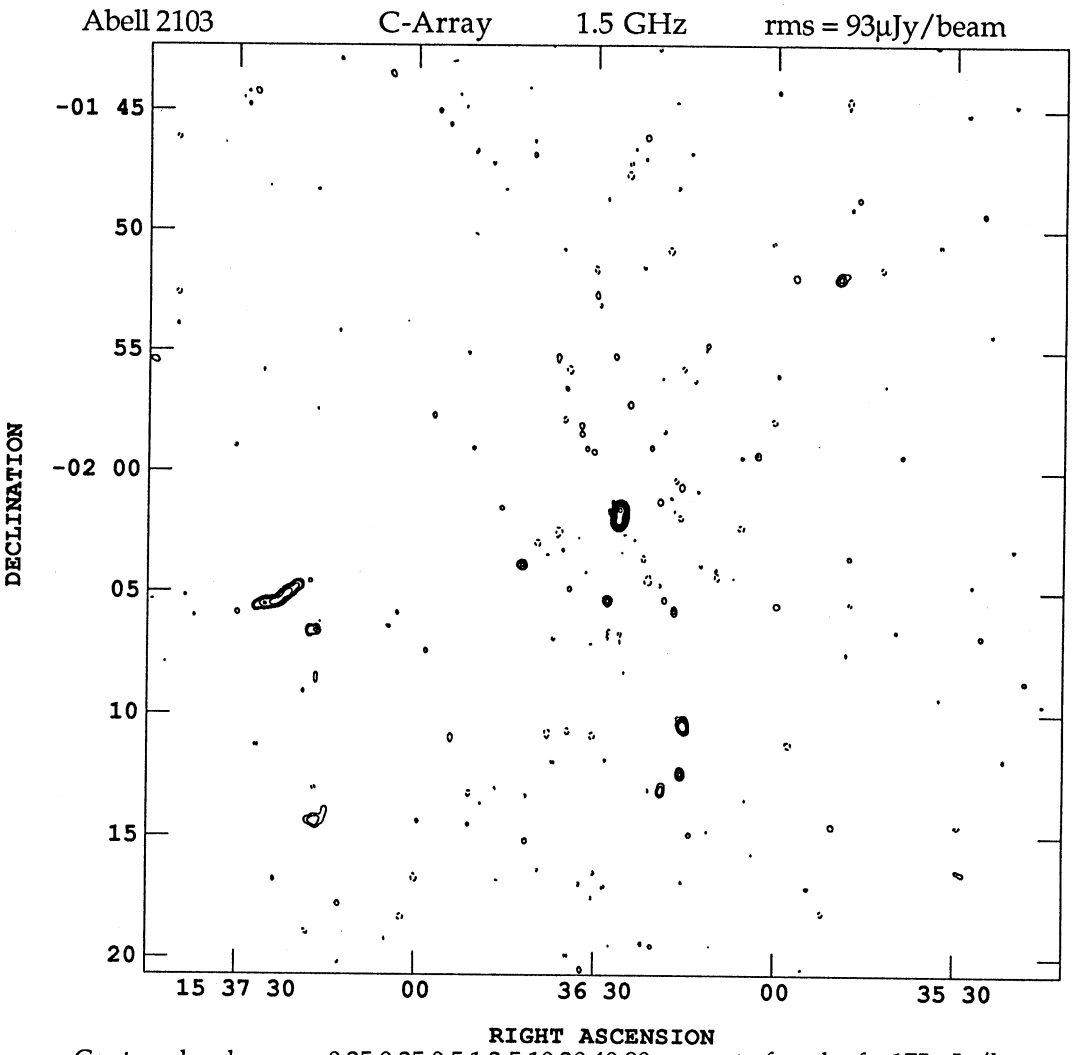


Contour levels: -0.25,0.25,0.5,1,2,5,10,20,40,80 percent of peak of 175mJy/beam

**Figure 53**

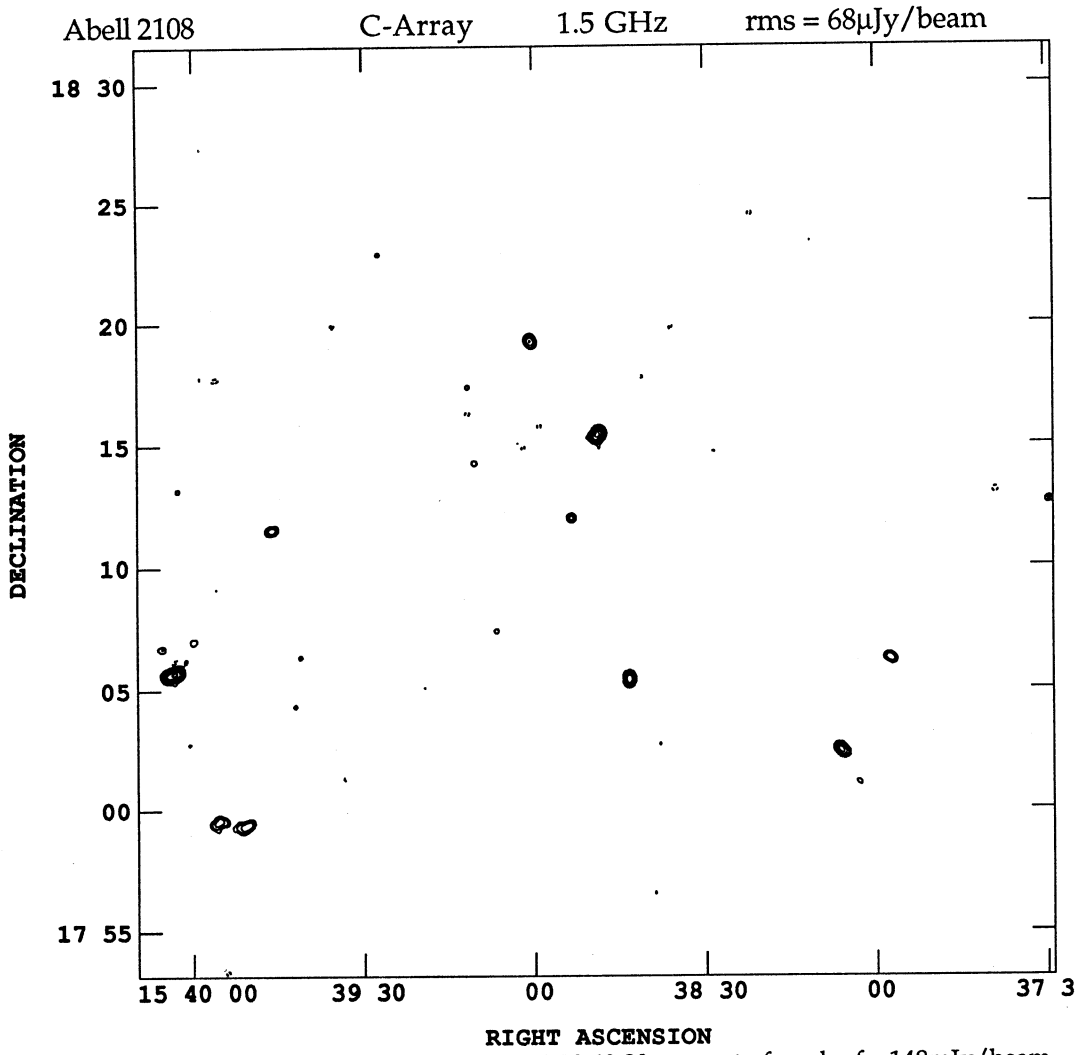


Contour levels: -0.5,0.5,1,2,5,10,20,40,80 percent of peak of 148mJy/beam

**Figure 54**

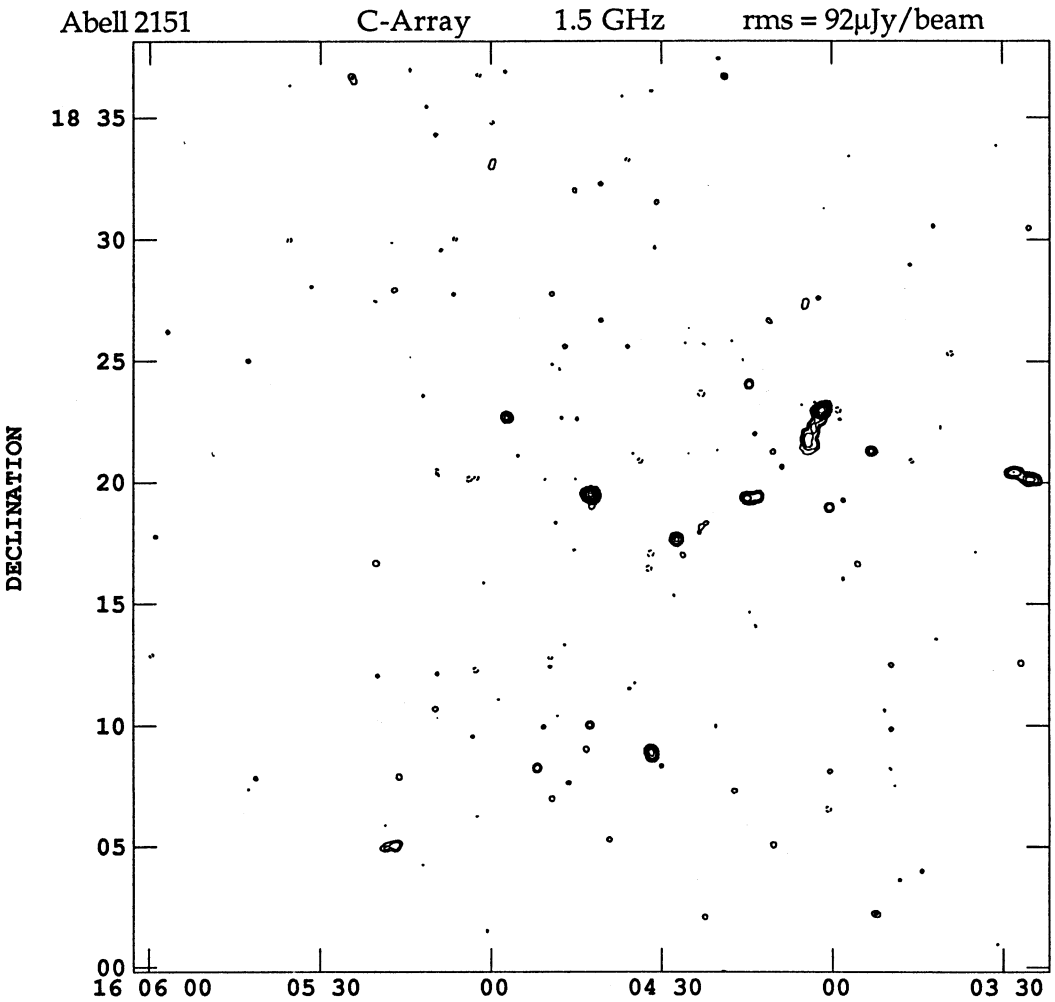


Contour levels: -0.25,0.25,0.5,1,2,5,10,20,40,80 percent of peak of 205mJy/beam

**Figure 55**

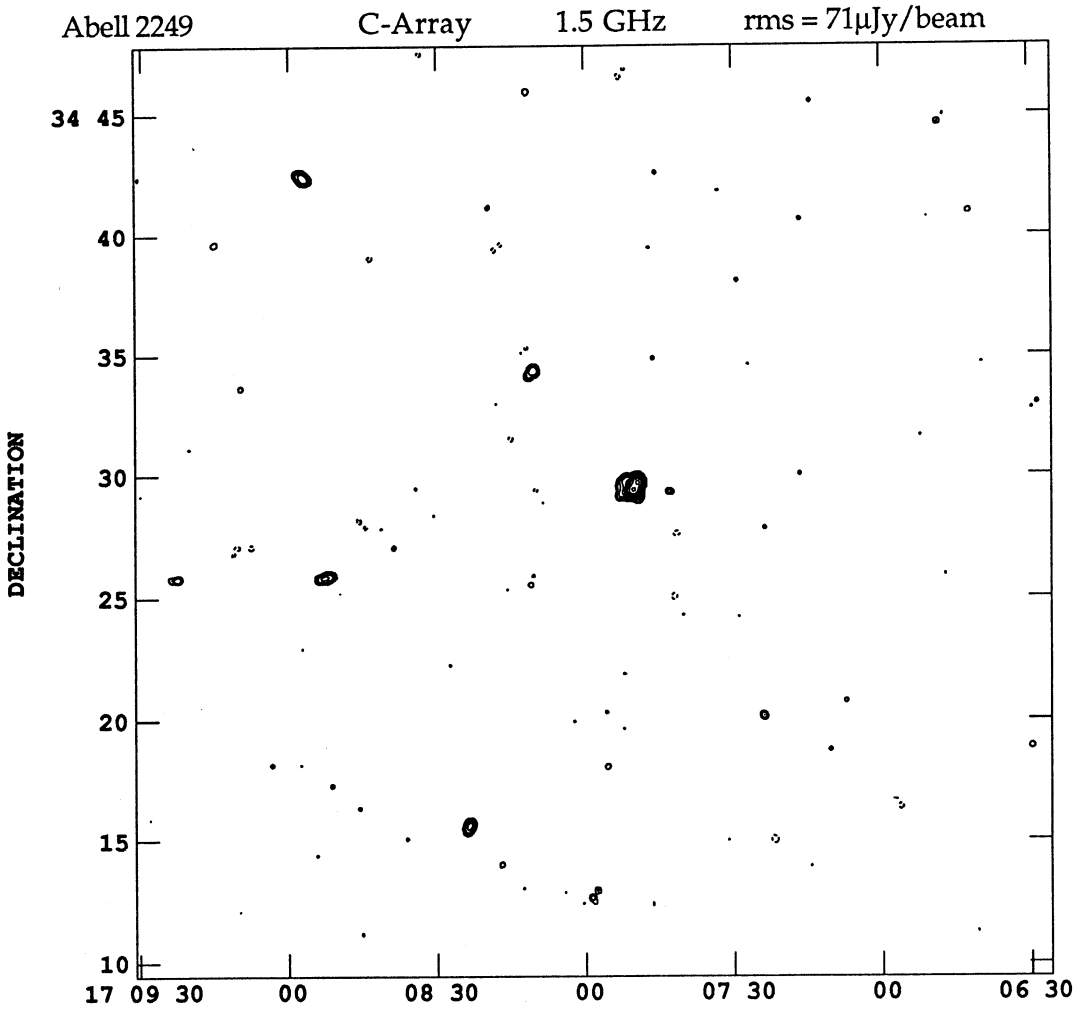


Contour levels: -0.25,0.25,0.5,1,2,5,10,20,40,80 percent of peak of 176mJy/beam

**Figure 56**

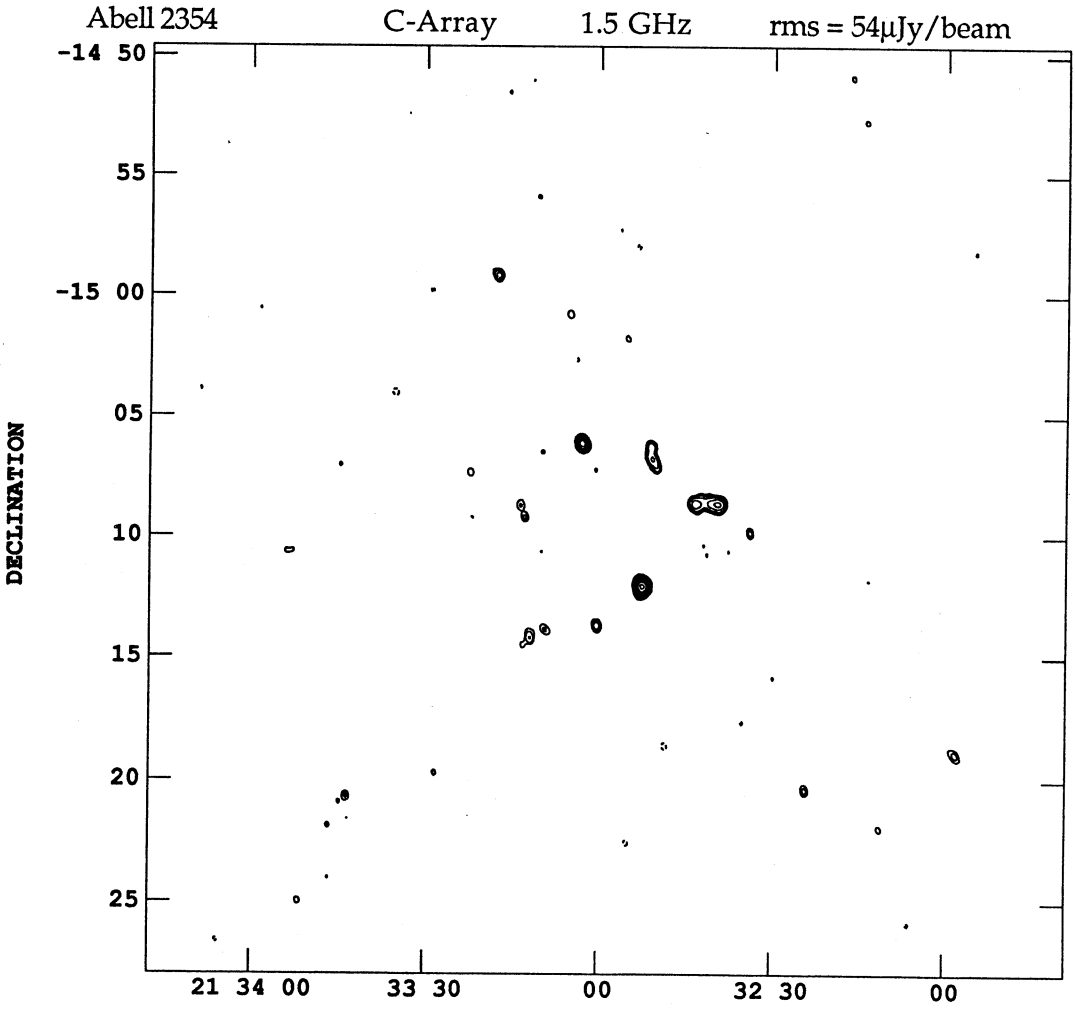


Contour levels: -0.5,0.5,1,2,5,10,20,40,80 percent of peak of 77.6mJy/beam

**Figure 57**

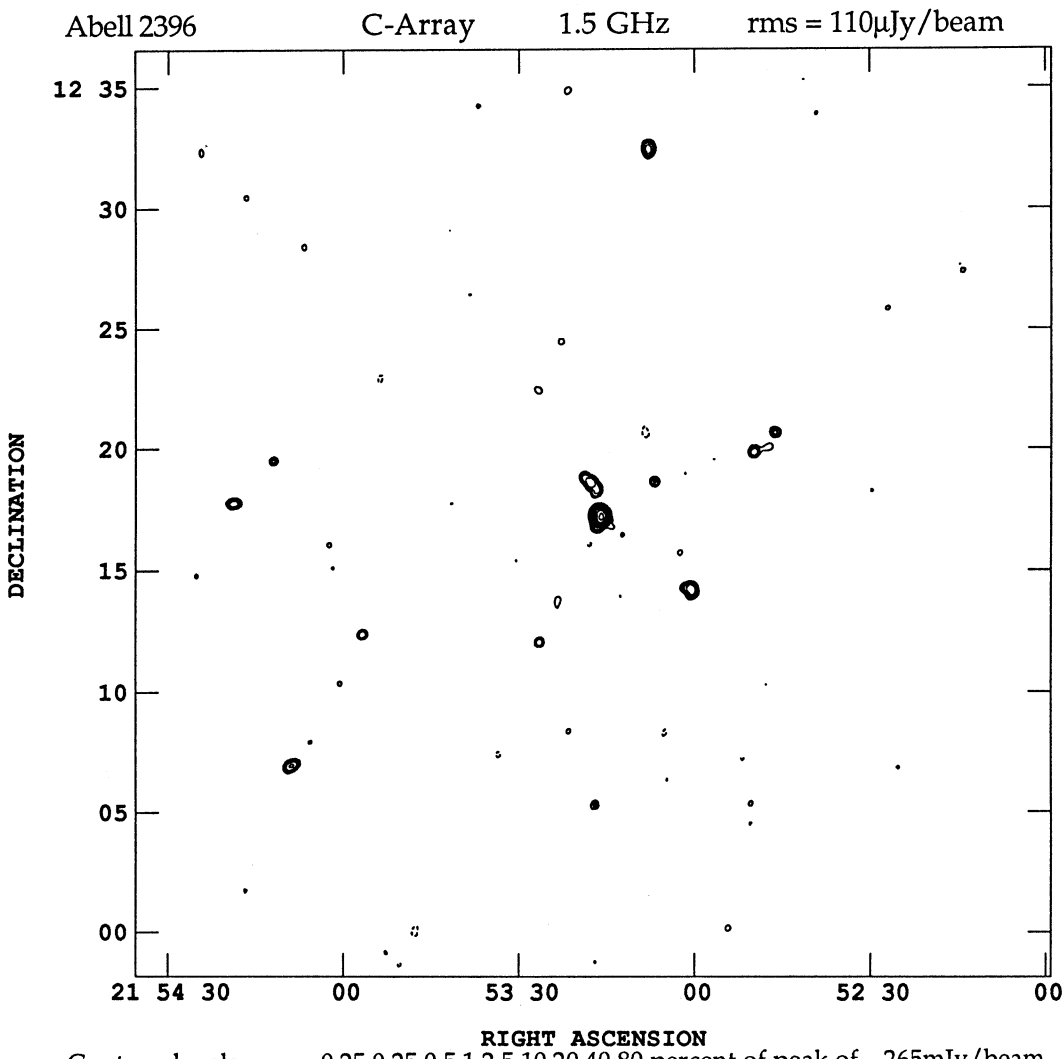


Contour levels: -0.25,0.25,0.5,1,2,5,10,20,40,80 percent of peak of 265mJy/beam

**Figure 58**

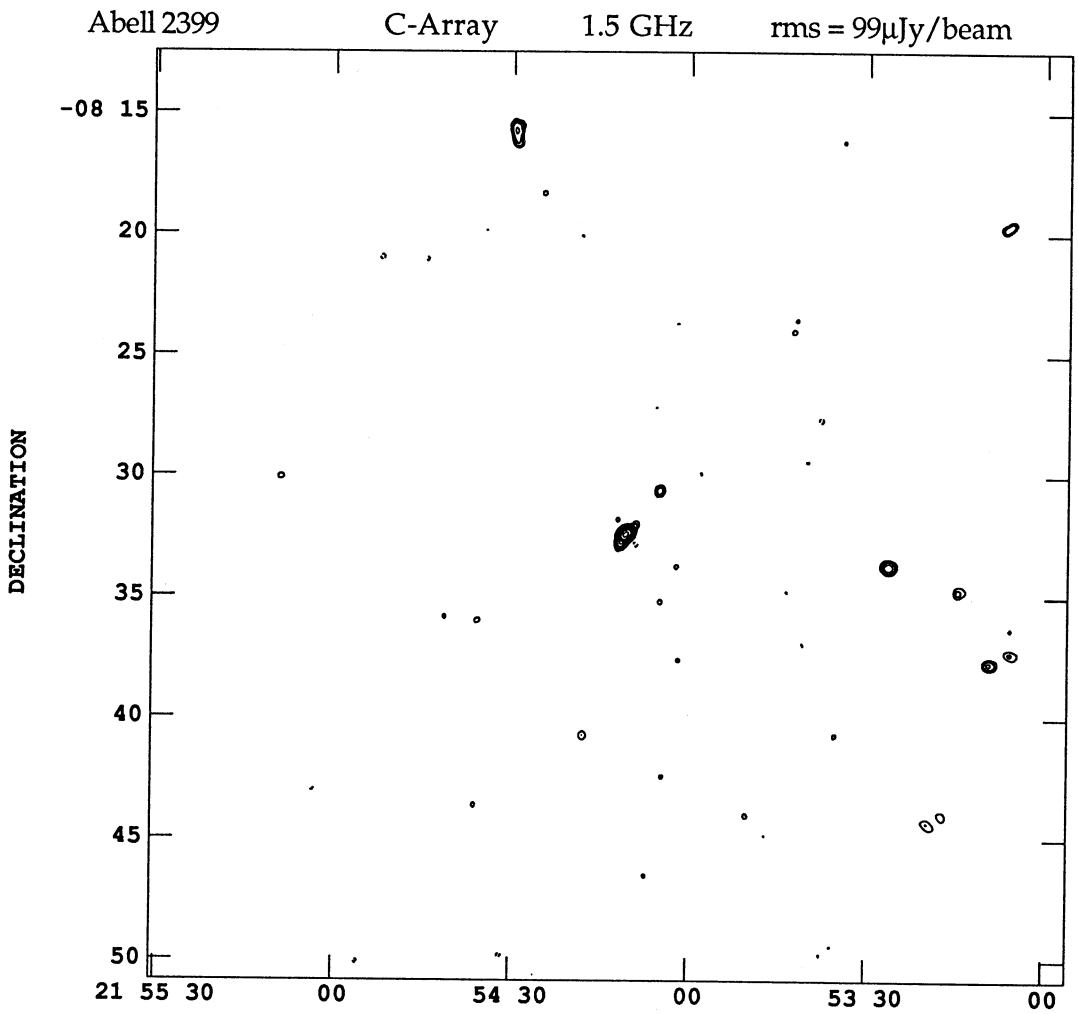


Contour levels: -0.5,0.5,1,2,5,10,20,40,80 percent of peak of 114mJy/beam

**Figure 59**

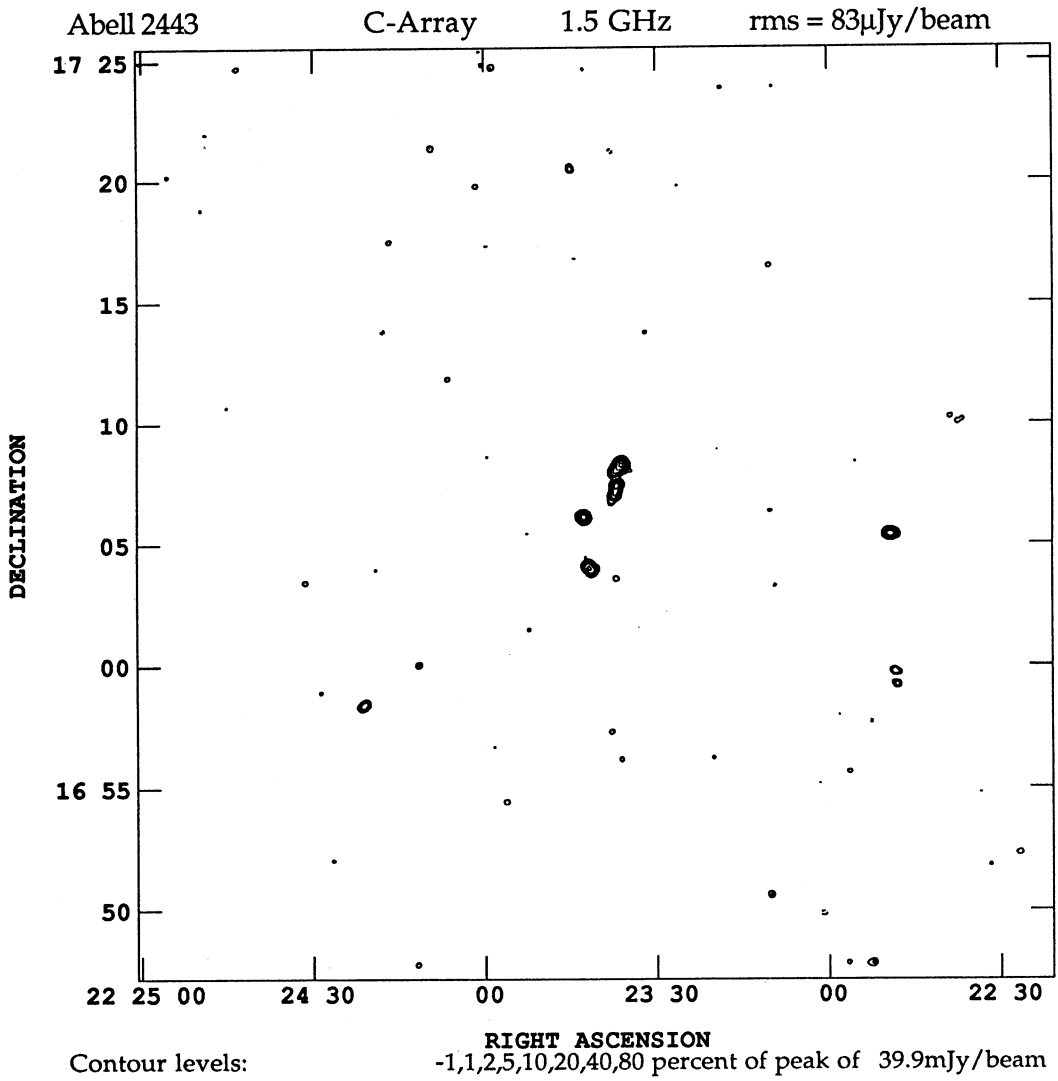
Abell 2443
C-Array
1.5 GHz
rms = 83μJy/beam
17 25
20
15
10
05
00
16 55
50
DECLINATION
22 25 00
24 30
00
23 30
00
22 30
RIGHT ASCENSION
Contour levels:
-1,1,2,5,10,20,40,80 percent of peak of 39.9mJy/beam

**Figure 60**

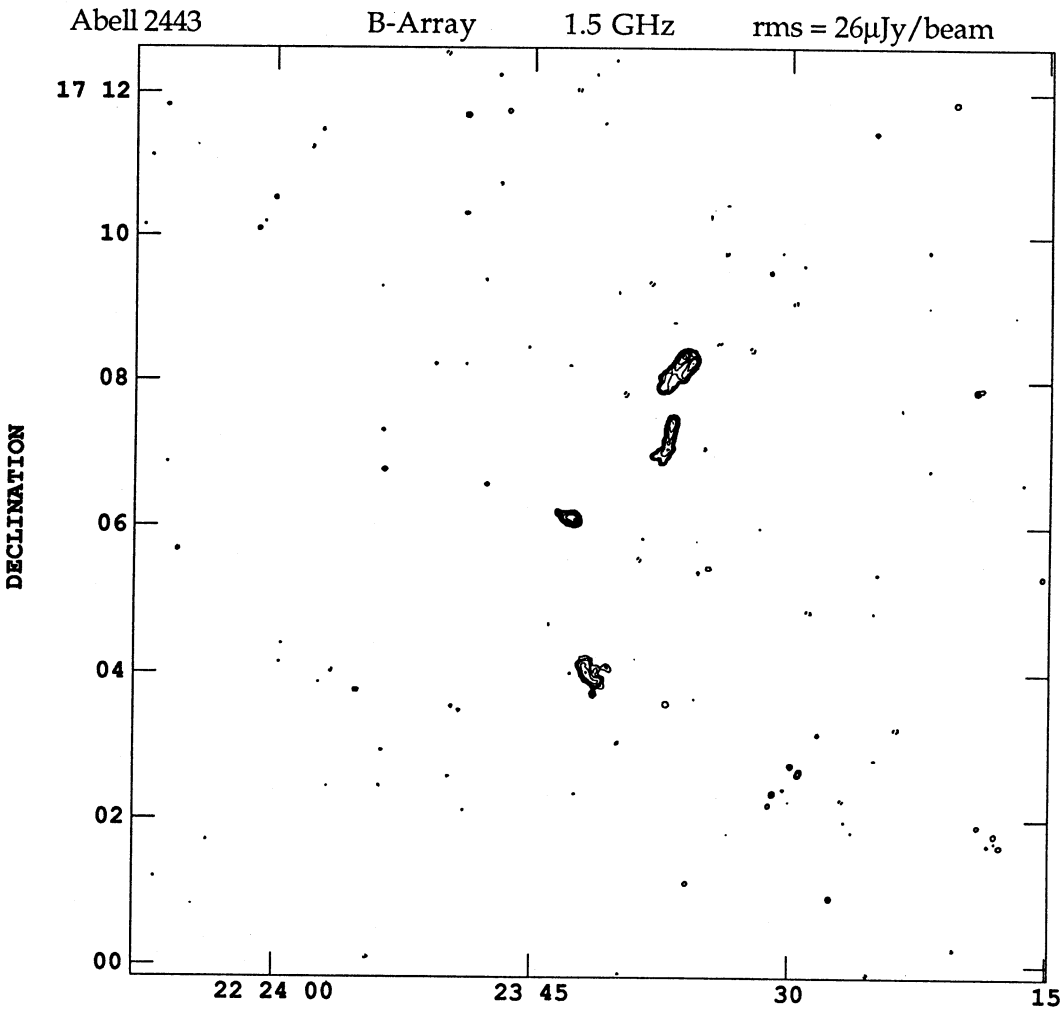


Contour levels: -1.5,1.5,3,5,10,20,40,80 percent of peak of 10.6mJy/beam

**Figure 61**

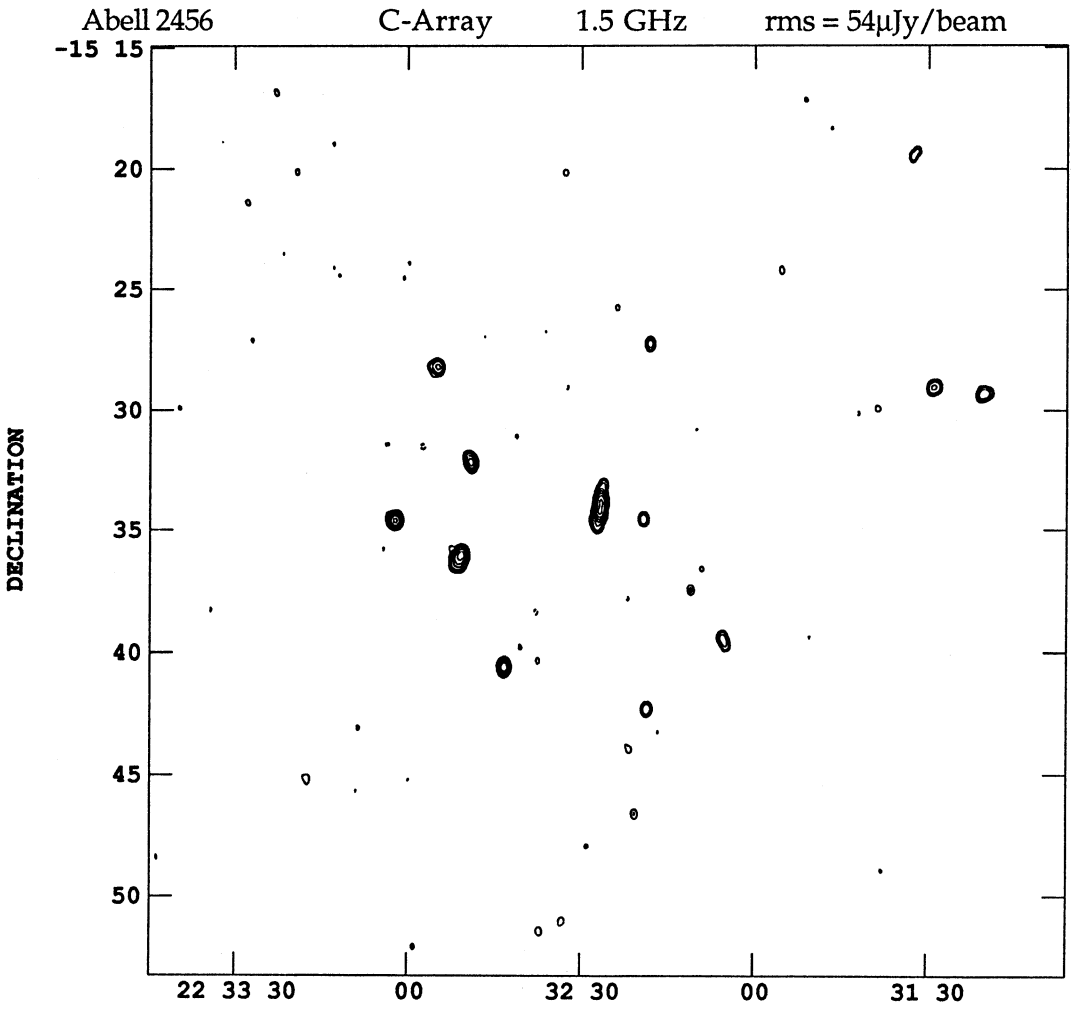


Contour levels: -0.5,0.5,1,2,5,10,20,40,80 percent of peak of 109mJy/beam

**Figure 62**

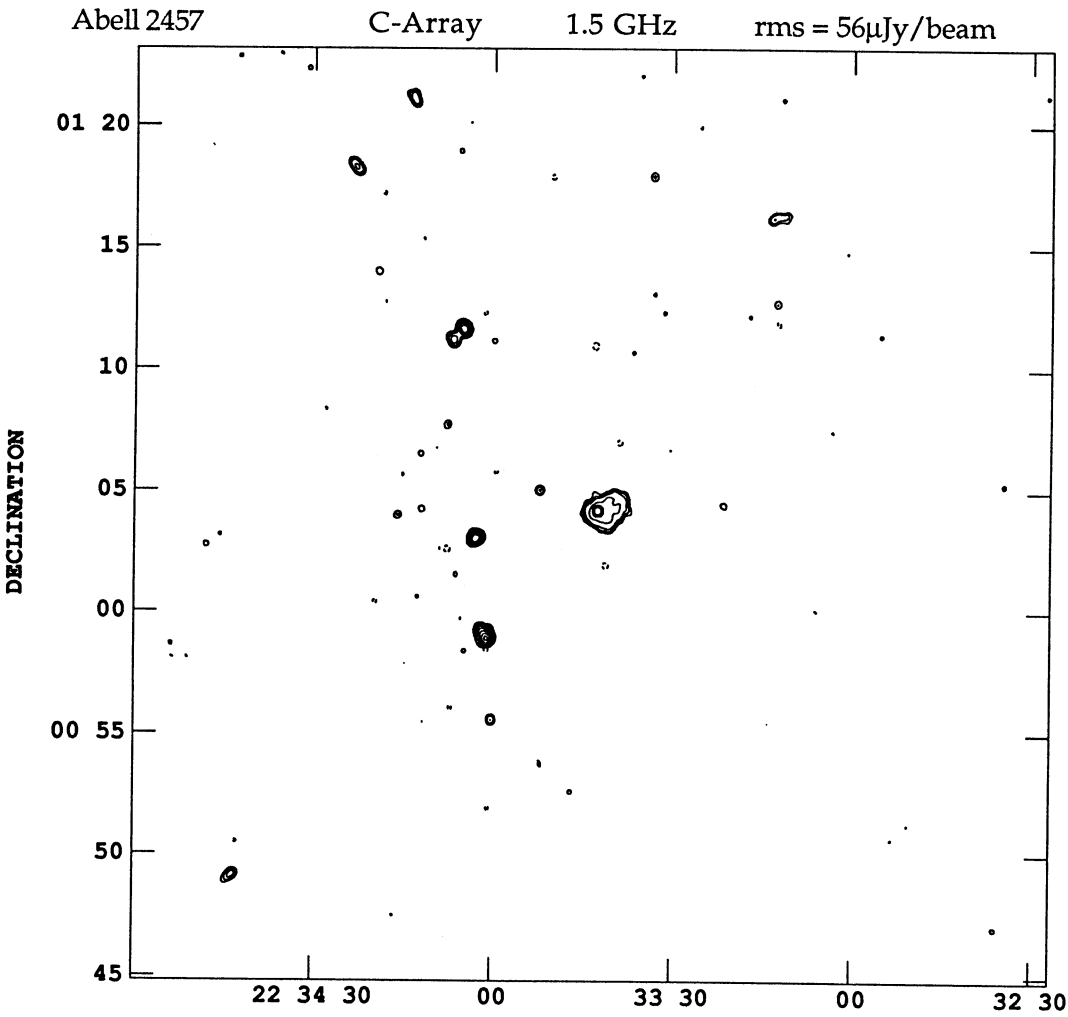


Contour levels: -0.5,0.5,1,2,5,10,20,40,80 percent of peak of 84mJy/beam

**Figure 63**

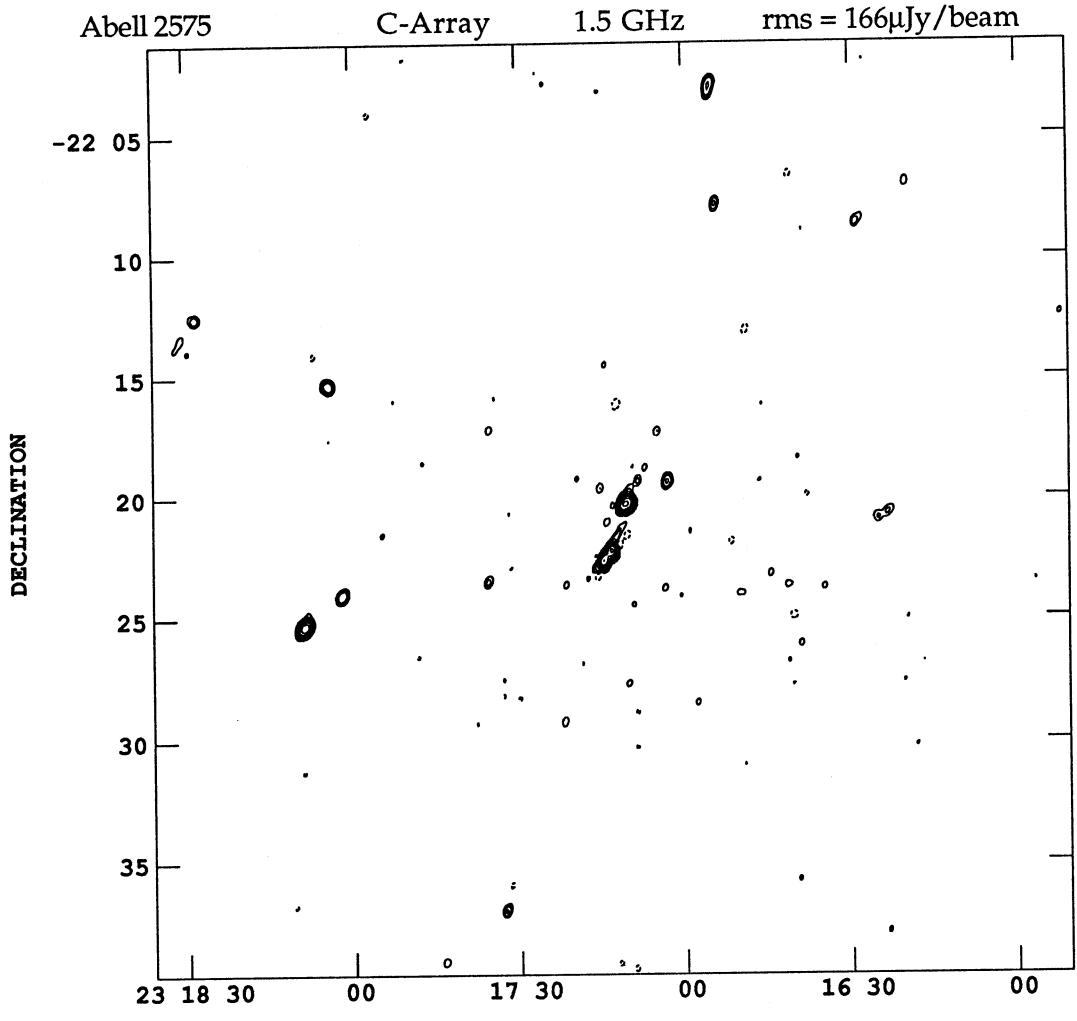


Contour levels: -0.5,0.5,1,2,5,10,20,40,80 percent of peak of 186mJy/beam

**Figure 64**

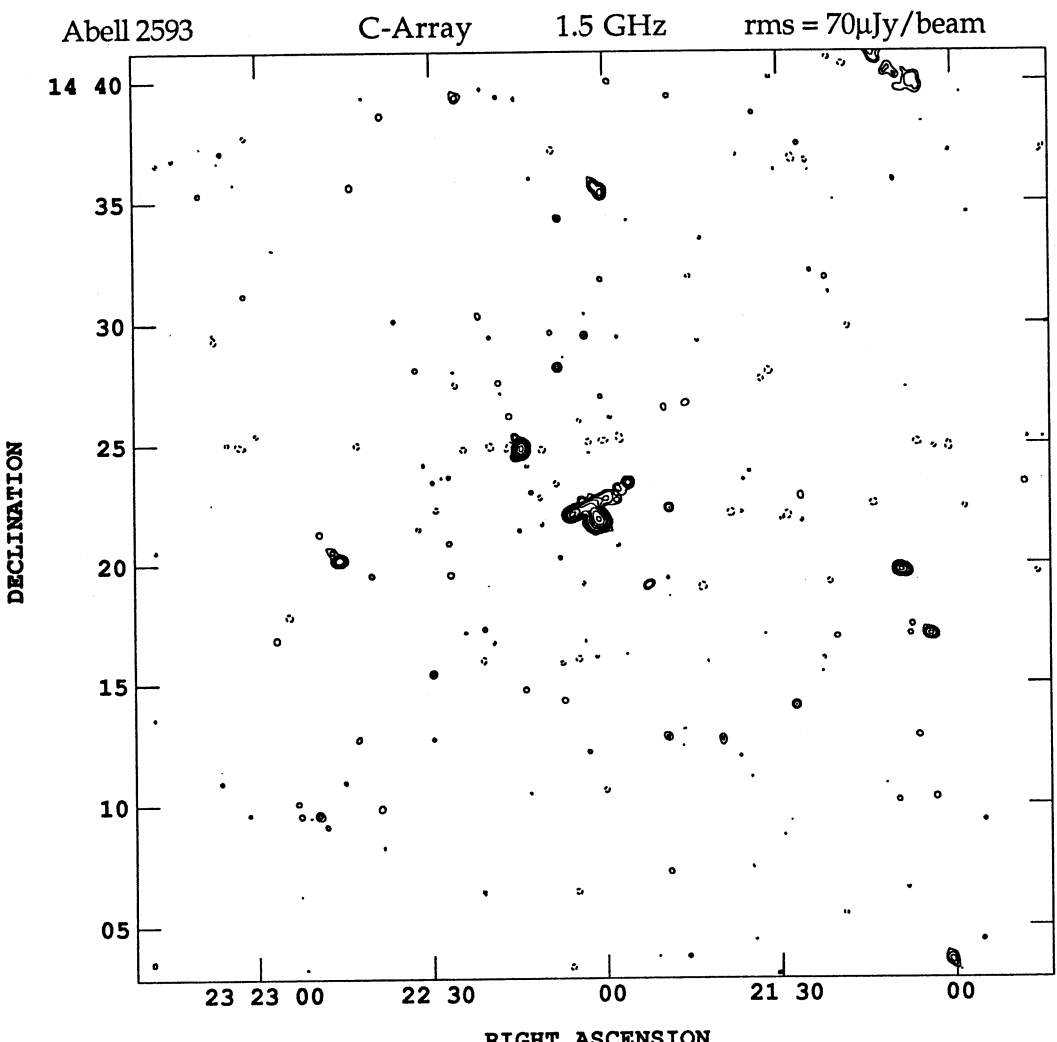


Contour levels: -0.25,0.25,0.5,1,2,5,10,20,40,80 percent of peak of 132mJy/beam

**Figure 65**

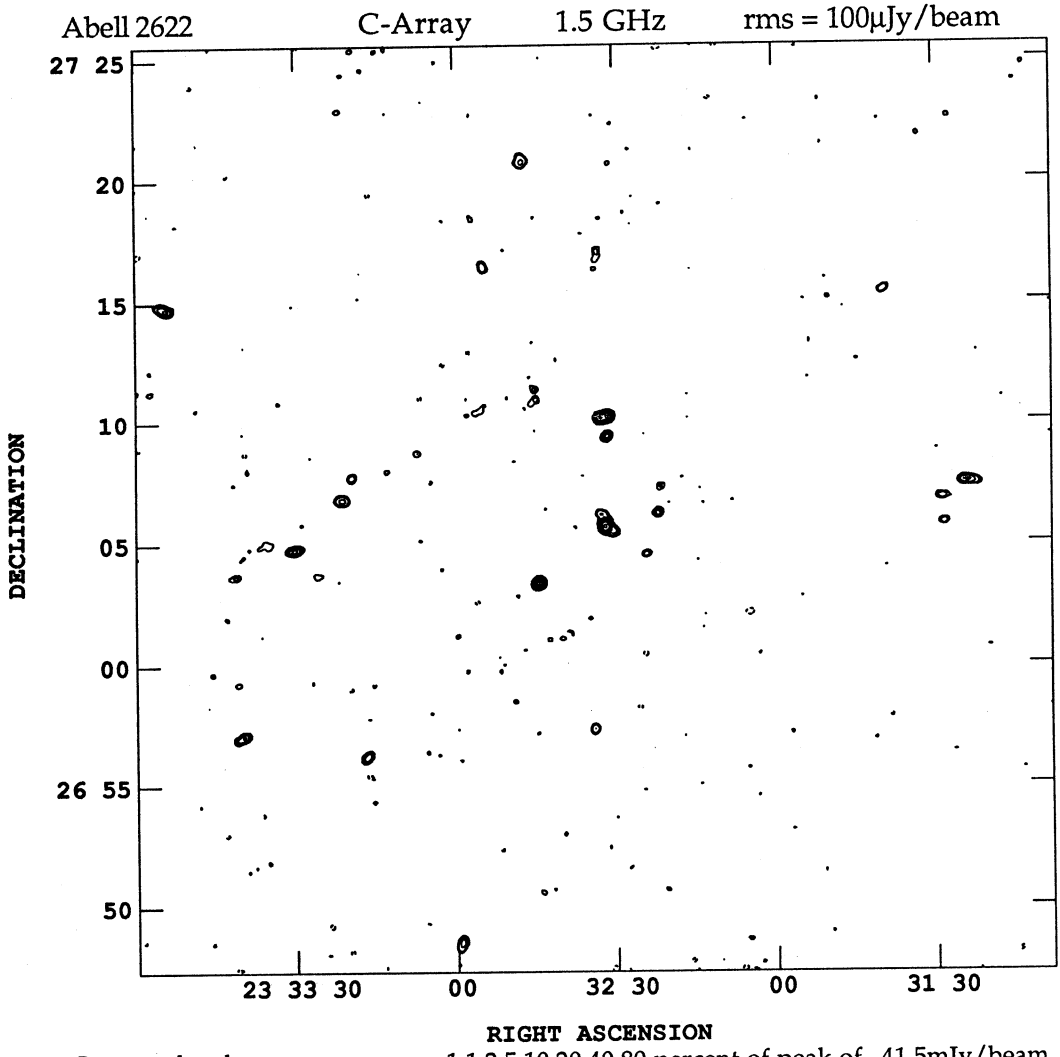


Contour levels: -1,1,2,5,10,20,40,80 percent of peak of 41.5mJy/beam

**Figure 66**

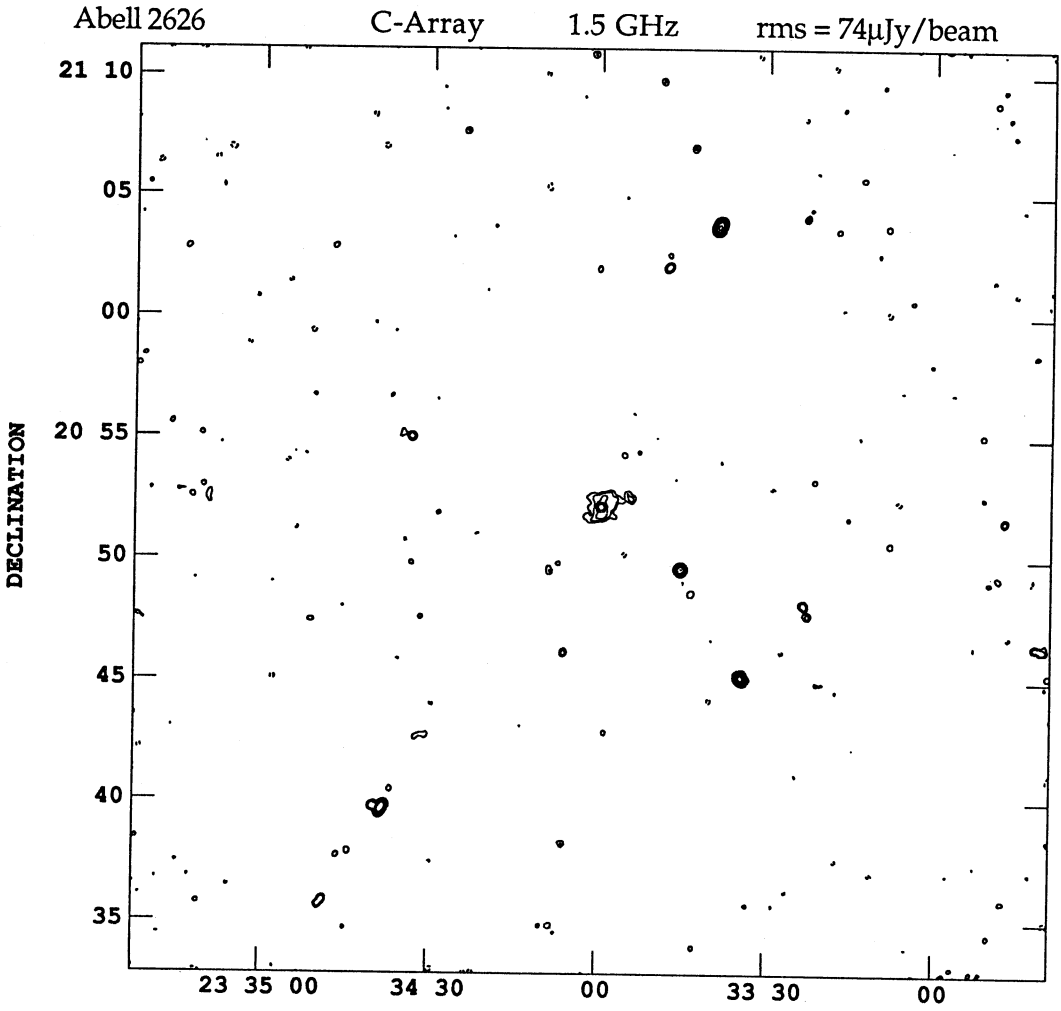


Contour levels: -1,1,2,5,10,20,40,80 percent of peak of 35.1mJy/beam

**Figure 67**

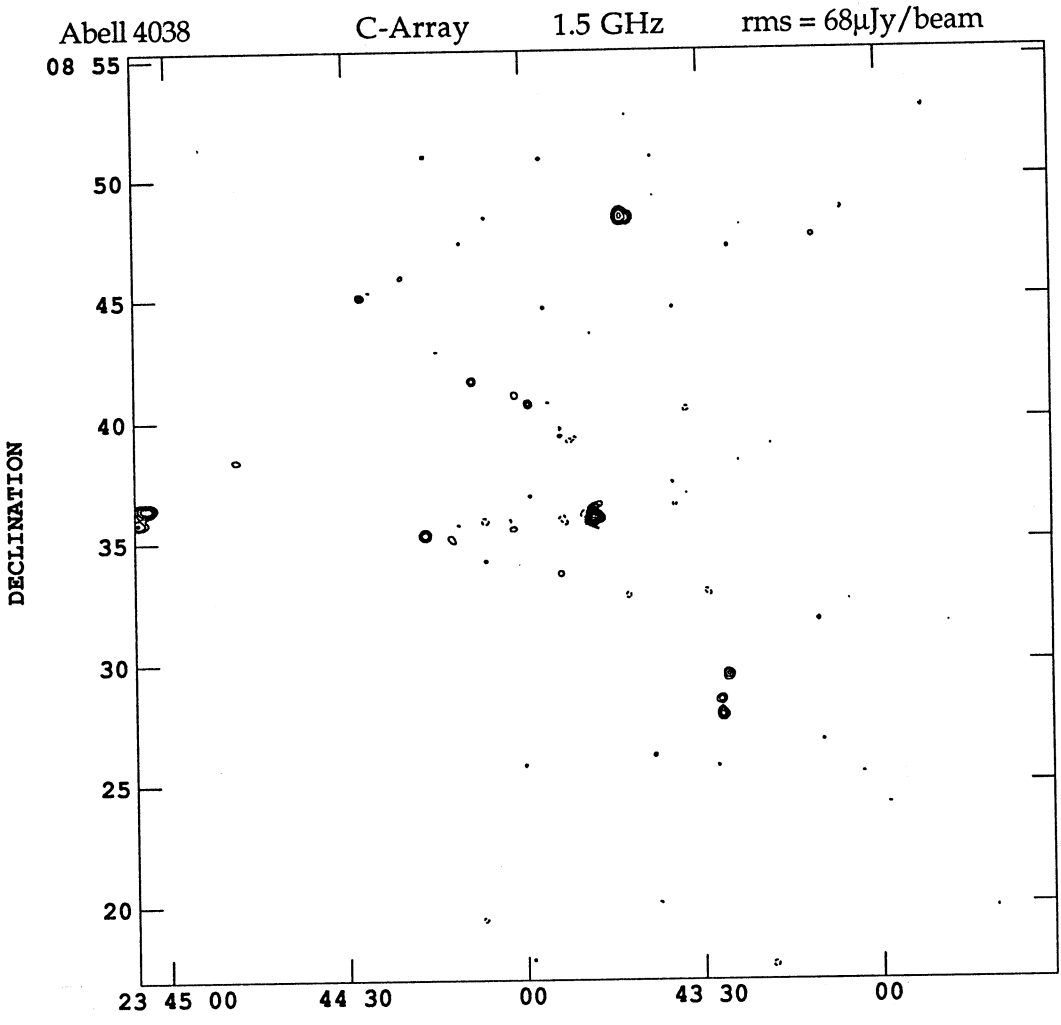


Contour levels: -0.25,0.25,0.5,1,2,5,10,20,40,80 percent of peak of 302mJy/beam

**Figure 68**

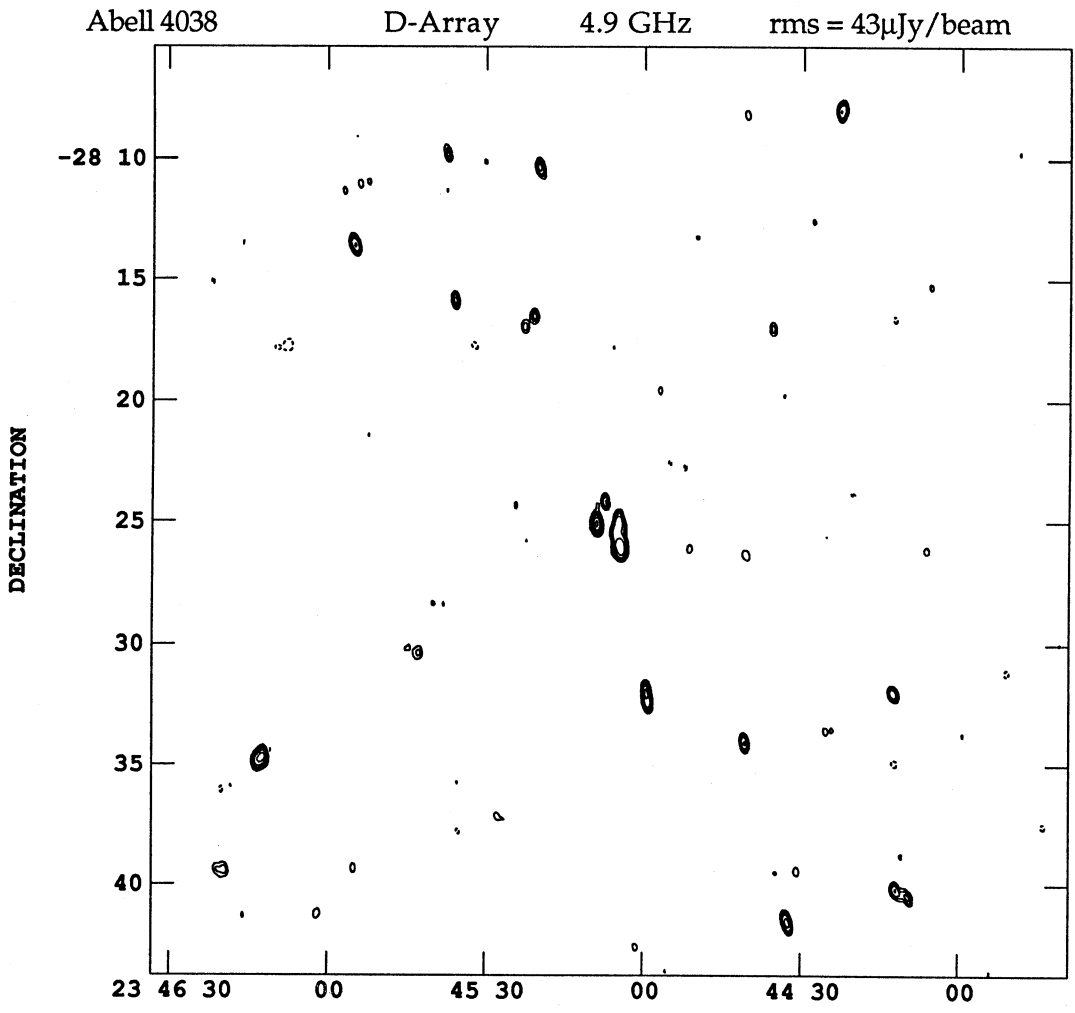


Contour levels: -2,2,4,6,10,20,40,80 percent of peak of 19.8mJy/beam

**Figure 69**

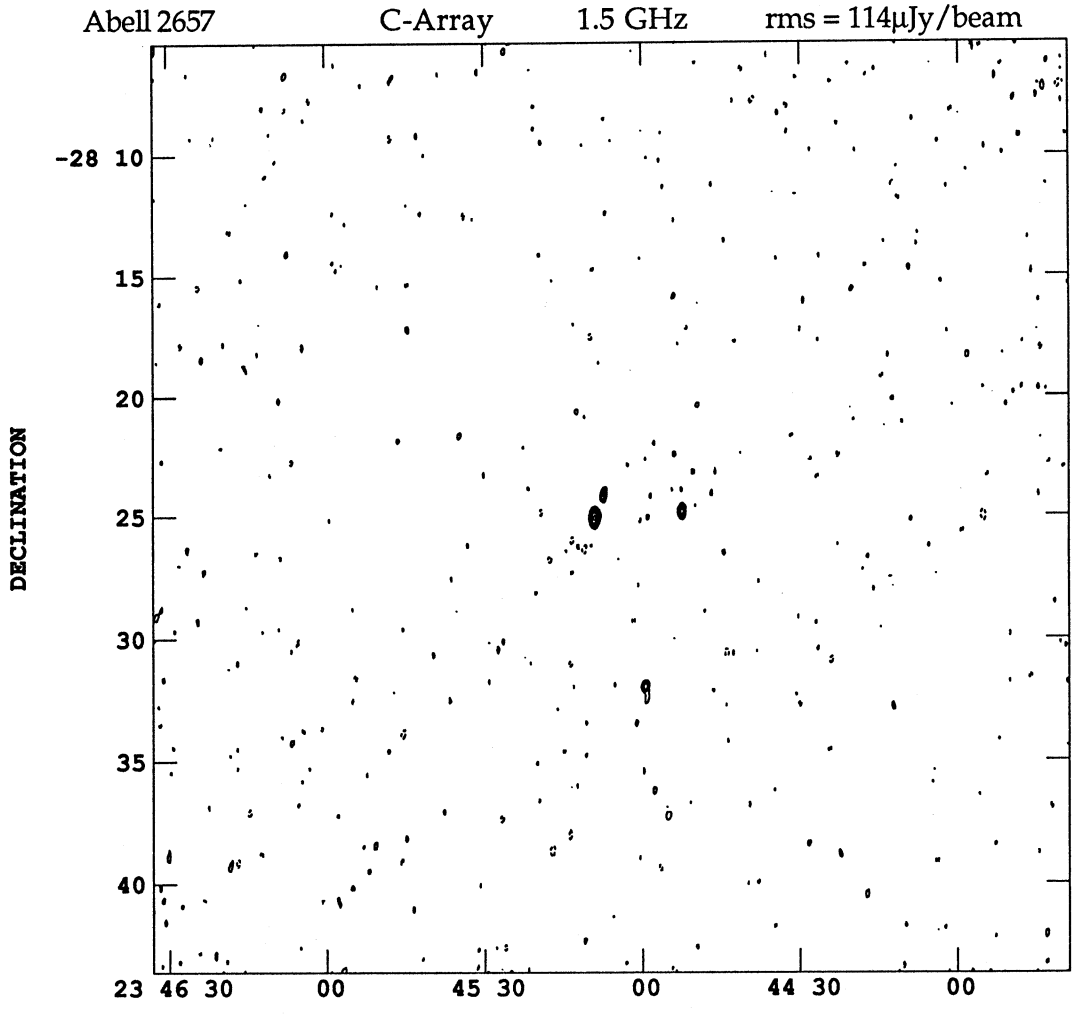


Contour levels: -2,2,4,6,10,20,40,80 percent of peak of 7.1mJy/beam

**Figure 70**

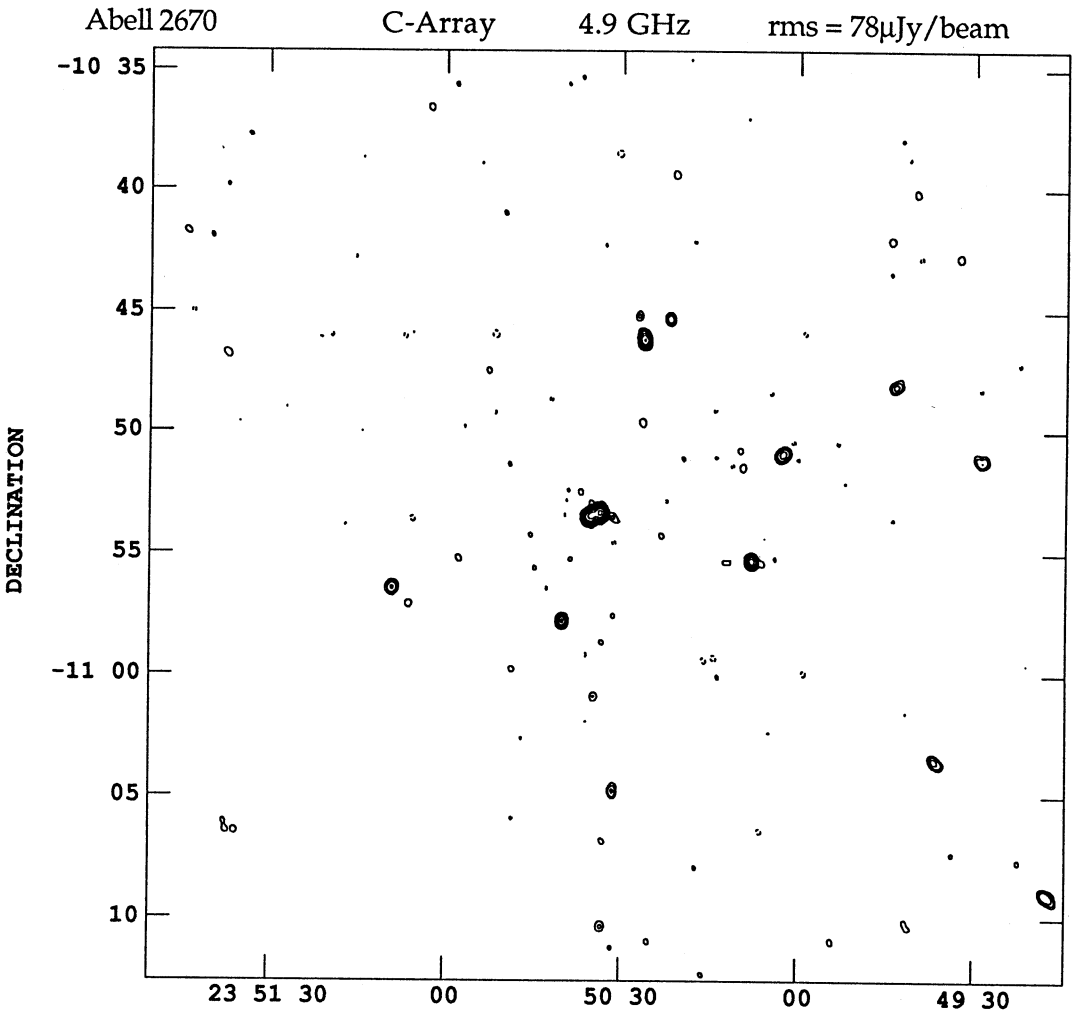


Contour levels: -0.5,0.5,1,2,5,10,20,40,80 percent of peak of 74.4mJy/beam

**Figure 71**

**Table 2. The source list**

| Cluster & Source | Ang. Dist. R/Rc | R.A. 1950 h m s | Dec. ° ' " | Flux Dens. 1.5 GHz mJy | Flux Dens. 4.9 GHz mJy | Spec. Index $\alpha_{1.5}^{4.9}$ |
|---|---|---|---|---|---|---|
| Abell 13 | | | | | | |
| 1 | 1.30 | 00 09 38.97 | -19 40 42.4 | 84.0 | | |
| 2 | 1.29 | 00 09 41.47 | -19 55 01.8 | 7.74 | | |
| 3 | 1.08 | 00 10 02.61 | -19 37 35.1 | 2.43 | | |
| 4 | 0.59 | 00 10 31.65 | -19 52 07.5 | 2.48 | | |
| 5 | 0.54 | 00 10 51.13 | -19 39 02.1 | 1.69 | | |
| 6 | 0.19 | 00 10 54.51 | -19 46 47.7 | 3.85 | | |
| 7 | 0.45 | 00 10 56.68 | -19 40 14.1 | 21.1 | | |
| 8 | 0.36 | 00 11 04.70 | -19 53 14.5 | 1.64 | | |
| 9 | 0.07 | 00 11 11.91 | -19 46 23.8 | 0.97 | | |
| 10 | 0.68 | 00 11 31.28 | -19 57 20.4 | 1.96 | | |
| 11 | 1.09 | 00 11 50.69 | -19 31 57.1 | 15.0 | | |
| 12 | 1.00 | 00 11 58.75 | -19 59 18.2 | 9.37 | | |
| 13 | 1.11 | 00 12 09.31 | -19 59 24.6 | 18.5 | | |
| 14 | 0.96 | 00 12 15.44 | -19 43 54.8 | 7.39 | | |
| Abell 76 | | | | | | |
| 1 | 0.82 | 00 36 39.42 | 06 56 32.7 | 31.8 | | |
| 2 | 0.78 | 00 36 59.37 | 06 56 16.1 | 3.30 | | |
| 3 | 0.80 | 00 37 12.52 | 06 57 14.0 | 3.05 | | |
| 4 | 0.67 | 00 37 12.79 | 06 52 52.8 | 5.10 | | |
| 5a/b | 1.14 | 00 37 17.56 | 07 08 32.7 | 20.7 | | |
| 6 | 1.16 | 00 37 20.88 | 07 09 26.5 | 6.88 | | |
| 7 | 0.99 | 00 37 24.35 | 07 03 19.3 | 1.14 | | |
| 8 | 1.00 | 00 37 31.45 | 07 03 31.9 | 24.6 | 10.1 | -0.73 |
| 9 | 0.81 | 00 37 32.38 | 06 57 05.7 | 9.19 | | |
| 10 | 0.99 | 00 37 40.47 | 07 02 47.2 | | 0.53 | |
| 11 | 1.20 | 00 37 40.54 | 07 10 08.8 | 2.18 | | |
| 12 | 0.97 | 00 37 47.58 | 07 01 50.3 | 2.16 | 0.35 | -1.50 |
| 13a/b | 0.93 | 00 37 47.96 | 07 00 08.3 | 157. | 51.6 | -0.92 |
| 14 | 1.11 | 00 37 59.28 | 07 05 48.0 | 2.09 | | |
| 15 | 1.13 | 00 38 05.87 | 07 05 46.4 | 7.54 | | |
| 16 | 1.31 | 00 38 16.86 | 07 11 28.2 | 4.20 | | |
| 17a/b | 0.72 | 00 38 17.31 | 06 48 26.9 | 29.6 | | |
| 18 | 1.18 | 00 38 23.50 | 07 06 02.3 | 3.00 | | |
| Abell 85 | | | | | | |
| 1 | 1.21 | 00 37 08.09 | -10 05 57.6 | 37.3 | | |
| 2 | 1.09 | 00 37 51.47 | -10 09 30.6 | 3.09 | | |
| 3a/b | 0.57 | 00 37 52.46 | -09 31 52.9 | 101. | | |
| 4 | 1.24 | 00 37 56.18 | -10 15 41.6 | 10.1 | | |
| 5 | 0.51 | 00 37 58.05 | -09 41 02.8 | 5.97 | | |
| 6 | 0.75 | 00 37 58.83 | -09 56 38.7 | 2.82 | | |
| 7a/b | 1.27 | 00 37 59.43 | -10 17 03.2 | 85.7 | | |
| 8 | 0.98 | 00 38 11.78 | -10 07 37.2 | 4.16 | 1.32 | -0.95 |
| 9 | 0.84 | 00 38 11.98 | -10 02 37.7 | | 0.89 | |
| 10 | 0.47 | 00 38 12.36 | -09 46 08.5 | 8.64 | | |
| 11 | 0.45 | 00 38 15.52 | -09 29 06.1 | 3.20 | | |
| 12a/b | 0.89 | 00 38 17.42 | -10 05 07.2 | 331. | 84.3 | -1.14 |
| 13 | 0.68 | 00 38 19.50 | -09 57 18.9 | 40.9 | | |
| 14 | 0.61 | 00 38 22.53 | -09 19 58.6 | 3.99 | | |
| 15 | 1.10 | 00 38 23.26 | -10 12 56.1 | 3.19 | | |
| 16 | 0.77 | 00 38 23.80 | -10 01 16.8 | | 1.63 | |
| 17 | 0.74 | 00 38 27.69 | -10 00 27.7 | 7.38 | | |
| 18 | 0.88 | 00 38 28.61 | -10 05 49.5 | 17.9 | 4.00 | -1.25 |
| 19 | 0.32 | 00 38 34.84 | -09 45 12.9 | 8.80 | | |
| 20 | 0.30 | 00 38 42.40 | -09 29 33.7 | 1.67 | | |
| 21 | 0.33 | 00 38 48.67 | -09 27 19.4 | 0.97 | | |
| 22 | 0.46 | 00 38 49.67 | -09 52 33.6 | 4.90 | | |
| 23 | 1.06 | 00 38 52.39 | -10 13 11.1 | 4.06 | | |
| 24 | 0.25 | 00 38 56.75 | -09 29 27.5 | 0.63 | | |
| 25a/b/c | 0.08 | 00 38 57.03 | -09 38 44.4 | 7.81 | | |
| 26 | 0.17 | 00 38 58.48 | -09 32 14.3 | 6.54 | | |
| 27 | 0.21 | 00 39 01.12 | -09 44 27.9 | 1.29 | | |
| 28 | 0.55 | 00 39 01.94 | -09 56 17.8 | 2.67 | | |
| 29 | 1.01 | 00 39 02.37 | -10 11 44.0 | 4.60 | | |
| 30 | 0.54 | 00 39 04.15 | -09 55 49.3 | 12.6 | | |
| 31 | 0.05 | 00 39 07.10 | -09 39 17.2 | 1.53 | | |
| 32 | 0.21 | 00 39 09.89 | -09 30 38.1 | 2.12 | | |
| 33 | 0.15 | 00 39 16.14 | -09 33 09.9 | 49.1 | | |
| 34 | 0.07 | 00 39 16.30 | -09 37 10.8 | 5.20 | | |
| 35a/b | 0.13 | 00 39 18.66 | -09 34 38.4 | 46.2 | | |
| 36a/b | 0.17 | 00 39 19.28 | -09 42 15.0 | 91.1 | | |

| Cluster & Source | Ang. Dist. R/Rc | R.A. 1950 h m s | Dec. ° ' " | Flux Dens. 1.5 GHz mJy | 4.9 GHz mJy | Spec. Index $\alpha_{1.5}^{4.9}$ |
|---|---|---|---|---|---|---|
| Abell 85(cont) | | | | | | |
| 37 | 0.16 | 00 39 21.28 | -09 41 31.1 | 2.47 | | |
| 38 | 0.27 | 00 39 21.35 | -09 45 56.2 | 1.47 | | |
| 39 | 0.49 | 00 39 23.73 | -09 21 37.0 | 2.49 | | |
| 40 | 0.19 | 00 39 26.47 | -09 33 21.9 | 2.66 | | |
| 41 | 0.56 | 00 39 27.08 | -09 55 48.0 | 4.36 | | |
| 42 | 0.17 | 00 39 27.50 | -09 40 17.9 | 0.89 | | |
| 43 | 0.27 | 00 39 32.24 | -09 31 13.2 | 1.04 | | |
| 44 | 0.57 | 00 39 34.30 | -09 55 46.4 | 3.49 | | |
| 45a/b | 0.40 | 00 39 36.11 | -09 48 59.0 | 27.6 | | |
| 46 | 0.63 | 00 39 37.39 | -09 57 19.4 | 20.7 | | |
| 47 | 0.28 | 00 39 39.48 | -09 32 59.9 | 0.77 | | |
| 48 | 0.43 | 00 39 42.43 | -09 49 11.5 | 2.64 | | |
| 49 | 0.32 | 00 39 44.39 | -09 42 55.5 | 0.85 | | |
| 50 | 0.31 | 00 39 44.88 | -09 42 10.5 | 1.32 | | |
| 51 | 0.49 | 00 39 47.50 | -09 50 47.1 | 48.1 | | |
| 52 | 0.59 | 00 39 49.76 | -09 20 45.3 | 4.98 | | |
| 53 | 0.39 | 00 39 53.44 | -09 43 29.6 | 1.29 | | |
| 54 | 0.38 | 00 39 58.61 | -09 38 27.9 | 81.2 | | |
| 55 | 0.54 | 00 39 59.62 | -09 50 32.0 | 2.51 | | |
| 56 | 0.41 | 00 40 02.08 | -09 38 35.7 | 1.32 | | |
| 57 | 0.47 | 00 40 09.29 | -09 41 37.6 | 1.73 | | |
| Abell 86 | | | | | | |
| 1 | 0.86 | 00 38 32.30 | -22 09 55.2 | 11.8 | | |
| 2 | 0.64 | 00 38 53.24 | -22 03 11.7 | 2.87 | | |
| 3 | 0.59 | 00 39 24.60 | -22 16 20.5 | 2.02 | | |
| 4 | 0.24 | 00 39 40.03 | -22 07 48.5 | 2.56 | | |
| 5a/b | 0.39 | 00 39 41.61 | -22 13 15.2 | 136. | 43.5 | -0.95 |
| 6 | 0.59 | 00 39 44.33 | -22 18 39.6 | 1.37 | | |
| 7 | 0.16 | 00 39 45.40 | -22 03 30.9 | 3.85 | | |
| 8 | 0.78 | 00 39 46.83 | -22 23 31.8 | 17.9 | | |
| 9 | 0.48 | 00 39 56.25 | -22 16 24.9 | 1.40 | | |
| 10 | 0.24 | 00 39 57.97 | -21 58 52.9 | 2.58 | | |
| 11 | 0.59 | 00 40 01.54 | -22 19 11.6 | 3.65 | | |
| 12 | 0.36 | 00 40 18.30 | -22 12 47.2 | 32.1 | | |
| 13 | 0.32 | 00 40 24.27 | -22 10 28.5 | 2.30 | | |
| 14 | 0.88 | 00 40 58.28 | -22 22 04.5 | 13.4 | | |

| Cluster & Source | Ang. Dist. R/Rc | R.A. 1950 h m s | Dec. ° ' " | Flux Dens. 1.5 GHz mJy | 4.9 GHz mJy | Spec. Index $\alpha_{1.5}^{4.9}$ |
|---|---|---|---|---|---|---|
| Abell 115 | | | | | | |
| 1 | 1.30 | 00 52 58.84 | 26 22 29.8 | 16.9 | | |
| 2a/b | 0.33 | 00 53 08.86 | 26 08 20.5 | 1255 | 140. | -1.82 |
| 3 | 0.71 | 00 53 09.92 | 26 14 13.2 | | 4.27 | |
| 4 | 0.15 | 00 53 17.56 | 26 01 40.5 | 4.75 | | |
| 5 | 0.49 | 00 53 21.56 | 26 11 01.8 | 247. | 87.3 | -0.86 |
| 6 | 0.37 | 00 53 27.11 | 26 08 57.6 | | 1.33 | |
| 7 | 0.41 | 00 53 41.15 | 26 06 48.8 | 11.5 | | |
| 8 | 0.64 | 00 53 41.68 | 26 11 38.7 | 5.28 | | |
| 9 | 0.51 | 00 53 46.23 | 26 07 45.6 | 14.9 | | |
| 10 | 1.15 | 00 54 13.26 | 26 15 13.2 | 138. | | |
| Abell 133 | | | | | | |
| 1 | 0.65 | 00 59 04.46 | -22 10 42.7 | 6.97 | | |
| 2 | 0.54 | 00 59 17.80 | -22 10 21.1 | 25.8 | | |
| 3 | 0.24 | 00 59 53.90 | -22 00 02.9 | 5.05 | | |
| 4 | 0.25 | 00 59 57.76 | -22 09 51.2 | 1.46 | | |
| 5 | 0.15 | 01 00 02.22 | -22 07 13.3 | 2.18 | | |
| 6 | 0.17 | 01 00 12.43 | -22 08 51.6 | 3.83 | 1.61 | -0.72 |
| 7a/b | 0.16 | 01 00 14.53 | -22 08 35.4 | 130. | 3.95 | -2.90 |
| 8 | 0.23 | 01 00 18.50 | -22 10 22.3 | 20.0 | 6.00 | -1.00 |
| 9 | 0.81 | 01 00 18.94 | -22 26 02.0 | 3.48 | | |
| 10 | 0.26 | 01 00 23.75 | -22 11 05.1 | | 0.59 | |
| 11 | 0.79 | 01 00 23.98 | -22 25 36.4 | 4.82 | | |
| 12 | 0.61 | 01 00 42.40 | -22 19 18.3 | 3.36 | | |
| 13 | 0.50 | 01 00 44.07 | -22 15 49.9 | 12.0 | | |
| 14 | 0.35 | 01 00 56.06 | -22 04 28.0 | 6.45 | | |
| Abell 154 | | | | | | |
| 1 | 0.13 | 01 08 30.40 | 17 31 21.8 | 5.34 | | |
| 2 | 0.27 | 01 08 53.19 | 17 37 31.3 | 32.3 | 16.4 | -0.56 |
| 3 | 0.31 | 01 09 00.59 | 17 38 48.1 | 2.01 | | |
| 4a/b | 0.39 | 01 09 02.40 | 17 44 03.3 | 21.5 | | |
| 5 | 0.32 | 01 09 09.80 | 17 37 57.3 | 457. | 149. | -0.93 |
| 6 | 0.28 | 01 09 27.31 | 17 25 35.1 | 4.31 | | |
| 7 | 0.31 | 01 09 31.19 | 17 27 44.8 | 31.3 | | |
| 8 | 0.44 | 01 09 55.26 | 17 34 08.9 | 2.61 | | |
| 9 | 0.52 | 01 09 55.76 | 17 43 08.9 | 6.80 | | |
| 10 | 0.42 | 01 09 55.77 | 17 31 06.3 | 4.15 | 1.81 | -0.69 |
| 11 | 0.46 | 01 09 57.02 | 17 36 08.8 | 327. | 96.3 | -1.01 |

| Cluster & Source | Ang. Dist. R/Rc | R.A. 1950 h m s | Dec. ° ' " | Flux Dens. 1.5 GHz mJy | 4.9 GHz mJy | Spec. Index $\alpha_{1.5}^{4.9}$ |
|---|---|---|---|---|---|---|
| Abell 154(cont) | | | | | | |
| 12a/b | 0.48 | 01 10 07.33 | 17 32 47.1 | 34.9 | 8.63 | -1.16 |
| Abell 196 | | | | | | |
| 1 | 1.40 | 01 23 12.30 | 22 47 26.3 | 206. | | |
| 2a/b | 1.09 | 01 24 19.62 | 22 41 56.1 | 44.7 | | |
| 3a/b | 0.17 | 01 24 24.78 | 22 55 28.8 | 47.4 | 16.9 | -0.86 |
| 4 | 0.10 | 01 24 26.01 | 22 58 52.8 | 316. | 76.3 | -1.18 |
| 5 | 0.52 | 01 24 57.24 | 23 01 38.4 | 28.1 | | |
| Abell 240 | | | | | | |
| 1 | 1.07 | 01 37 37.98 | 07 09 55.6 | 13.2 | | |
| 2 | 1.08 | 01 37 44.04 | 07 38 47.8 | 101. | | |
| 3 | 0.88 | 01 37 49.01 | 07 15 54.4 | 3.15 | | |
| 4 | 0.90 | 01 37 50.99 | 07 32 30.1 | 2.21 | | |
| 5 | 0.82 | 01 37 57.61 | 07 31 09.6 | 3.99 | | |
| 6a/b | 0.75 | 01 37 58.78 | 07 21 54.0 | 338. | | |
| 7 | 1.06 | 01 38 05.36 | 07 43 45.8 | 7.68 | | |
| 8 | 0.74 | 01 38 14.52 | 07 34 06.5 | 46.4 | 27.6 | -0.43 |
| 9a/b | 0.61 | 01 38 16.97 | 07 28 21.1 | 168. | 56.8 | -0.90 |
| 10 | 0.60 | 01 38 22.69 | 07 30 28.6 | 6.17 | | |
| 11 | 0.80 | 01 38 24.21 | 07 38 51.5 | 3.71 | | |
| 12 | 0.50 | 01 38 25.87 | 07 20 16.0 | 2.66 | | |
| 13a/b | 0.47 | 01 38 34.17 | 07 28 55.7 | 6.73 | 3.49 | -0.55 |
| 14 | 0.43 | 01 38 40.15 | 07 29 29.5 | 15.2 | 3.67 | -1.18 |
| 15 | 0.75 | 01 39 01.66 | 07 41 56.2 | 15.5 | | |
| 16 | 0.13 | 01 39 19.85 | 07 26 16.4 | 17.9 | | |
| 17 | 0.08 | 01 39 25.07 | 07 23 18.0 | 27.8 | | |
| 18 | 0.15 | 01 39 25.25 | 07 26 13.6 | 8.71 | | |
| 19 | 0.11 | 01 39 26.89 | 07 23 54.1 | 20.0 | | |
| Abell 278 | | | | | | |
| 1 | 0.58 | 01 53 48.93 | 32 13 00.8 | 8.77 | | |
| 2 | 0.36 | 01 53 57.72 | 31 50 47.5 | 19.0 | | |
| 3 | 0.23 | 01 53 58.82 | 32 02 39.0 | 5.33 | | |
| 4 | 0.24 | 01 53 59.36 | 31 55 02.5 | 56.0 | 123. | 0.65 |
| 5 | 0.72 | 01 54 21.52 | 31 39 42.1 | 845. | | |
| 6a/b | 0.03 | 01 54 23.54 | 31 59 52.6 | 346. | 110. | -0.95 |
| 7 | 0.05 | 01 54 27.59 | 31 58 17.2 | 8.70 | 2.62 | -1.00 |
| 8 | 0.54 | 01 54 28.54 | 31 44 27.3 | 22.9 | | |
| Abell 278(cont) | | | | | | |
| 9 | 0.72 | 01 54 51.08 | 31 40 41.1 | 17.7 | | |
| 10 | 0.44 | 01 55 05.02 | 32 06 57.5 | 73.5 | | |
| 11 | 0.37 | 01 55 07.03 | 32 02 12.9 | 8.76 | | |
| Abell 357 | | | | | | |
| 1 | 0.70 | 02 25 31.40 | 12 56 17.1 | 4.19 | | |
| 2 | 0.69 | 02 25 42.68 | 13 12 19.2 | 3.40 | | |
| 3 | 0.58 | 02 25 44.68 | 13 06 40.7 | 5.23 | | |
| 4 | 0.60 | 02 26 01.50 | 13 13 56.3 | 5.48 | | |
| 5 | 0.35 | 02 26 11.42 | 12 57 14.0 | 309. | 71.7 | -1.21 |
| 6 | 0.30 | 02 26 40.71 | 13 09 36.1 | 5.11 | | |
| 7 | 0.27 | 02 26 45.33 | 13 08 49.3 | 8.29 | | |
| 8 | 0.34 | 02 26 45.88 | 13 10 43.1 | 21.4 | | |
| 9 | 0.46 | 02 26 51.20 | 12 49 10.7 | 78.3 | | |
| 10a/b | 0.14 | 02 26 53.58 | 12 58 32.3 | 31.7 | | |
| 11 | 0.29 | 02 26 54.63 | 13 09 16.3 | 47.7 | | |
| 12 | 0.85 | 02 27 06.20 | 12 39 09.8 | 15.2 | | |
| Abell 362 | | | | | | |
| 1 | 1.03 | 02 28 22.46 | -05 04 36.7 | 4.70 | | |
| 2 | 0.92 | 02 28 27.42 | -05 04 53.5 | 41.5 | | |
| 3 | 1.01 | 02 28 44.03 | -04 55 58.5 | 2.30 | | |
| 4 | 0.46 | 02 28 55.49 | -05 01 29.3 | 0.96 | | |
| 5 | 1.01 | 02 28 56.75 | -04 54 34.7 | 1.64 | | |
| 6 | 0.10 | 02 29 06.76 | -05 06 31.2 | 122. | 51.3 | -0.72 |
| 7 | 0.01 | 02 29 09.06 | -05 05 20.7 | 2.12 | | |
| 8 | 0.07 | 02 29 10.73 | -05 06 11.4 | 132. | 42.1 | -0.95 |
| 9 | 0.64 | 02 29 12.47 | -05 12 36.8 | 5.09 | 0.84 | -1.50 |
| 10 | 0.16 | 02 29 12.61 | -05 04 00.8 | 21.9 | 8.60 | -0.78 |
| 11 | 0.40 | 02 29 18.16 | -05 01 35.3 | 0.94 | | |
| 12 | 0.69 | 02 29 23.34 | -05 12 21.2 | 1.27 | | |
| 13 | 0.58 | 02 29 24.93 | -05 10 38.6 | 1.24 | | |
| 14a/b | 1.21 | 02 29 43.82 | -04 55 02.6 | 126. | | |
| 15 | 1.60 | 02 30 03.09 | -05 17 27.3 | 5.86 | | |
| 16 | 1.33 | 02 30 03.70 | -04 59 16.5 | 8.86 | | |
| 17 | 1.46 | 02 30 07.39 | -04 57 52.6 | 28.8 | | |
| Abell 407 | | | | | | |
| 1 | 0.50 | 02 57 15.56 | 35 35 17.5 | 16.0 | | |

| Cluster & Source | Ang. Dist. R/Rc | R.A. 1950 h m s | Dec. ° ' " | Flux Dens. 1.5 GHz mJy | 4.9 GHz mJy | Spec. Index $\alpha_{1.5}^{4.9}$ |
|---|---|---|---|---|---|---|
| Abell 407(cont) | | | | | | |
| 2 | 0.47 | 02 57 19.51 | 35 42 06.8 | 19.3 | | |
| 3a/b | 0.47 | 02 57 19.65 | 35 36 01.0 | 105. | | |
| 4 | 0.38 | 02 57 35.52 | 35 35 52.8 | 23.6 | | |
| 5 | 0.34 | 02 57 40.56 | 35 37 56.5 | 10.4 | | |
| 6a/b | 0.36 | 02 57 43.37 | 35 33 47.3 | 187. | | |
| 7 | 0.20 | 02 58 08.27 | 35 35 28.8 | 1.95 | | |
| 8 | 0.27 | 02 58 10.36 | 35 31 29.1 | 7.14 | | |
| 9 | 0.49 | 02 58 15.75 | 35 22 48.2 | 21.0 | | |
| 10 | 0.25 | 02 58 24.60 | 35 46 53.6 | 3.23 | | |
| 11 | 0.55 | 02 58 34.07 | 35 20 27.4 | 21.6 | | |
| 12 | 0.07 | 02 58 34.77 | 35 36 33.9 | 2.49 | | |
| 13 | 0.40 | 02 58 38.42 | 35 25 12.2 | 6.34 | | |
| 14 | 0.37 | 02 58 38.69 | 35 26 27.3 | 4.14 | | |
| 15a/b | 0.05 | 02 58 44.33 | 35 38 35.8 | 694. | 208. | -1.00 |
| 16 | 0.09 | 02 58 50.96 | 35 37 36.0 | 22.1 | | |
| 17 | 0.18 | 02 58 53.03 | 35 33 51.7 | 4.58 | | |
| 18 | 0.46 | 02 58 55.78 | 35 54 03.1 | 10.3 | | |
| 19 | 0.39 | 02 59 18.74 | 35 48 52.4 | 6.98 | | |
| 20 | 0.48 | 02 59 26.08 | 35 26 13.3 | 153. | | |
| 21 | 0.36 | 02 59 30.36 | 35 33 17.0 | 6.70 | | |
| 22 | 0.52 | 02 59 30.41 | 35 24 55.9 | 8.94 | | |
| 23 | 0.41 | 02 59 42.80 | 35 41 36.9 | 8.89 | | |
| 24 | 0.62 | 03 00 17.45 | 35 34 38.9 | 7.98 | | |
| 25 | 0.62 | 03 00 17.45 | 35 34 38.9 | 8.04 | | |
| Abell 416 | | | | | | |
| 1 | 1.16 | 03 04 05.24 | -16 53 30.3 | 8.41 | | |
| 2 | 1.22 | 03 04 12.52 | -16 48 12.1 | 2.39 | | |
| 3 | 0.73 | 03 04 25.00 | -16 52 51.8 | 2.94 | | |
| 4 | 0.43 | 03 04 36.64 | -16 54 05.5 | 5.58 | | |
| 5 | 0.36 | 03 04 38.53 | -16 55 05.8 | 6.18 | | |
| 6 | 0.42 | 03 04 51.13 | -17 00 00.3 | 9.60 | | |
| 7 | 0.47 | 03 05 05.07 | -16 51 49.5 | 171. | 41.4 | -1.18 |
| 8 | 0.76 | 03 05 07.61 | -16 48 52.5 | 3.38 | | |
| 9 | 0.68 | 03 05 09.69 | -16 50 02.3 | 1.63 | | |
| 10 | 0.61 | 03 05 11.72 | -16 51 22.5 | 58.8 | 14.3 | -1.18 |
| 11a/b | 0.75 | 03 05 14.49 | -16 50 02.7 | 143. | 41.9 | -1.02 |
| 12 | 0.88 | 03 05 16.66 | -17 02 46.7 | 34.2 | | |
| 13 | 0.64 | 03 05 17.11 | -16 52 33.5 | 12.1 | 5.22 | -0.70 |
| Abell 416(cont) | | | | | | |
| 14 | 1.29 | 03 05 28.02 | -17 05 55.1 | 39.9 | | |
| 15 | 0.92 | 03 05 28.87 | -16 59 38.6 | 81.6 | | |
| 16 | 1.11 | 03 05 40.79 | -16 55 18.5 | 3.19 | | |
| 17 | 1.17 | 03 05 42.07 | -16 53 03.3 | 21.8 | | |
| 18 | 1.42 | 03 05 48.51 | -16 49 58.5 | 20.3 | | |
| Abell 474 | | | | | | |
| 1 | 2.23 | 04 04 15.82 | -16 43 12.9 | 3.06 | | |
| 2 | 2.31 | 04 04 32.53 | -16 35 04.3 | 7.39 | | |
| 3 | 1.80 | 04 04 51.69 | -16 37 07.0 | 27.1 | | |
| 4a/b | 1.64 | 04 04 51.71 | -17 00 00.3 | 3.80 | | |
| 5 | 1.62 | 04 04 55.88 | -17 00 36.7 | 3.77 | | |
| 6 | 1.55 | 04 04 56.14 | -16 39 15.0 | 2.93 | | |
| 7 | 1.01 | 04 05 02.46 | -16 53 56.4 | 1.76 | | |
| 8 | 0.98 | 04 05 02.64 | -16 45 28.5 | 1.25 | | |
| 9 | 1.43 | 04 05 04.78 | -16 38 58.6 | 13.0 | | |
| 10 | 1.55 | 04 05 10.27 | -17 02 09.1 | 3.62 | | |
| 11 | 1.80 | 04 05 10.50 | -17 04 36.5 | 4.21 | | |
| 12 | 0.69 | 04 05 20.98 | -16 54 39.3 | 1.96 | | |
| 13a/b | 0.35 | 04 05 31.54 | -16 46 28.9 | 159. | 42.4 | -1.10 |
| 14 | 0.12 | 04 05 33.90 | -16 48 32.1 | 1.56 | | |
| 15 | 0.89 | 04 05 45.96 | -16 57 08.9 | 1.97 | | |
| 16 | 0.97 | 04 05 47.57 | -16 41 17.4 | 9.87 | | |
| 17 | 1.60 | 04 05 48.02 | -17 03 42.4 | 4.70 | | |
| 18 | 0.57 | 04 05 52.13 | -16 46 14.3 | 4.24 | 2.16 | -0.56 |
| 19a/b | 1.51 | 04 06 24.10 | -16 56 40.7 | 6.38 | | |
| 20 | 1.68 | 04 06 38.39 | -16 47 32.4 | 635. | | |
| Abell 496 | | | | | | |
| 1 | 0.44 | 04 30 06.90 | -13 11 48.7 | 22.3 | | |
| 2 | 0.31 | 04 30 36.15 | -13 11 56.6 | 6.69 | | |
| 3 | 0.06 | 04 31 13.11 | -13 19 08.0 | | 2.13 | |
| 4 | 0.01 | 04 31 18.81 | -13 21 56.2 | 106. | 57.1 | -0.52 |
| 5 | 0.11 | 04 31 23.92 | -13 26 34.3 | | 1.25 | |
| 6 | 0.06 | 04 31 29.37 | -13 22 20.4 | 15.1 | 5.87 | -0.79 |
| 7 | 0.15 | 04 31 29.51 | -13 15 44.4 | 2.85 | | |
| 8 | 0.35 | 04 31 37.04 | -13 06 50.1 | 6.97 | | |
| 9a/b | 0.23 | 04 31 50.48 | -13 28 38.4 | 598. | | |
| 10 | 0.23 | 04 31 54.12 | -13 27 10.1 | 43.8 | | |

| Cluster & Source | Ang. Dist. R/Rc | R.A. 1950 h m s | Dec. ° ' " | Flux Dens. 1.5 GHz mJy | 4.9 GHz mJy | Spec. Index $\alpha_{1.5}^{4.9}$ |
|---|---|---|---|---|---|---|
| Abell 496(cont) | | | | | | |
| 11a/b | 0.25 | 04 31 58.28 | -13 16 05.3 | 1569 | | |
| 12 | 0.25 | 04 32 04.19 | -13 23 07.2 | 4.45 | | |
| 13 | 0.31 | 04 32 05.77 | -13 29 22.6 | 5.29 | | |
| Abell 514 | | | | | | |
| 1 | 0.11 | 04 45 14.49 | -20 31 59.1 | 6.52 | | |
| 2 | 0.20 | 04 45 22.52 | -20 38 05.2 | 149. | | |
| 3 | 0.64 | 04 45 48.57 | -20 52 52.9 | 6.04 | | |
| 4a/b | 0.15 | 04 45 51.29 | -20 32 31.4 | 114. | | |
| 5 | 0.69 | 04 45 56.82 | -20 54 00.6 | 34.1 | | |
| 6a/b | 0.20 | 04 45 59.46 | -20 30 13.3 | 129. | | |
| 7 | 0.31 | 04 46 09.61 | -20 36 30.1 | 3.15 | | |
| 8a/b | 0.39 | 04 46 20.70 | -20 37 13.8 | 609. | 193. | -0.95 |
| 19 | 0.43 | 04 46 21.39 | -20 40 00.8 | 7.20 | 3.93 | -0.50 |
| 10 | 0.66 | 04 46 23.96 | -20 49 52.9 | 31.7 | | |
| 11 | 0.63 | 04 46 27.12 | -20 48 04.6 | 4.43 | | |
| 12 | 0.45 | 04 46 32.95 | -20 27 50.9 | 8.18 | | |
| 13 | 0.48 | 04 46 34.45 | -20 25 12.2 | 8.16 | | |
| 14 | 0.49 | 04 46 34.46 | -20 38 18.9 | 8.26 | 2.52 | -0.99 |
| 15a/b/c | 0.77 | 04 46 49.07 | -20 49 52.4 | 202. | | |
| 16 | 0.66 | 04 46 52.16 | -20 43 06.0 | 17.4 | | |
| 17 | 0.68 | 04 46 56.58 | -20 42 52.2 | 17.7 | | |
| 18 | 0.73 | 04 47 10.53 | -20 23 53.4 | 10.4 | | |
| 19 | 0.90 | 04 47 27.47 | -20 44 24.6 | 20.6 | | |
| Abell 519 | | | | | | |
| 1a/b | 0.81 | 04 50 06.18 | 00 26 14.1 | 22.7 | | |
| 2 | 0.78 | 04 50 22.20 | 00 22 40.3 | 12.5 | | |
| 3a/b | 0.72 | 04 50 33.54 | 00 22 21.8 | 26.7 | | |
| 4 | 0.61 | 04 50 35.98 | 00 25 08.8 | 9.61 | | |
| 5 | 0.60 | 04 50 37.04 | 00 48 03.7 | 7.10 | | |
| 6 | 0.71 | 04 50 45.36 | 00 21 07.6 | 3.97 | | |
| 7 | 0.71 | 04 51 04.13 | 00 53 14.1 | 7.42 | | |
| 8a/b | 0.06 | 04 51 15.17 | 00 35 52.3 | 311. | 96.0 | -0.98 |
| 9 | 0.21 | 04 51 29.13 | 00 35 15.5 | 2.99 | | |
| 10 | 0.34 | 04 51 29.81 | 00 30 15.4 | 9.11 | 1.39 | -1.56 |
| 11 | 0.44 | 04 51 38.70 | 00 44 20.1 | 2.34 | | |
| 12 | 0.56 | 04 52 02.99 | 00 36 30.2 | 3.33 | | |
| 13 | 0.70 | 04 52 04.33 | 00 27 16.5 | 36.9 | | |

| Cluster & Source | Ang. Dist. R/Rc | R.A. 1950 h m s | Dec. ° ' " | Flux Dens. 1.5 GHz mJy | 4.9 GHz mJy | Spec. Index $\alpha_{1.5}^{4.9}$ |
|---|---|---|---|---|---|---|
| Abell 531 | | | | | | |
| 1 | 0.99 | 04 57 51.45 | -03 26 55.1 | 40.1 | | |
| 2 | 0.66 | 04 58 06.38 | -03 42 14.2 | 9.22 | | |
| 3 | 0.38 | 04 58 27.13 | -03 33 25.0 | 1.26 | | |
| 4 | 0.65 | 04 58 33.98 | -03 26 25.1 | 7.61 | | |
| 5 | 0.18 | 04 58 38.52 | -03 35 32.7 | 1.17 | | |
| 6 | 0.35 | 04 58 40.52 | -03 43 19.4 | 1.39 | | |
| 7a/b | 0.83 | 04 58 45.52 | -03 52 17.2 | 68.9 | | |
| 8 | 0.46 | 04 58 48.46 | -03 29 08.0 | 1.94 | | |
| 9 | 0.05 | 04 58 49.67 | -03 38 11.2 | 15.1 | 0.35 | -3.12 |
| 10 | 0.85 | 04 58 50.15 | -03 22 07.7 | 1.91 | | |
| 11a/b | 0.04 | 04 58 51.06 | -03 36 51.2 | 314. | 84.6 | -1.09 |
| 12 | 0.34 | 04 58 52.05 | -03 43 29.1 | 6.05 | | |
| 13 | 0.40 | 04 59 00.28 | -03 30 47.4 | 1.82 | | |
| 14 | 0.38 | 04 59 07.22 | -03 32 04.8 | 3.45 | 1.35 | -0.78 |
| 15 | 0.26 | 04 59 08.16 | -03 36 44.4 | 4.81 | 1.86 | -0.79 |
| 16 | 0.53 | 04 59 11.27 | -03 29 39.1 | 8.28 | | |
| 17 | 0.50 | 04 59 12.20 | -03 44 23.8 | 3.30 | | |
| 18 | 0.75 | 04 59 13.95 | -03 49 22.6 | 41.4 | | |
| 19 | 0.43 | 04 59 19.95 | -03 36 02.9 | 2.17 | | |
| 20 | 0.69 | 04 59 29.93 | -03 44 28.5 | 13.1 | | |
| Abell 658 | | | | | | |
| 1 | 1.51 | 08 20 08.00 | 15 32 28.9 | 5.15 | | |
| 2 | 0.84 | 08 20 33.88 | 16 01 48.6 | 51.1 | | |
| 3 | 1.19 | 08 20 34.43 | 15 34 30.8 | 22.5 | | |
| 4 | 1.11 | 08 20 35.91 | 15 35 34.3 | 5.04 | | |
| 5 | 0.87 | 08 20 38.91 | 16 02 51.4 | 7.48 | | |
| 6 | 0.56 | 08 20 42.27 | 15 43 38.6 | 65.7 | | |
| 7 | 0.69 | 08 20 46.25 | 15 41 20.6 | 6.51 | | |
| 8 | 0.20 | 08 20 48.24 | 15 52 56.8 | 4.79 | | |
| 9 | 0.12 | 08 20 50.76 | 15 51 49.5 | 3.67 | | |
| 10 | 0.40 | 08 21 01.97 | 15 56 37.7 | 22.4 | | |
| 11a/b | 0.50 | 08 21 11.73 | 15 44 30.0 | 224. | 80.5 | -0.85 |
| 12 | 0.58 | 08 21 24.63 | 15 56 11.4 | 1.41 | | |
| 13 | 1.12 | 08 21 33.77 | 15 37 12.5 | 0.81 | | |
| 14 | 1.81 | 08 21 46.75 | 15 27 29.3 | 5.83 | | |
| 15 | 1.54 | 08 21 48.11 | 15 32 15.9 | 2.18 | | |
| 16 | 2.02 | 08 21 48.83 | 15 24 20.2 | 6.43 | | |

| Cluster & Source | Ang. Dist. R/Rc | R.A. 1950 h m s | Dec. ° ' " | Flux Dens. 1.5 GHz mJy | 4.9 GHz mJy | Spec. Index $\alpha_{1.5}^{4.9}$ |
|---|---|---|---|---|---|---|
| Abell 658(cont) | | | | | | |
| 17 | 0.98 | 08 21 56.56 | 15 49 31.9 | 2.94 | | |
| 18 | 1.88 | 08 21 57.54 | 15 27 47.0 | 9.05 | | |
| 19 | 1.23 | 08 22 10.35 | 15 47 55.8 | 8.97 | | |
| 20 | 1.23 | 08 22 10.35 | 15 47 55.8 | 8.53 | | |
| 21 | 1.56 | 08 22 14.37 | 15 37 47.4 | 3.66 | | |
| Abell 912 | | | | | | |
| 1a/b | 0.68 | 09 57 43.60 | 00 19 49.4 | 825. | | |
| 2 | 0.40 | 09 57 56.42 | 00 11 10.5 | 23.5 | | |
| 3 | 0.41 | 09 58 32.90 | 00 18 58.1 | | 1.15 | |
| 4 | 0.70 | 09 58 34.87 | 00 25 56.5 | 43.2 | | |
| 5 | 0.46 | 09 58 40.05 | 00 20 00.3 | | 1.06 | |
| 6 | 0.54 | 09 58 52.15 | 00 21 16.4 | | 1.42 | |
| 7 | 0.46 | 09 59 19.15 | 00 06 59.6 | 32.4 | | |
| Abell 1142 | | | | | | |
| 1 | 0.34 | 10 58 51.45 | 10 41 57.9 | 10.5 | | |
| 2 | 0.73 | 10 59 20.38 | 10 30 26.5 | 10.9 | | |
| 3 | 0.63 | 10 59 34.72 | 10 40 15.8 | 2.84 | | |
| 4 | 0.63 | 10 59 34.75 | 10 40 15.9 | | 2.90 | |
| 5 | 0.63 | 10 59 35.09 | 10 41 00.5 | 4.03 | | |
| 6 | 0.63 | 10 59 40.52 | 10 45 17.6 | 553. | 104. | -1.39 |
| 7 | 0.74 | 10 59 57.48 | 10 47 58.0 | 3.99 | | |
| 8 | 0.76 | 10 59 59.93 | 10 51 11.9 | 3.32 | | |
| 9 | 0.78 | 11 00 02.95 | 10 48 48.6 | 3.36 | | |
| 10 | 0.81 | 11 00 05.80 | 10 43 49.3 | 3.08 | | |
| 11 | 0.80 | 11 00 06.04 | 10 46 56.2 | 3.42 | | |
| 12 | 0.87 | 11 00 10.14 | 10 58 33.3 | 65.2 | | |
| 13 | 0.95 | 11 00 12.69 | 10 35 13.2 | 4.81 | | |
| 14 | 0.91 | 11 00 14.16 | 10 59 54.6 | 6.65 | | |
| 15 | 0.94 | 11 00 22.35 | 10 42 45.2 | 5.32 | | |
| 16 | 1.01 | 11 00 32.25 | 10 42 15.6 | 7.50 | | |
| Abell 1171 | | | | | | |
| 1 | 0.59 | 11 03 47.92 | 03 11 40.6 | 3.30 | | |
| 2 | 1.08 | 11 03 58.20 | 02 46 17.6 | 4.99 | | |
| 3 | 0.55 | 11 04 00.88 | 03 05 31.6 | 2.06 | | |
| 4 | 0.69 | 11 04 05.81 | 02 57 58.8 | 2.03 | | |
| 5 | 0.55 | 11 04 06.07 | 03 03 23.0 | 1.10 | | |
| Abell 1171(cont) | | | | | | |
| 6 | 0.46 | 11 04 13.25 | 03 21 08.5 | 3.02 | | |
| 7 | 0.48 | 11 04 16.29 | 03 03 36.9 | 1.16 | | |
| 8a/b | 0.74 | 11 04 18.63 | 02 54 21.0 | 4.59 | | |
| 9 | 0.42 | 11 04 21.28 | 03 04 48.3 | 0.71 | 0.27 | -0.79 |
| 10 | 0.61 | 11 04 21.32 | 02 58 07.7 | 1.51 | | |
| 11a/b | 0.40 | 11 04 31.55 | 03 03 24.0 | 141. | 42.1 | -1.00 |
| 12 | 0.29 | 11 04 35.83 | 03 06 40.1 | | 1.03 | |
| 13 | 0.29 | 11 04 35.84 | 03 06 40.8 | 0.71 | | |
| 14 | 0.15 | 11 04 38.10 | 03 14 39.8 | 1.89 | | |
| 15 | 0.17 | 11 04 38.65 | 03 10 35.7 | 2.27 | | |
| 16a/b | 0.08 | 11 04 51.46 | 03 11 05.0 | 80.0 | | |
| 17 | 0.93 | 11 04 51.57 | 02 47 15.7 | 2.35 | | |
| 18 | 0.44 | 11 04 57.78 | 03 00 58.2 | 3.74 | | |
| 19 | 0.08 | 11 04 59.64 | 03 15 07.1 | 2.73 | | |
| 20 | 0.08 | 11 05 01.73 | 03 12 10.5 | 1.84 | | |
| 21 | 0.92 | 11 05 01.98 | 02 47 36.2 | 3.02 | | |
| 22a/b | 0.48 | 11 05 27.40 | 03 02 35.0 | 64.2 | | |
| 23 | 0.32 | 11 05 28.59 | 03 15 44.4 | 14.4 | | |
| 24 | 0.79 | 11 05 38.27 | 02 54 07.9 | 5.11 | | |
| Abell 1189 | | | | | | |
| 1 | 0.64 | 11 07 38.38 | 01 33 31.0 | 66.8 | | |
| 2 | 0.62 | 11 07 49.54 | 01 12 23.3 | 28.7 | | |
| 3 | 0.11 | 11 08 21.62 | 01 26 09.8 | 6.93 | 2.57 | -0.82 |
| 4 | 0.16 | 11 08 23.02 | 01 27 36.7 | 13.5 | 4.52 | -0.91 |
| 5 | 0.03 | 11 08 30.68 | 01 24 39.9 | 273. | 77.7 | -1.04 |
| 6 | 0.53 | 11 08 39.80 | 01 36 53.6 | 24.0 | | |
| 7 | 0.18 | 11 08 46.55 | 01 23 31.7 | 2.61 | | |
| 8 | 0.33 | 11 08 48.31 | 01 17 25.6 | 2.84 | | |
| 9a/b | 0.26 | 11 08 49.77 | 01 27 51.3 | 4.48 | | |
| 10 | 0.47 | 11 08 53.54 | 01 33 47.8 | 22.5 | | |
| 11 | 0.55 | 11 08 54.21 | 01 36 08.2 | 2.83 | | |
| 12 | 0.29 | 11 08 56.82 | 01 25 48.9 | 16.0 | | |
| 13 | 0.48 | 11 09 04.14 | 01 16 12.4 | 29.8 | | |
| 14 | 0.90 | 11 09 41.62 | 01 36 59.3 | 30.2 | | |
| Abell 1238 | | | | | | |
| 1 | 1.21 | 11 19 31.67 | 01 10 29.7 | 9.08 | | |
| 2 | 1.40 | 11 19 40.23 | 01 05 18.1 | 22.9 | | |

| Cluster & Source | Ang. Dist. R/Rc | R.A. 1950 h m s | Dec. ° ' " | Flux Dens. 1.5 GHz mJy | 4.9 GHz mJy | Spec. Index $\alpha_{1.5}^{4.9}$ |
|---|---|---|---|---|---|---|
| .Abell 1238(cont) | | | | | | |
| 3 | 0.82 | 11 19 52.30 | 01 32 01.4 | 3.07 | | |
| 4 | 0.52 | 11 19 53.89 | 01 20 10.2 | 1.86 | | |
| 5a/b | 0.84 | 11 19 57.20 | 01 12 18.0 | 3.35 | | |
| 6 | 1.39 | 11 19 57.18 | 01 42 04.8 | 8.30 | | |
| 7 | 0.44 | 11 19 57.30 | 01 22 08.0 | 13.3 | 5.86 | -0.68 |
| 8 | 0.36 | 11 20 12.57 | 01 27 25.7 | 1.70 | 1.36 | -0.18 |
| 9 | 0.12 | 11 20 15.73 | 01 23 18.9 | 2.78 | | |
| 10 | 0.39 | 11 20 17.81 | 01 28 19.8 | 1.26 | | |
| 11a/b | 0.06 | 11 20 20.01 | 01 23 17.2 | 203. | 70.1 | -0.88 |
| 12 | 0.62 | 11 20 23.08 | 01 13 44.0 | 4.23 | | |
| 13 | 0.19 | 11 20 26.06 | 01 25 24.9 | 1.59 | | |
| 14 | 0.74 | 11 20 26.85 | 01 12 07.0 | 2.56 | | |
| 15 | 0.10 | 11 20 27.79 | 01 22 11.7 | | 0.38 | |
| 16 | 0.53 | 11 20 31.99 | 01 15 26.2 | 5.58 | | |
| 17 | 0.27 | 11 20 36.81 | 01 21 13.1 | 1.79 | | |
| 18 | 0.40 | 11 20 38.82 | 01 27 02.9 | 1.16 | | |
| 19 | 0.45 | 11 20 46.22 | 01 25 40.7 | 2.37 | | |
| 20 | 0.77 | 11 20 50.02 | 01 13 53.4 | 2.88 | | |
| 21 | 0.82 | 11 20 53.51 | 01 13 46.2 | 2.51 | | |
| 22 | 0.66 | 11 20 57.73 | 01 26 46.7 | 3.04 | | |
| 23 | 1.20 | 11 20 59.91 | 01 37 34.4 | 3.20 | | |
| 24a/b | 0.71 | 11 21 03.98 | 01 23 31.8 | 36.9 | | |
| 25 | 1.29 | 11 21 06.29 | 01 37 58.3 | 2.45 | | |
| 26 | 1.22 | 11 21 33.00 | 01 25 29.9 | 2.75 | | |
| 27 | 1.37 | 11 21 33.25 | 01 13 27.6 | 3.88 | | |
| Abell 1273 | | | | | | |
| 1 | 0.71 | 11 26 23.71 | -06 51 01.2 | 20.3 | 6.43 | -0.96 |
| 2 | 1.06 | 11 26 26.67 | -06 56 49.9 | 32.2 | | |
| 3 | 0.37 | 11 26 34.62 | -06 48 03.8 | | 2.98 | |
| 4 | 0.36 | 11 26 34.78 | -06 47 58.0 | 7.90 | | |
| 5 | 0.22 | 11 26 40.28 | -06 46 47.4 | 487. | 133. | -1.08 |
| 6 | 0.18 | 11 26 44.58 | -06 45 00.2 | 2.71 | | |
| 7 | 0.18 | 11 26 44.92 | -06 44 54.0 | | 1.51 | |
| 8 | 0.97 | 11 27 24.07 | -06 39 38.3 | 12.2 | | |
| 9 | 1.54 | 11 27 35.32 | -06 33 19.0 | 27.7 | | |
| Abell 1620 | | | | | | |
| 1 | 0.61 | 12 46 51.11 | -01 31 56.7 | 33.2 | | |
| Abell 1620(cont) | | | | | | |
| 2 | 0.26 | 12 47 18.14 | -01 13 42.8 | 14.8 | 5.52 | -0.82 |
| 3a/b | 0.25 | 12 47 30.05 | -01 16 11.5 | 330. | 135. | -0.74 |
| 4 | 0.29 | 12 47 36.90 | -01 20 07.6 | | 5.19 | |
| 5 | 0.58 | 12 47 56.23 | -01 25 42.0 | 22.3 | | |
| 6 | 0.58 | 12 47 57.30 | -01 13 11.9 | 3.39 | | |
| 7 | 0.57 | 12 47 59.86 | -01 15 30.0 | 7.98 | | |
| 8 | 0.88 | 12 48 25.59 | -01 12 40.6 | 16.7 | | |
| 9 | 0.97 | 12 48 35.53 | -01 14 01.7 | 23.6 | | |
| Abell 1631 | | | | | | |
| 1a/b | 0.72 | 12 49 18.76 | -14 54 10.5 | 22.9 | | |
| 2 | 0.94 | 12 49 19.82 | -14 46 35.7 | 26.6 | | |
| 3a/b | 0.49 | 12 49 32.91 | -15 20 19.2 | 6.00 | | |
| 4a/b | 0.30 | 12 49 37.69 | -15 07 27.2 | 65.0 | | |
| 5 | 0.38 | 12 49 39.24 | -15 02 45.5 | 12.2 | | |
| 6 | 0.52 | 12 49 54.02 | -14 55 54.9 | 20.4 | | |
| 7 | 0.17 | 12 49 54.32 | -15 12 31.0 | 16.4 | | |
| 8a/b | 0.36 | 12 49 55.99 | -15 00 30.3 | 1.29 | | |
| 9 | 0.72 | 12 49 59.99 | -14 49 59.4 | 14.5 | | |
| 10 | 0.47 | 12 50 02.06 | -14 57 08.8 | 7.90 | | |
| 11 | 0.35 | 12 50 05.31 | -15 00 15.9 | 1.53 | | |
| 12 | 0.09 | 12 50 05.72 | -15 07 56.8 | 1.04 | | |
| 13 | 0.06 | 12 50 06.88 | -15 11 27.5 | 2.61 | | |
| 14 | 0.41 | 12 50 07.37 | -14 58 33.9 | 1.04 | | |
| 15 | 0.72 | 12 50 12.13 | -14 49 55.7 | 1.41 | | |
| 16 | 0.06 | 12 50 17.43 | -15 09 38.7 | 0.78 | | |
| 17a/b | 0.22 | 12 50 17.46 | -15 04 07.6 | 260. | 90.7 | -0.87 |
| 18a/b | 0.21 | 12 50 24.53 | -15 05 13.3 | 26.8 | 9.09 | -0.90 |
| 19 | 0.24 | 12 50 35.92 | -15 07 20.7 | 0.77 | | |
| 20 | 0.48 | 12 51 05.46 | -15 13 00.3 | 4.71 | | |
| 21 | 0.55 | 12 51 13.52 | -15 13 38.5 | 10.2 | | |
| 22 | 0.90 | 12 51 15.99 | -14 50 06.1 | 13.2 | | |
| 23 | 0.77 | 12 51 17.21 | -14 55 27.8 | 3.24 | | |
| 24 | 0.75 | 12 51 22.90 | -14 58 16.5 | 3.39 | | |
| Abell 3528 | | | | | | |
| 1a/b | 0.22 | 12 51 58.63 | -28 57 26.5 | 1251 | 202. | -1.52 |
| 2a/b | 0.32 | 12 52 09.39 | -29 00 09.3 | | 19.4 | |
| 3 | 0.25 | 12 52 23.61 | -28 55 03.8 | | 6.87 | |

| Cluster & Source | Ang. Dist. R/Rc | R.A. 1950 h m s | Dec. ° ' " | Flux Dens. 1.5 GHz mJy | Flux Dens. 4.9 GHz mJy | Spec. Index $\alpha_{1.5}^{4.9}$ |
|---|---|---|---|---|---|---|
| Abell 1689 | | | | | | |
| 1 | 1.85 | 13 07 50.08 | -00 54 34.3 | 24.2 | | |
| 2a/b | 1.86 | 13 07 52.04 | -00 53 44.5 | 86.4 | | |
| 3 | 1.20 | 13 08 05.39 | -01 08 46.2 | 1.36 | | |
| 4 | 1.57 | 13 08 11.12 | -00 53 15.3 | 6.24 | | |
| 5 | 0.94 | 13 08 21.39 | -01 11 27.6 | 3.35 | | |
| 6 | 0.94 | 13 08 21.39 | -01 11 27.6 | 3.35 | | |
| 7 | 0.93 | 13 08 40.58 | -01 15 49.7 | 11.6 | | |
| 8 | 0.58 | 13 08 40.61 | -01 01 43.6 | 1.05 | | |
| 9 | 1.06 | 13 08 41.88 | -01 17 32.9 | 12.4 | | |
| 10 | 0.78 | 13 08 51.53 | -01 15 02.6 | 1.47 | | |
| 11 | 0.12 | 13 08 53.07 | -01 06 05.7 | 1.10 | | |
| 12 | 0.13 | 13 08 54.86 | -01 05 16.1 | 3.96 | 0.74 | -1.39 |
| 13 | 0.18 | 13 08 55.81 | -01 04 33.5 | 10.4 | 2.75 | -1.11 |
| 14 | 0.23 | 13 08 57.21 | -01 03 50.8 | 3.24 | 0.75 | -1.21 |
| 15 | 0.25 | 13 08 57.35 | -01 03 35.9 | 41.1 | 10.7 | -1.12 |
| 16 | 1.04 | 13 09 02.82 | -01 18 05.8 | 4.17 | | |
| 17 | 0.99 | 13 09 03.30 | -01 17 25.3 | 14.8 | | |
| 18 | 0.25 | 13 09 08.00 | -01 07 48.5 | 11.5 | 6.46 | -0.48 |
| 19a/b | 0.35 | 13 09 09.26 | -01 03 34.1 | 11.7 | 5.93 | -0.57 |
| 20 | 0.64 | 13 09 15.57 | -01 12 09.0 | 2.57 | | |
| 21 | 1.32 | 13 09 26.71 | -01 19 26.6 | 4.29 | | |
| 22 | 1.24 | 13 09 26.77 | -01 18 25.5 | 43.3 | | |
| 23 | 1.04 | 13 09 31.95 | -00 58 18.9 | 6.81 | | |
| Abell 1772 | | | | | | |
| 1 | 1.40 | 13 38 17.54 | -10 43 05.2 | 5.27 | | |
| 2 | 1.30 | 13 38 20.15 | -10 57 15.0 | 4.59 | | |
| 3 | 1.38 | 13 38 41.31 | -11 05 51.6 | 19.1 | | |
| 4 | 0.83 | 13 38 44.44 | -10 47 12.9 | 3.77 | | |
| 5 | 1.05 | 13 38 52.56 | -10 39 42.0 | 12.7 | | |
| 6 | 0.65 | 13 39 05.89 | -10 58 01.4 | 4.46 | | |
| 7a/b | 0.02 | 13 39 26.58 | -10 51 17.8 | 188. | 49.7 | -1.10 |
| 8 | 0.70 | 13 39 55.79 | -10 57 17.0 | 1.07 | | |
| 9a/b | 0.72 | 13 40 02.88 | -10 54 57.7 | 2.08 | | |
| 10 | 0.93 | 13 40 14.37 | -10 46 33.8 | 41.5 | | |
| 11 | 0.97 | 13 40 14.38 | -10 45 08.8 | 58.7 | | |
| 12 | 1.13 | 13 40 27.24 | -10 47 41.4 | 3.65 | | |

| Cluster & Source | Ang. Dist. R/Rc | R.A. 1950 h m s | Dec. ° ' " | Flux Dens. 1.5 GHz mJy | Flux Dens. 4.9 GHz mJy | Spec. Index $\alpha_{1.5}^{4.9}$ |
|---|---|---|---|---|---|---|
| Abell 1775 | | | | | | |
| 1 | 0.71 | 13 38 20.03 | 26 26 57.2 | 2.27 | | |
| 2 | 0.60 | 13 38 27.70 | 26 30 30.6 | 1.46 | | |
| 3 | 0.54 | 13 38 37.07 | 26 44 20.3 | 24.0 | | |
| 4 | 0.71 | 13 38 38.19 | 26 52 11.0 | 22.7 | | |
| 5 | 0.38 | 13 38 54.59 | 26 32 09.7 | 1.06 | | |
| 6 | 0.31 | 13 39 07.46 | 26 42 37.4 | 4.40 | | |
| 7 | 0.17 | 13 39 22.25 | 26 40 24.4 | | 0.66 | |
| 8 | 0.46 | 13 39 29.37 | 26 24 08.1 | 10.1 | | |
| 9 | 0.66 | 13 39 30.31 | 26 55 35.1 | 2.79 | | |
| 10a/b | 0.05 | 13 39 31.13 | 26 37 29.3 | 331. | 95.7 | -1.03 |
| 11 | 0.58 | 13 39 31.55 | 26 53 25.4 | 3.23 | | |
| 12 | 0.63 | 13 39 31.67 | 26 19 18.9 | 3.71 | | |
| 13 | 0.57 | 13 39 37.98 | 26 21 00.2 | 39.5 | | |
| 14 | 0.64 | 13 39 44.76 | 26 19 02.8 | 8.33 | | |
| 15 | 0.32 | 13 39 49.13 | 26 45 46.7 | 6.56 | | |
| 16 | 0.35 | 13 40 01.96 | 26 28 56.4 | 0.82 | | |
| 17 | 0.26 | 13 40 08.75 | 26 39 18.8 | 4.82 | | |
| 18 | 0.27 | 13 40 09.53 | 26 34 37.4 | 1.28 | | |
| 19 | 0.45 | 13 40 16.62 | 26 46 05.4 | 6.72 | | |
| 20 | 0.71 | 13 40 32.00 | 26 21 12.1 | 30.8 | | |
| Abell 1791 | | | | | | |
| 1 | 0.18 | 13 45 48.03 | -25 10 54.2 | | 1.50 | |
| 2a | 0.02 | 13 46 05.09 | -25 12 20.3 | 100. | 34.8 | -0.88 |
| 2b | 0.03 | 13 46 09.09 | -25 12 12.9 | 64.8 | 15.5 | -1.19 |
| Abell 1913 | | | | | | |
| 1 | 0.65 | 14 23 36.33 | 17 01 28.6 | 14.9 | | |
| 2 | 0.61 | 14 23 40.67 | 16 46 57.3 | 18.3 | | |
| 3 | 0.53 | 14 23 42.87 | 16 58 30.7 | 4.27 | | |
| 4 | 0.39 | 14 23 52.88 | 16 54 34.8 | 4.88 | | |
| 5 | 0.68 | 14 24 01.33 | 17 07 53.5 | 6.79 | | |
| 6 | 0.27 | 14 24 10.84 | 16 58 17.9 | 12.9 | | |
| 7 | 0.49 | 14 24 11.35 | 17 04 15.2 | 4.70 | | |
| 8 | 0.26 | 14 24 12.34 | 16 58 29.8 | 21.9 | | |
| 9 | 0.24 | 14 24 15.50 | 16 58 25.4 | 1.57 | | |
| 10 | 0.32 | 14 24 16.04 | 16 47 44.1 | 4.59 | | |
| 11 | 0.12 | 14 24 20.34 | 16 52 25.4 | 15.7 | 3.40 | -1.27 |

| Cluster & Source | Ang. Dist. R/Rc | R.A. 1950 h m s | Dec. ° ' " | Flux Dens. 1.5 GHz mJy | 4.9 GHz mJy | Spec. Index $\alpha_{1.5}^{4.9}$ |
|---|---|---|---|---|---|---|
| Abell 1913(cont) | | | | | | |
| 12 | 0.10 | 14 24 23.75 | 16 56 04.9 | 0.68 | | |
| 13 | 0.27 | 14 24 30.29 | 16 48 12.7 | 0.96 | | |
| 14a/b | 0.17 | 14 24 40.30 | 16 56 44.9 | 136. | 47.3 | -0.88 |
| 15 | 0.55 | 14 24 50.85 | 17 05 20.1 | 1.38 | | |
| 16a/b | 0.43 | 14 24 56.01 | 16 47 07.2 | 58.1 | | |
| 17 | 0.78 | 14 24 57.00 | 17 10 27.3 | 3.94 | | |
| 18 | 0.37 | 14 24 57.43 | 16 59 03.8 | 1.32 | 0.65 | -0.58 |
| 19 | 0.87 | 14 24 59.51 | 17 12 21.8 | 7.96 | | |
| 20 | 0.41 | 14 25 01.99 | 16 49 18.0 | 12.7 | | |
| 21 | 0.74 | 14 25 27.33 | 17 03 14.8 | 3.94 | | |
| 22a/b | 0.67 | 14 25 31.13 | 16 51 40.1 | 77.2 | | |
| 23 | 0.70 | 14 25 34.91 | 16 54 31.6 | 3.64 | | |
| 24 | 0.93 | 14 25 39.06 | 17 06 45.1 | 4.07 | | |
| 25 | 1.01 | 14 25 49.58 | 16 42 18.4 | 22.3 | | |
| Abell 2009 | | | | | | |
| 1 | 1.43 | 14 57 20.62 | 21 21 04.5 | 16.0 | | |
| 2 | 1.11 | 14 57 24.65 | 21 24 56.3 | 1.84 | | |
| 3 | 0.54 | 14 57 36.39 | 21 36 41.6 | 1.18 | | |
| 4 | 0.99 | 14 57 36.46 | 21 24 39.9 | 0.80 | | |
| 5 | 0.46 | 14 57 38.95 | 21 32 37.9 | 5.81 | 1.91 | -0.92 |
| 6 | 0.71 | 14 57 44.53 | 21 41 27.7 | 6.52 | | |
| 7 | 1.52 | 14 57 47.90 | 21 51 09.9 | 4.22 | | |
| 8 | 0.75 | 14 57 49.29 | 21 42 17.9 | 1.00 | | |
| 9 | 0.80 | 14 57 49.40 | 21 42 55.2 | 0.65 | | |
| 10 | 0.22 | 14 57 59.59 | 21 36 48.6 | 0.52 | | |
| 11 | 1.01 | 14 58 00.82 | 21 45 35.4 | 2.37 | | |
| 12a/b | 0.11 | 14 58 02.67 | 21 35 25.7 | 43.2 | 2.16 | -2.49 |
| 13 | 0.09 | 14 58 04.23 | 21 34 01.5 | 21.7 | 6.37 | -1.02 |
| 14 | 0.12 | 14 58 05.30 | 21 34 46.8 | | 0.88 | |
| 15 | 0.81 | 14 58 07.22 | 21 43 14.6 | 0.51 | | |
| 16 | 0.27 | 14 58 13.01 | 21 34 54.8 | | 0.60 | |
| 17 | 0.97 | 14 58 19.48 | 21 44 14.6 | 9.12 | | |
| 18 | 1.30 | 14 58 40.98 | 21 23 08.8 | 3.34 | | |
| 19 | 1.49 | 14 58 53.06 | 21 45 34.7 | 8.22 | | |
| 20 | 1.35 | 14 59 04.58 | 21 36 45.0 | 33.7 | | |
| 21 | 1.78 | 14 59 05.95 | 21 47 12.9 | 53.3 | | |
| 22 | 1.41 | 14 59 07.68 | 21 36 27.8 | 2.78 | | |
| 23 | 1.93 | 14 59 08.03 | 21 19 21.1 | 8.82 | | |
| Abell 2009(cont) | | | | | | |
| 24 | 2.02 | 14 59 11.38 | 21 18 50.6 | 4.27 | | |
| 25a/b | 1.84 | 14 59 13.12 | 21 46 11.9 | 182. | | |
| 26 | 1.56 | 14 59 15.16 | 21 36 19.5 | 4.00 | | |
| 27 | 2.05 | 14 59 23.34 | 21 46 46.7 | 6.92 | | |
| Abell 2029 | | | | | | |
| 1 | 0.11 | 15 08 19.68 | 05 57 12.6 | | 0.61 | |
| 2a/b | 0.06 | 15 08 27.33 | 05 55 58.9 | 385. | 57.5 | -1.58 |
| 3 | 0.09 | 15 08 29.72 | 05 55 09.4 | | 2.32 | |
| 4 | 0.15 | 15 08 31.72 | 06 00 36.7 | 2.23 | 4.95 | 0.66 |
| 5 | 0.22 | 15 08 37.64 | 05 52 40.5 | | 1.80 | |
| Abell 2052 | | | | | | |
| 1 | 0.03 | 15 14 17.03 | 07 12 16.8 | 5169 | 868. | -1.48 |
| 2 | 0.46 | 15 14 34.00 | 07 20 58.6 | 34.6 | | |
| ZW 1518.8 | | | | | | |
| 1 | 0.21 | 15 18 18.82 | 07 43 14.5 | 374. | | |
| 2 | 0.59 | 15 18 21.10 | 08 08 18.8 | 6.50 | | |
| 3 | 0.42 | 15 18 35.20 | 08 02 44.7 | 0.99 | | |
| 4 | 0.11 | 15 18 43.07 | 07 51 09.4 | 0.55 | | |
| 5 | 0.11 | 15 19 01.34 | 07 49 18.3 | 2.05 | 0.58 | -1.05 |
| 6 | 0.19 | 15 19 01.67 | 07 53 30.6 | 0.57 | | |
| 7 | 0.46 | 15 19 13.50 | 08 03 18.9 | 43.5 | | |
| 8 | 0.26 | 15 19 14.80 | 07 54 07.9 | | 0.40 | |
| 9 | 0.28 | 15 19 15.70 | 07 55 03.5 | 7.47 | 2.81 | -0.81 |
| 10 | 0.26 | 15 19 16.24 | 07 39 59.4 | 0.80 | | |
| 11a/b | 0.27 | 15 19 24.02 | 07 52 19.1 | 79.2 | 7.30 | -1.98 |
| 12 | 0.41 | 15 19 37.25 | 07 37 18.8 | 0.82 | | |
| 13 | 0.35 | 15 19 41.94 | 07 45 11.7 | 5.21 | | |
| 14 | 0.45 | 15 19 46.81 | 07 56 02.7 | 2.86 | | |
| 15 | 0.51 | 15 19 51.62 | 07 58 23.0 | 1.94 | | |
| 16a/b | 0.72 | 15 19 52.33 | 08 09 12.9 | 3.53 | | |
| 17 | 0.48 | 15 19 55.00 | 07 54 18.5 | 2.10 | | |
| 18 | 0.77 | 15 19 56.25 | 08 11 04.5 | 3.65 | | |
| 19 | 0.51 | 15 19 56.64 | 07 56 17.0 | 0.68 | | |
| 20 | 0.45 | 15 19 57.13 | 07 48 46.5 | 1.96 | | |
| 21 | 0.46 | 15 19 57.36 | 07 44 12.0 | 89.3 | | |
| 22 | 0.65 | 15 20 03.64 | 08 03 16.1 | 0.91 | | |

| Cluster & Source | Ang. Dist. R/Rc | R.A. 1950 h m s | Dec. ° ' " | Flux Dens. 1.5 GHz mJy | Flux Dens. 4.9 GHz mJy | Spec. Index $\alpha_{1.5}^{4.9}$ |
|---|---|---|---|---|---|---|
| ZW1518.8(cont) | | | | | | |
| 23 | 0.65 | 15 20 27.81 | 07 48 43.9 | 2.24 | | |
| Abell 2082 | | | | | | |
| 1 | 0.10 | 15 28 08.63 | 03 39 52.4 | 6.48 | | |
| 2 | 0.21 | 15 28 17.55 | 03 32 02.0 | 4.96 | | |
| 3a/b | 0.21 | 15 28 19.51 | 03 42 18.0 | 15.0 | | |
| 4 | 0.21 | 15 28 30.18 | 03 35 05.2 | 1.53 | | |
| 5 | 0.52 | 15 28 36.40 | 03 49 04.0 | 2.43 | | |
| 6 | 0.34 | 15 28 42.20 | 03 41 12.0 | 90.5 | 29.2 | -0.94 |
| 7 | 0.66 | 15 28 49.21 | 03 51 30.5 | 3.67 | | |
| 8 | 0.91 | 15 28 49.71 | 03 58 32.6 | 20.3 | | |
| 9 | 0.51 | 15 28 57.26 | 03 31 09.1 | 4.26 | | |
| 10a/b | 0.62 | 15 28 57.44 | 03 48 07.6 | 95.9 | 30.1 | -0.96 |
| 11 | 0.55 | 15 28 58.35 | 03 44 59.9 | 4.38 | 2.09 | -0.61 |
| 12 | 0.65 | 15 29 01.35 | 03 48 21.6 | 23.9 | 2.40 | -1.91 |
| 13 | 0.52 | 15 29 04.27 | 03 35 58.2 | 143. | | |
| 14 | 0.81 | 15 29 19.37 | 03 49 10.6 | 4.95 | | |
| 15 | 0.73 | 15 29 25.29 | 03 39 24.7 | 6.75 | | |
| 16 | 0.80 | 15 29 29.55 | 03 43 27.8 | 2.97 | | |
| 17 | 0.78 | 15 29 30.97 | 03 39 53.6 | 2.60 | | |
| 18 | 1.01 | 15 29 36.27 | 03 52 08.4 | 197. | | |
| 19 | 0.90 | 15 29 42.56 | 03 41 35.1 | 19.7 | | |
| 20 | 1.09 | 15 30 01.57 | 03 31 36.2 | 24.4 | | |
| Abell 2091 | | | | | | |
| 1a/b | 1.58 | 15 31 16.21 | 10 35 37.1 | 6.49 | | |
| 2 | 0.77 | 15 31 24.81 | 10 24 34.7 | 2.54 | | |
| 3 | 1.87 | 15 31 27.33 | 10 09 14.9 | 5.28 | | |
| 4 | 1.85 | 15 31 41.80 | 10 08 23.2 | 5.58 | | |
| 5 | 0.59 | 15 31 43.50 | 10 29 27.5 | 15.3 | 5.35 | -0.87 |
| 6a/b | 0.22 | 15 31 54.46 | 10 26 36.3 | 281. | 68.1 | -1.18 |
| 7a/b | 0.35 | 15 31 57.83 | 10 21 51.6 | 16.4 | 5.74 | -0.87 |
| 8 | 0.36 | 15 32 00.41 | 10 27 19.7 | 40.1 | 12.7 | -0.96 |
| 9 | 0.57 | 15 32 01.86 | 10 29 21.1 | 1.29 | 0.88 | -0.32 |
| 10 | 1.56 | 15 32 08.31 | 10 11 17.5 | 2.87 | | |
| 11 | 0.78 | 15 32 12.66 | 10 19 46.6 | 2.21 | | |
| 12 | 0.79 | 15 32 18.14 | 10 27 58.0 | 3.44 | | |
| 13 | 1.79 | 15 32 25.00 | 10 10 49.0 | 7.41 | | |
| 14 | 1.07 | 15 32 31.63 | 10 23 50.0 | 50.8 | | |
| Abell 2091(cont) | | | | | | |
| 15 | 1.23 | 15 32 37.41 | 10 24 03.2 | 2.08 | | |
| 16 | 1.49 | 15 32 38.57 | 10 31 47.6 | 9.65 | | |
| 17 | 1.75 | 15 32 53.51 | 10 29 16.0 | 4.93 | | |
| 18 | 1.78 | 15 32 55.40 | 10 28 33.6 | 4.46 | | |
| 19 | 1.81 | 15 32 57.05 | 10 28 01.4 | 11.6 | | |
| Abell 2094 | | | | | | |
| 1 | 1.62 | 15 33 00.40 | -01 42 34.8 | 4.69 | | |
| 2 | 1.33 | 15 33 12.01 | -01 44 04.7 | 216. | | |
| 3 | 0.51 | 15 33 40.25 | -01 50 52.7 | 105. | 29.4 | -1.06 |
| 4 | 0.51 | 15 33 41.29 | -01 50 13.7 | 1.76 | | |
| 5a/b | 0.31 | 15 33 55.25 | -01 55 01.9 | 152. | 43.6 | -1.04 |
| 6 | 0.18 | 15 34 03.07 | -01 50 04.4 | 0.99 | | |
| 7 | 0.47 | 15 34 06.20 | -01 46 53.6 | 11.1 | 4.11 | -0.82 |
| 8 | 1.18 | 15 34 07.50 | -01 38 57.5 | 3.02 | | |
| 9a/b | 0.12 | 15 34 07.76 | -01 51 42.7 | 212. | 83.2 | -0.77 |
| 10 | 0.30 | 15 34 10.50 | -01 49 24.7 | 4.45 | 0.53 | -1.77 |
| 11 | 0.66 | 15 34 13.05 | -01 45 09.6 | 19.7 | 5.75 | -1.02 |
| 12a/b | 0.93 | 15 34 18.46 | -02 01 44.1 | 9.09 | | |
| 13 | 1.38 | 15 34 24.59 | -02 06 38.0 | 8.80 | | |
| 14 | 1.23 | 15 34 29.56 | -01 40 05.1 | 2.30 | | |
| 15 | 1.33 | 15 34 36.53 | -01 39 45.4 | 2.82 | | |
| 16 | 1.05 | 15 34 38.43 | -01 59 48.1 | 2.17 | | |
| 17 | 1.03 | 15 34 40.53 | -01 58 49.2 | 4.40 | | |
| 18 | 1.46 | 15 34 49.65 | -02 03 39.2 | 3.32 | | |
| 19 | 1.06 | 15 34 49.96 | -01 53 20.3 | 8.56 | | |
| Abell 2103 | | | | | | |
| 1 | 0.95 | 15 35 49.22 | -01 51 55.8 | 7.94 | | |
| 2 | 0.74 | 15 36 15.20 | -02 10 30.3 | 17.5 | | |
| 3 | 0.78 | 15 36 15.63 | -02 12 26.9 | 5.08 | | |
| 4 | 0.65 | 15 36 16.84 | -02 05 46.6 | 2.02 | | |
| 5 | 0.77 | 15 36 18.85 | -02 13 07.7 | 4.65 | | |
| 6a/b | 0.54 | 15 36 26.04 | -02 01 46.1 | 419. | 137. | -0.93 |
| 7 | 0.55 | 15 36 28.00 | -02 05 21.9 | 2.82 | 1.67 | -0.43 |
| 8 | 0.40 | 15 36 42.33 | -02 03 53.1 | 3.45 | | |
| 9 | 0.53 | 15 37 16.84 | -02 14 25.3 | 17.1 | | |
| 10 | 0.23 | 15 37 17.20 | -02 06 36.6 | 8.18 | | |
| 11a/b | 0.18 | 15 37 22.69 | -02 05 16.8 | 70.9 | | |

| Cluster & Source | Ang. Dist. R/Rc | R.A. 1950 h m s | Dec. ° ' " | Flux Dens. 1.5 GHz mJy | Flux Dens. 4.9 GHz mJy | Spec. Index $\alpha_{1.5}^{4.9}$ |
|---|---|---|---|---|---|---|
| Abell 2108 | | | | | | |
| 1 | 0.65 | 15 37 29.24 | 18 12 37.2 | 7.00 | | |
| 2 | 0.23 | 15 37 57.27 | 18 06 13.0 | 16.1 | | |
| 3 | 0.26 | 15 38 02.82 | 18 01 02.0 | 3.95 | | |
| 4 | 0.28 | 15 38 06.02 | 18 02 22.6 | 67.1 | | |
| 5 | 0.84 | 15 38 43.36 | 18 05 24.0 | 44.7 | | |
| 6 | 1.19 | 15 38 48.91 | 18 15 25.1 | 245. | 91.5 | -0.82 |
| 7 | 1.13 | 15 38 53.51 | 18 11 58.8 | 4.44 | 0.94 | -1.29 |
| 8 | 1.49 | 15 39 00.68 | 18 19 16.5 | 25.8 | | |
| 9 | 1.20 | 15 39 06.68 | 18 07 23.7 | 1.39 | | |
| 10 | 1.42 | 15 39 10.88 | 18 14 12.0 | 2.42 | | |
| 11 | 1.54 | 15 39 11.80 | 18 17 24.7 | 1.25 | | |
| 12 | 1.94 | 15 39 27.52 | 18 22 54.2 | 2.03 | | |
| 13 | 1.70 | 15 39 41.30 | 18 06 20.0 | 2.39 | | |
| 14 | 1.71 | 15 39 42.23 | 18 04 18.2 | 1.80 | | |
| 15 | 1.84 | 15 39 46.32 | 18 11 31.2 | 14.0 | | |
| 16a/b | 1.86 | 15 39 51.00 | 17 59 17.4 | 101. | | |
| 17 | 1.99 | 15 40 00.10 | 18 06 59.2 | 5.05 | | |
| 18 | 2.11 | 15 40 02.98 | 18 13 08.5 | 3.09 | | |
| 19 | 2.03 | 15 40 03.70 | 18 05 40.3 | 453. | | |
| 20 | 2.07 | 15 40 05.83 | 18 06 41.9 | 6.90 | | |
| Abell 2151 | | | | | | |
| 1a/b | 0.99 | 16 03 25.66 | 18 20 12.9 | 65.3 | | |
| 2 | 0.56 | 16 03 52.08 | 18 02 08.6 | 7.92 | | |
| 3 | 1.11 | 16 03 52.91 | 18 21 18.4 | 5.47 | | |
| 4 | 1.06 | 16 04 00.35 | 18 18 58.9 | 5.56 | | |
| 5a/b | 1.19 | 16 04 01.71 | 18 23 00.5 | 299. | | |
| 6 | 1.34 | 16 04 04.57 | 18 27 24.8 | 2.99 | | |
| 7a/b | 1.14 | 16 04 14.27 | 18 19 22.4 | 18.7 | 4.10 | -1.26 |
| 8 | 1.28 | 16 04 14.49 | 18 24 04.5 | 2.89 | | |
| 9 | 1.70 | 16 04 18.86 | 18 36 48.0 | 3.67 | | |
| 10 | 1.15 | 16 04 27.31 | 18 17 39.1 | 15.5 | 6.14 | -0.77 |
| 11 | 0.97 | 16 04 31.75 | 18 08 51.9 | 36.3 | | |
| 12 | 1.29 | 16 04 42.45 | 18 19 30.2 | 290. | 76.3 | -1.11 |
| 13 | 1.07 | 16 04 42.60 | 18 09 59.9 | 2.21 | | |
| 14 | 1.11 | 16 04 51.92 | 18 08 14.9 | 3.34 | | |
| 15 | 1.46 | 16 04 57.28 | 18 22 43.0 | 6.84 | 3.03 | -0.68 |
| 16 | 1.76 | 16 04 59.90 | 18 33 09.0 | 4.41 | | |
| Abell 2151(cont) | | | | | | |
| 17 | 1.25 | 16 05 17.42 | 18 04 59.2 | 14.2 | | |
| 18 | 1.99 | 16 05 24.59 | 18 36 42.8 | 7.87 | | |
| Abell 2249 | | | | | | |
| 1 | 0.52 | 17 07 23.77 | 34 20 08.7 | 2.85 | | |
| 2 | 0.52 | 17 07 23.77 | 34 20 08.7 | 2.90 | | |
| 3a/b | 0.10 | 17 07 49.84 | 34 29 33.4 | 598. | 196. | -0.93 |
| 4 | 0.74 | 17 07 58.45 | 34 12 38.7 | 8.87 | | |
| 5 | 0.15 | 17 08 10.59 | 34 34 22.0 | 17.2 | 4.47 | -1.12 |
| 6 | 0.66 | 17 08 23.62 | 34 15 33.1 | 46.9 | | |
| 7 | 0.50 | 17 08 52.83 | 34 25 49.8 | 18.5 | | |
| 8 | 0.64 | 17 08 57.36 | 34 42 28.6 | 47.0 | | |
| 9 | 0.73 | 17 09 23.09 | 34 25 45.8 | 8.19 | | |
| Abell 2354 | | | | | | |
| 1 | 1.74 | 21 31 57.88 | -15 18 56.0 | 6.63 | | |
| 2 | 1.39 | 21 32 23.95 | -15 20 24.6 | 3.08 | | |
| 3 | 0.72 | 21 32 33.71 | -15 09 50.6 | 1.75 | | |
| 4a/b | 0.57 | 21 32 40.47 | -15 08 38.6 | 39.2 | | |
| 5a/b | 0.40 | 21 32 50.73 | -15 06 40.3 | 12.5 | | |
| 6 | 0.43 | 21 32 52.37 | -15 12 07.3 | 107. | | |
| 7 | 0.46 | 21 33 00.23 | -15 13 44.0 | 2.47 | | |
| 8 | 0.24 | 21 33 02.91 | -15 06 17.9 | 27.0 | | |
| 9 | 0.71 | 21 33 05.17 | -15 00 47.2 | 1.01 | | |
| 10a/b | 0.50 | 21 33 11.87 | -15 14 13.3 | 6.13 | | |
| 11a/b | 0.13 | 21 33 13.11 | -15 08 57.4 | 2.58 | | |
| 12 | 0.89 | 21 33 17.68 | -14 59 09.2 | 4.55 | | |
| 13 | 0.35 | 21 33 22.23 | -15 07 21.8 | 0.86 | | |
| 14 | 1.33 | 21 33 43.84 | -15 20 45.9 | 3.53 | | |
| Abell 2396 | | | | | | |
| 1 | 0.96 | 21 52 46.16 | 12 20 41.0 | 5.46 | | |
| 2 | 0.82 | 21 52 49.76 | 12 19 51.9 | 8.45 | | |
| 3 | 0.44 | 21 53 00.57 | 12 14 11.6 | 21.1 | 3.87 | -1.41 |
| 4 | 0.38 | 21 53 06.82 | 12 18 38.6 | 2.98 | 1.50 | -0.57 |
| 5 | 1.87 | 21 53 07.85 | 12 32 30.0 | 29.1 | | |
| 6a/b | 0.15 | 21 53 16.02 | 12 17 13.3 | 482. | 123. | -1.13 |
| 7 | 1.20 | 21 53 17.06 | 12 05 16.2 | 3.42 | | |
| 8 | 0.31 | 21 53 17.77 | 12 18 35.8 | 27.1 | 8.54 | -0.96 |

| Cluster & Source | Ang. Dist. R/Rc | R.A. 1950 h m s | Dec. ° ' " | Flux Dens. 1.5 GHz mJy | 4.9 GHz mJy | Spec. Index $\alpha_{1.5}^{4.9}$ |
|---|---|---|---|---|---|---|
| Abell 2396(cont) | | | | | | |
| 9 | 0.53 | 21 53 26.56 | 12 12 04.6 | 3.08 | | |
| 10 | 1.21 | 21 53 56.88 | 12 12 23.3 | 5.45 | | |
| 11 | 1.79 | 21 54 09.05 | 12 06 56.0 | 23.6 | | |
| 12 | 1.61 | 21 54 12.23 | 12 19 30.7 | 4.25 | | |
| 13 | 1.76 | 21 54 19.02 | 12 17 45.0 | 14.6 | | |
| Abell 2399 | | | | | | |
| 1 | 1.73 | 21 53 05.37 | -08 37 19.8 | 11.4 | | |
| 2 | 1.26 | 21 53 06.05 | -08 19 36.2 | 13.2 | | |
| 3 | 1.73 | 21 53 08.83 | -08 37 43.3 | 10.3 | | |
| 4 | 1.60 | 21 53 14.05 | -08 34 44.8 | 9.04 | | |
| 5 | 1.89 | 21 53 18.69 | -08 44 18.9 | 24.9 | | |
| 6 | 1.50 | 21 53 26.10 | -08 33 44.2 | 25.6 | | |
| 7 | 1.21 | 21 54 04.98 | -08 30 37.9 | 4.24 | | |
| 8 | 1.26 | 21 54 10.71 | -08 32 25.7 | 181. | | |
| 9 | 1.55 | 21 54 17.79 | -08 40 47.0 | 2.41 | | |
| 10 | 0.59 | 21 54 29.68 | -08 15 44.6 | 43.6 | | |
| Abell 2443 | | | | | | |
| 1a/b | 1.30 | 22 22 37.32 | 17 10 08.0 | 6.63 | | |
| 2a/b | 1.15 | 22 22 48.07 | 16 59 43.4 | 4.44 | | |
| 3 | 1.03 | 22 22 48.89 | 17 05 22.5 | 36.1 | | |
| 4 | 1.75 | 22 22 52.28 | 16 47 44.2 | 8.48 | | |
| 5 | 1.38 | 22 23 10.03 | 16 50 33.9 | 2.83 | | |
| 6 | 1.06 | 22 23 10.27 | 17 16 31.2 | 1.24 | | |
| 7 | 0.22 | 22 23 36.23 | 17 08 14.1 | 88.8 | 29.1 | -0.93 |
| 8 | 0.21 | 22 23 36.97 | 17 03 34.0 | 1.03 | | |
| 9 | 0.15 | 22 23 37.02 | 17 07 19.2 | 51.3 | 13.3 | -1.12 |
| 10 | 0.70 | 22 23 37.88 | 16 57 16.3 | 1.46 | | |
| 11 | 0.15 | 22 23 41.65 | 17 03 59.8 | 25.1 | 10.3 | -0.74 |
| 12 | 0.03 | 22 23 42.75 | 17 06 06.5 | 34.2 | 9.15 | -1.09 |
| 13 | 1.19 | 22 23 45.05 | 17 20 32.5 | 3.15 | | |
| 14 | 0.97 | 22 23 56.42 | 16 54 24.6 | 1.65 | | |
| 15 | 1.58 | 22 23 59.33 | 17 24 52.7 | 6.63 | | |
| 16 | 1.20 | 22 24 01.55 | 17 19 50.1 | 2.38 | | |
| 17 | 0.68 | 22 24 06.59 | 17 11 53.2 | 0.89 | | |
| 18 | 1.37 | 22 24 09.53 | 17 21 24.1 | 2.22 | | |
| 19 | 0.74 | 22 24 11.65 | 17 00 02.3 | 1.17 | | |
| 20 | 1.58 | 22 24 11.92 | 16 47 41.2 | 3.13 | | |
| Abell 2443(cont) | | | | | | |
| 21 | 1.17 | 22 24 17.05 | 17 17 31.4 | 21.9 | | |
| 22 | 0.98 | 22 24 21.23 | 16 58 21.4 | 8.87 | | |
| 23 | 0.98 | 22 24 31.59 | 17 03 25.1 | 1.58 | | |
| Abell 2456 | | | | | | |
| 1 | 2.03 | 22 31 20.06 | -15 29 17.5 | 19.1 | | |
| 2 | 1.79 | 22 31 28.74 | -15 29 01.3 | 19.9 | | |
| 3 | 2.42 | 22 31 32.25 | -15 19 21.1 | 9.34 | | |
| 4 | 1.47 | 22 31 38.55 | -15 29 55.6 | 1.74 | | |
| 5 | 1.49 | 22 31 55.38 | -15 24 09.9 | 2.11 | | |
| 6 | 0.94 | 22 32 05.21 | -15 39 32.3 | 8.08 | | |
| 7 | 0.62 | 22 32 10.94 | -15 37 28.9 | 1.84 | | |
| 8 | 0.84 | 22 32 18.11 | -15 27 14.2 | 5.13 | | |
| 9 | 1.12 | 22 32 18.57 | -15 42 20.6 | 7.77 | | |
| 10 | 0.18 | 22 32 19.19 | -15 34 33.7 | 5.34 | 1.39 | -1.12 |
| 11 | 1.66 | 22 32 20.62 | -15 46 40.2 | 2.35 | | |
| 12 | 1.31 | 22 32 21.73 | -15 43 56.9 | 2.02 | | |
| 13a/b | 0.10 | 22 32 26.66 | -15 34 03.1 | 273. | 79.4 | -1.02 |
| 14 | 1.07 | 22 32 43.33 | -15 40 36.7 | 28.4 | | |
| 15 | 0.81 | 22 32 49.21 | -15 32 10.6 | 27.1 | 1.64 | -2.33 |
| 16 | 0.90 | 22 32 50.98 | -15 36 06.2 | 71.7 | 12.4 | -1.46 |
| 17 | 1.19 | 22 32 55.02 | -15 28 11.6 | 15.4 | | |
| 18 | 1.20 | 22 33 02.33 | -15 34 37.0 | 44.7 | | |
| 19 | 2.22 | 22 33 17.77 | -15 45 13.2 | 4.52 | | |
| Abell 2457 | | | | | | |
| 1a/b | 0.14 | 22 33 12.55 | 01 16 19.2 | 11.7 | | |
| 2 | 0.24 | 22 33 33.37 | 01 17 59.5 | 2.06 | | |
| 3a/b | 0.42 | 22 33 42.35 | 01 04 11.5 | 130. | 24.5 | -1.38 |
| 4 | 0.45 | 22 33 52.13 | 01 05 03.4 | 1.77 | | |
| 5 | 0.79 | 22 34 00.15 | 00 55 32.4 | 3.01 | | |
| 6 | 0.69 | 22 34 01.02 | 00 58 54.2 | 142. | | |
| 7 | 0.58 | 22 34 02.84 | 01 03 01.8 | 44.4 | 11.9 | -1.09 |
| 8a/b | 0.46 | 22 34 05.10 | 01 11 40.4 | 65.7 | | |
| 9 | 0.52 | 22 34 07.76 | 01 07 44.5 | 1.32 | | |
| 10 | 0.63 | 22 34 13.57 | 01 21 11.6 | 21.8 | | |
| 11 | 0.67 | 22 34 23.30 | 01 18 21.8 | 24.7 | | |
| 12 | 1.25 | 22 34 43.60 | 00 49 02.5 | 23.4 | | |

| Cluster & Source | Ang. Dist. R/Rc | R.A. 1950 h m s | Dec. ° ' " | Flux Dens. 1.5 GHz mJy | Flux Dens. 4.9 GHz mJy | Spec. Index $\alpha_{1.5}^{4.9}$ |
|---|---|---|---|---|---|---|
| Abell 2575 | | | | | | |
| 1a/b | 1.78 | 23 16 23.91 | -22 20 49.1 | 13.3 | | |
| 2 | 2.53 | 23 16 28.52 | -22 08 34.5 | 9.40 | | |
| 3 | 2.18 | 23 16 54.12 | -22 07 50.0 | 8.48 | | |
| 4 | 2.86 | 23 16 54.97 | -22 02 59.1 | 55.9 | | |
| 5 | 0.54 | 23 17 03.13 | -22 19 22.9 | 12.1 | | |
| 6 | 0.26 | 23 17 10.63 | -22 20 19.5 | 308. | | |
| 7a/b | 0.13 | 23 17 13.88 | -22 22 28.6 | 377. | | |
| 8 | 2.36 | 23 17 32.76 | -22 37 01.8 | 11.4 | | |
| 9 | 0.75 | 23 17 35.59 | -22 23 32.7 | 4.31 | | |
| 10 | 1.65 | 23 18 02.09 | -22 24 05.7 | 19.9 | | |
| 11 | 1.93 | 23 18 04.39 | -22 15 18.9 | 19.0 | | |
| 12 | 1.92 | 23 18 08.91 | -22 25 21.0 | 175. | | |
| 13 | 2.86 | 23 18 28.61 | -22 12 30.0 | 17.9 | | |
| Abell 2593 | | | | | | |
| 1 | 0.51 | 23 21 03.77 | 14 17 01.9 | 10.5 | | |
| 2 | 0.44 | 23 21 08.79 | 14 19 42.1 | 44.0 | | |
| 3 | 0.40 | 23 21 27.20 | 14 14 02.9 | 1.99 | | |
| 4 | 0.08 | 23 21 49.04 | 14 22 21.4 | 1.60 | | |
| 5 | 0.12 | 23 21 52.56 | 14 19 06.8 | 1.77 | | |
| 6 | 0.05 | 23 21 56.10 | 14 23 24.7 | 5.30 | 2.16 | -0.75 |
| 7a/b | 0.47 | 23 22 00.88 | 14 35 30.8 | 16.2 | | |
| 8a/b | 0.03 | 23 22 01.27 | 14 21 55.2 | 288. | 103. | -0.85 |
| 9 | 0.23 | 23 22 08.20 | 14 28 13.6 | 2.31 | | |
| 10 | 0.17 | 23 22 14.53 | 14 24 51.2 | 230. | 80.6 | -0.87 |
| 11 | 0.66 | 23 22 25.66 | 14 39 26.6 | 5.77 | | |
| 12 | 0.42 | 23 22 46.07 | 14 20 11.2 | 16.4 | | |
| Abell 2622 | | | | | | |
| 1 | 0.69 | 23 31 23.53 | 27 07 26.0 | 26.5 | | |
| 2 | 0.66 | 23 31 28.00 | 27 05 46.6 | 3.32 | | |
| 3 | 0.65 | 23 31 28.27 | 27 06 48.2 | 4.98 | | |
| 4 | 0.59 | 23 31 39.24 | 27 15 26.7 | 5.52 | | |
| 5 | 0.12 | 23 32 21.40 | 27 07 18.1 | 1.81 | | |
| 6 | 0.17 | 23 32 21.89 | 27 06 14.0 | 4.01 | 1.66 | -0.73 |
| 7 | 0.24 | 23 32 24.05 | 27 04 33.4 | 1.67 | | |
| 8 | 0.07 | 23 32 31.45 | 27 09 23.9 | 5.94 | 1.76 | -1.01 |
| 9 | 0.20 | 23 32 31.78 | 27 05 41.4 | 72.2 | 7.67 | -1.86 |
| 10a/b | 0.08 | 23 32 32.02 | 27 10 11.8 | 87.9 | 26.3 | -1.00 |
| Abell 2622(cont) | | | | | | |
| 11 | 0.38 | 23 32 33.26 | 27 16 57.2 | 5.11 | | |
| 12 | 0.61 | 23 32 33.97 | 26 57 17.7 | 3.96 | | |
| 13 | 0.37 | 23 32 44.44 | 27 03 21.4 | 49.5 | 26.5 | -0.52 |
| 14a/b | 0.23 | 23 32 45.19 | 27 11 07.3 | 5.55 | | |
| 15 | 0.61 | 23 32 47.29 | 27 20 50.0 | 13.2 | | |
| 16 | 0.47 | 23 32 54.69 | 27 16 28.7 | 4.60 | | |
| 17 | 1.11 | 23 32 59.31 | 26 48 25.5 | 19.1 | | |
| 18 | 0.87 | 23 33 16.79 | 26 56 10.6 | 11.0 | | |
| 19 | 0.60 | 23 33 19.55 | 27 07 43.7 | 3.78 | | |
| 20 | 0.63 | 23 33 21.37 | 27 06 48.2 | 8.50 | | |
| 21 | 0.75 | 23 33 30.34 | 27 04 46.0 | 16.1 | | |
| 22 | 1.03 | 23 33 40.17 | 26 57 00.2 | 23.2 | | |
| 23 | 0.89 | 23 33 41.67 | 27 03 40.8 | 6.09 | | |
| 24 | 1.02 | 23 33 54.78 | 27 14 46.9 | 40.2 | | |
| Abell 2626 | | | | | | |
| 1 | 0.79 | 23 32 40.70 | 20 46 24.8 | 11.3 | | |
| 2 | 0.67 | 23 32 47.13 | 20 51 38.7 | 2.91 | | |
| 3 | 0.55 | 23 33 22.89 | 21 04 13.1 | 2.52 | | |
| 4a/b | 0.40 | 23 33 22.98 | 20 48 02.0 | 5.02 | | |
| 5 | 0.41 | 23 33 34.35 | 20 45 08.6 | 37.1 | | |
| 6 | 0.46 | 23 33 38.82 | 21 03 48.6 | 94.8 | | |
| 7 | 0.57 | 23 33 43.30 | 21 07 04.8 | 2.41 | | |
| 8 | 0.20 | 23 33 45.24 | 20 49 37.2 | 18.0 | 9.28 | -0.55 |
| 9 | 0.36 | 23 33 47.75 | 21 02 07.0 | 3.04 | | |
| 10 | 0.06 | 23 33 54.70 | 20 52 33.7 | 3.90 | 1.22 | -0.97 |
| 11a/b | 0.06 | 23 33 59.47 | 20 52 10.0 | 41.7 | 9.75 | -1.21 |
| 12 | 0.62 | 23 34 06.04 | 20 38 15.0 | 2.71 | | |
| 13 | 0.31 | 23 34 06.12 | 20 46 10.1 | 1.31 | | |
| 14 | 0.19 | 23 34 08.63 | 20 49 37.2 | 1.47 | 2.06 | 0.28 |
| 15 | 0.63 | 23 34 24.20 | 21 07 45.4 | 2.41 | | |
| 16 | 0.35 | 23 34 33.79 | 20 55 03.3 | 3.33 | | |
| 17 | 0.68 | 23 34 38.41 | 20 39 37.7 | 30.5 | | |
| 18 | 0.87 | 23 34 49.15 | 20 35 43.1 | 9.32 | | |
| Abell 2657 | | | | | | |
| 1 | 1.10 | 23 43 25.55 | 08 29 27.7 | 8.42 | | |
| 2a/b | 1.16 | 23 43 26.61 | 08 27 48.7 | 13.1 | | |
| 3a/b | 0.82 | 23 43 43.23 | 08 48 24.9 | 55.6 | | |

| Cluster & Source | Ang. Dist. R/Rc | R.A. 1950 h m s | Dec. ° ' " | Flux Dens. 1.5 GHz mJy | Flux Dens. 4.9 GHz mJy | Spec. Index $\alpha_{1.5}^{4.9}$ |
|---|---|---|---|---|---|---|
| Abell 2657(cont) | | | | | | |
| 4 | 1.06 | 23 43 48.16 | 08 36 01.1 | 333. | 90.3 | -1.08 |
| 5 | 1.06 | 23 43 59.16 | 08 40 41.1 | 2.57 | | |
| 6 | 1.13 | 23 44 08.70 | 08 41 36.6 | 2.84 | | |
| 7 | 1.31 | 23 44 16.70 | 08 35 16.0 | 8.11 | | |
| 8 | 1.26 | 23 44 27.53 | 08 45 05.8 | 3.76 | | |
| 9a/b | 1.69 | 23 45 03.99 | 08 36 24.5 | 96.0 | | |
| Abell 4038 | | | | | | |
| 1a/b | 0.37 | 23 44 10.81 | -28 40 22.7 | 21.2 | | |
| 2 | 0.29 | 23 44 12.33 | -28 32 01.8 | 5.09 | | |
| 3 | 0.32 | 23 44 22.69 | -28 07 55.4 | 17.5 | | |
| 4 | 0.34 | 23 44 32.38 | -28 41 37.7 | 23.1 | | |
| 5 | 0.19 | 23 44 35.63 | -28 17 02.1 | 1.92 | | |
| 6 | 0.23 | 23 44 40.66 | -28 34 06.6 | 7.12 | | |
| 7 | 0.11 | 23 44 52.38 | -28 24 51.9 | | 1.57 | |
| 8a/b | 0.17 | 23 44 59.29 | -28 32 09.5 | 21.4 | | |
| 9 | 0.08 | 23 45 04.61 | -28 25 53.0 | 31.0 | | |
| 10 | 0.06 | 23 45 07.36 | -28 24 12.7 | 2.89 | 0.90 | -0.97 |
| 11 | 0.06 | 23 45 08.96 | -28 25 06.7 | 22.6 | 7.87 | -0.87 |
| 12 | 0.20 | 23 45 20.05 | -28 10 20.1 | 7.66 | | |
| 13a/b | 0.10 | 23 45 21.66 | -28 16 40.9 | 4.63 | | |
| 14 | 0.12 | 23 45 36.05 | -28 15 51.8 | 4.28 | | |
| 15 | 0.21 | 23 45 37.58 | -28 09 45.5 | 4.78 | | |
| 16 | 0.13 | 23 45 43.22 | -28 30 22.4 | 3.45 | | |
| 17 | 0.18 | 23 45 55.10 | -28 13 33.6 | 13.3 | | |
| 18 | 0.25 | 23 46 12.81 | -28 34 47.7 | 58.9 | | |
| 19 | 0.32 | 23 46 20.41 | -28 39 28.8 | 14.5 | | |
| Abell 2670 | | | | | | |
| 1 | 1.45 | 23 49 28.56 | -10 51 09.7 | 8.93 | | |
| 2 | 1.64 | 23 49 36.30 | -11 03 35.2 | 8.76 | | |
| 3 | 1.26 | 23 49 43.23 | -10 48 04.7 | 5.69 | | |
| 4 | 1.10 | 23 50 02.52 | -10 50 55.5 | 10.1 | | |
| 5 | 1.15 | 23 50 07.78 | -10 55 19.2 | 14.8 | 9.22 | -0.40 |
| 6 | 0.82 | 23 50 21.89 | -10 45 17.3 | 3.28 | | |
| 7 | 0.79 | 23 50 26.27 | -10 46 10.3 | 25.5 | | |
| 8 | 0.77 | 23 50 27.17 | -10 45 10.7 | 1.31 | | |
| 9 | 1.27 | 23 50 31.35 | -11 04 49.8 | 3.91 | | |
| 10 | 1.47 | 23 50 33.27 | -11 10 24.5 | 3.84 | | |
| Abell 2670(cont) | | | | | | |
| 11a/b | 0.86 | 23 50 34.18 | -10 53 23.8 | 155. | 38.3 | -1.16 |
| 12 | 1.11 | 23 50 34.61 | -11 00 57.5 | 1.22 | | |
| 13 | 0.96 | 23 50 40.05 | -10 57 47.4 | 9.94 | 4.33 | -0.69 |
| 14 | 0.74 | 23 51 09.08 | -10 56 26.8 | 7.74 | | |

class (column 4) and richness class (column 5) are from Abell's (1958) catalogue. The Bautz–Morgan (1970) classification of optical morphology in column 6 is as listed by Struble and Rood (1987*a*), who also give the Rood–Sastry classification in column 7. The angular radius of the cluster ($R_C$) is that measured from Palomar Sky Survey plates and quoted by Struble and Rood (1987*a*). For the few southern clusters without such measurements we have used Abell's definition ($1 \cdot 7/Z$ min of arc). The median linear cluster radius for all clusters in Table 1 is $2 \cdot 0$ Mpc. The redshift in column 3 is usually a measured value from Struble and Rood (1987*b*). Otherwise, we have used the calibrated empirical relationship between the magnitude of the tenth brightest galaxy and redshift, derived by Mills and Hoskins (1977). Asterisks against 21 cluster names in Table 1 denote VLA fields that were centred on steep spectrum sources displaced from the cluster centre by $>R_C/3$. In 10 of these cases the $1 \cdot 5$ GHz FHPW beamwidth of $30'$ ensured that the central regions of the clusters were surveyed. The remaining 11 fields were deliberately chosen to be outside the central regions of the nearby clusters in order to obtain comparative data on the morphology of sources inside and outside clusters.

The $1 \cdot 5$ GHz maps are shown in Figs 1–71. These $512 \times 512$ pixel cleaned maps were made predominantly from $1 \cdot 5$ GHz data taken with the C-Array. The pixel size of $4'' \cdot 5 \times 4'' \cdot 5$ results in maps of $38' \cdot 4 \times 38' \cdot 4$, i.e. extending well outside the half-power points of the antennae primary beams. We observed three clusters (A3528, A1791, A2029) only in the B/C scaled configurations and the resulting $512 \times 512$ maps with a pixel size of $1'' \cdot 5 \times 1'' \cdot 5$ have dimensions of $12' \cdot 8 \times 12' \cdot 8$. Four clusters (A85, A133, ZW1518·8+0747, A2443) are represented by $1 \cdot 5$ GHz maps in both the B- and C-Arrays. In some cases the dynamic range of the $1 \cdot 5$ GHz C-Array maps was limited by side-lobes of strong cluster sources rather than by the system noise; this prevented our detecting at $1 \cdot 5$ GHz some weaker sources that appear on the corresponding $4 \cdot 9$ GHz D-Array maps. For these clusters (A115, A496, A912, A1273, A1620, A2029, A4038) the $4 \cdot 9$ GHz maps of $512 \times 512$ pixels and pixel size $4'' \cdot 5 \times 4'' \cdot 5$ are given in addition to the $1 \cdot 5$ GHz maps. None of the maps in Figs 1–71 has been corrected for primary beam attenuation.

## 4. The Source List

We examined all the maps carefully for the presence of radio sources at $1 \cdot 5$ GHz and $4 \cdot 9$ GHz and noted the sources common to both frequencies. After correcting the sources for primary beam attenuation, we measured their flux densities, positions and angular sizes. The source list is given in Table 2.

The sources in each field are numbered in order of increasing right ascension with multiple components, identified by a, b, c, etc. following the number. The angular distance from the cluster centre in column 2 is expressed as a fraction of the cluster radius $R_C$. The positions in columns 3 and 4 are from the $1 \cdot 5$ GHz maps except for a few flat spectrum sources that appear only on the $4 \cdot 9$ GHz maps. The positions were obtained by fitting an elliptical Gaussian; in the case of sources with multiple components, such a fit produces a position that approximates the centroid of the brightness distribution. The positions have been corrected for an error dependent on the angular radial distance

from the phase centre of the map. For this we have used the equation derived by Condon and Mitchell (1984). The resultant positional errors, confirmed by comparing the 1·5 GHz and 4·9 GHz positions of compact sources, are <1″ in each coordinate.

We believe that very few of the sources listed in Table 2 are products of system noise or incomplete sampling of the UV plane and the cleaning process. Our reasons for this claim are that: (i) the weakest sources have flux densities 10 times the rms levels over the maps; (ii) the sources have survived a variety of cleaning processes involving a range of numbers of clean iterations and two or three cleaning windows ranging from 256×256 to 1024×1024 pixels and (iii) most of the sources within 5′ of the maps' centres were detected at both 1·5 GHz and 4·9 GHz with positional agreement usually better than 1″ arc.

## 5. Radio Source Statistics

Earlier studies with radio telescopes of lower resolution and sensitivity (e.g. Slee *et al.* 1983) have shown that radio sources in the directions of clusters are concentrated toward the cluster centres. This provides convincing evidence that the sources are associated with cluster galaxies, despite the absence of positive optical identifications for some sources or redshift measurements of galaxies that appear to be associated with radio sources. Our VLA study has detected sources with 1·5 GHz flux densities up to two orders of magnitude weaker than those of the sources in earlier studies, raising the possibility of many of the weaker sources being background galaxies or QSOs rather than cluster members. To resolve this question we examined the source number distribution with $R/R_C$ (angular distance from the cluster centre normalised by the cluster radius) as a function of source flux density.

We estimated the lowest flux density at which our VLA sample is complete. We plotted the numbers of 1·5 GHz sources in intervals of decreasing flux density, using sources out to the half-power circle on the maps, which were restricted to those with rms noise <100 μJy/beam. We found that the resulting plot of source numbers against flux density flattened abruptly below 2 mJy, indicating that at that level we were failing to detect a significant number of weak sources. We estimate that the source count for the better maps is 90 per cent complete at a flux density of 2·5 mJy, which is 12 to 30 times the rms noise at the half-power circle. The noisier maps containing side lobes of strong sources had rms noise that only rarely exceeded 200 μJy/beam; the 90 per cent completeness level on the noisiest maps is therefore ~5 mJy.

Following the analysis of Slee *et al.* (1983) we selected sources from the 26 clusters with rms noise ≤100 μJy/beam (ensuring a completeness level of 2·5 mJy at 1·5 GHz), which had been fully mapped out to $R/R_C \geq 0{\cdot}40$. The clusters used are denoted by asterisks in Table 3. The selected sources were then divided into two classes: (i) sources with $2{\cdot}5 \leq S_{1{\cdot}5} \leq 20$ mJy; (ii) the stronger sources with $S_{1{\cdot}5} > 20$ mJy. Next, the sources in each class were allocated to four equal area annuli extending out to $R/R_C = 0{\cdot}40$ and the numbers summed over the 26 clusters. The resulting plots in Fig. 72 summarise the results; the dashed horizontal line in each plot denotes the expected source count obtained by integrating the differential source counts

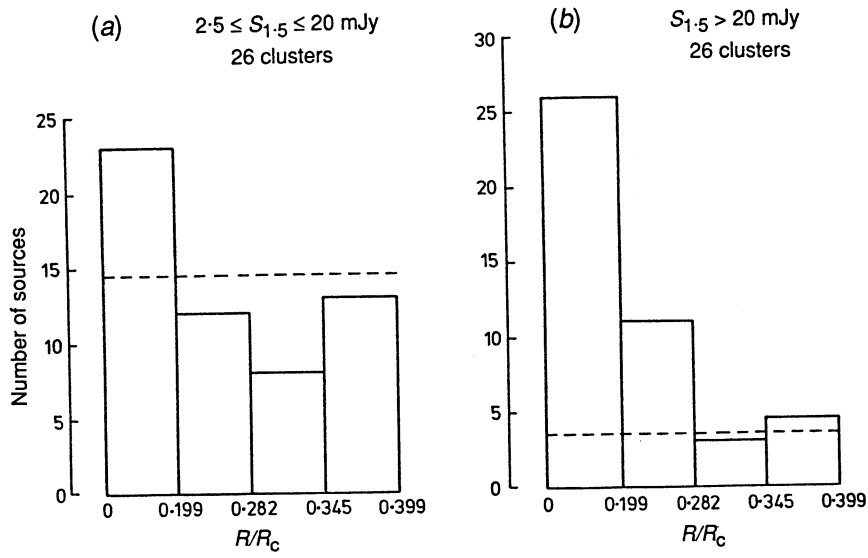


**Fig. 72.** Summed numbers of sources in annuli of equal area surrounding the centres of 26 clusters which were surveyed out to an angular radius $R/R_C > 0 \cdot 40$ and are complete to a flux density of $2 \cdot 5$ mJy at $1 \cdot 5$ GHz. The dashed line is the number of expected background sources computed from deep VLA and Westerbork surveys of a field free of clusters of galaxies. Parts (*a*) and (*b*) refer to the 'weak' and 'strong' samples of radio sources.

**Table 3. Maps used to establish cluster membership**

| | | | | |
|---|---|---|---|---|
| A13* | A407† | A1189† | A2009* | A2443* |
| A85E* | A416* | A1238* | A2052† | A2456* |
| A86§ | A474† | A1273† | ZW1518·8* | A2457§ |
| A115† | A496§ | A1620† | A20912* | A2575† |
| A133* | A519* | A1631* | A2094* | A2593* |
| A196† | A531* | A1689* | A2103§ | A2622* |
| A278† | A658* | A1772* | A2249* | A2626* |
| A357§ | A912§ | A1775* | A2354* | A4038§ |
| A362* | A1171§ | A1913* | A2396* | |

* Surveyed out to $R/R_C \geq 0 \cdot 40$ and complete to $S_{1 \cdot 5} = 2 \cdot 5$ mJy.
† Surveyed out to $R/R_C \geq 0 \cdot 40$ and complete to $S_{1 \cdot 5} = 20$ mJy.
§ Surveyed out to $R/R_C \geq 0 \cdot 20$ and complete to $S_{1 \cdot 5} = 20$ mJy.

from a deep survey of a cluster-free field obtained by Oort and Windhorst (1985).

Assuming Poisson statistics, the standard error in the source counts is $\sqrt{N}$, where $N$ is the number of sources in each bin. Thus the error in the background count of Fig. 72*a* is $\pm 3 \cdot 8$ sources, while for Fig. 72*b* it is $\pm 1 \cdot 9$ sources. When our sampling errors are added to those of the background counts we see that there is probably a small excess of weak (<20 mJy) sources in the first bin of Fig. 72*a* but that there are no significant departures from the expected counts in the bins further from the cluster centres. On the

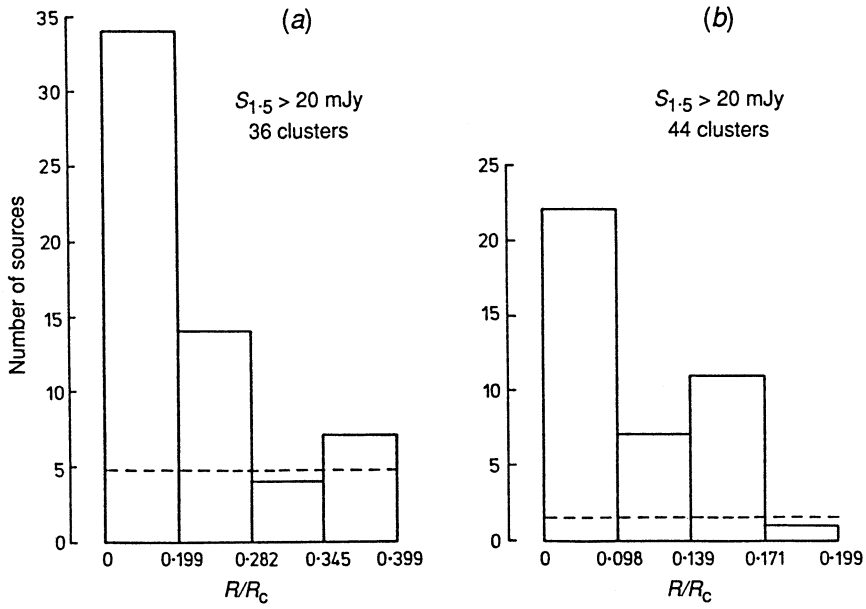


**Fig. 73.** Summed numbers of sources in annuli of equal area surrounding the centres of clusters. Part (*a*) refers to the sources in 36 clusters surveyed out to $R/R_C \geq 0\cdot40$ and complete to $S_{1\cdot5} = 20$ mJy. Part (*b*) is for the 44 clusters surveyed out to $R/R_C \geq 0\cdot20$ i.e. covering the first bin of the left hand distribution. The dashed line in each case is the expected number of background sources.

other hand, the strong sources (Fig. 72*b*) show significant excesses over the background count in the two bins nearest the cluster centre. We can conclude therefore that sources with 1·5 GHz flux density >20 mJy are very likely to be in clusters if their radial distance from the cluster centre is $R/R_C \leq 0\cdot28$. From Fig. 72*a* we see that most of the sources with $S_{1\cdot5} < 20$ mJy are likely to be unrelated background objects with the exception of a few per cent of the sources within $0\cdot20R/R_C$ of the cluster centre. Our criterion for cluster membership is therefore considerably more restrictive than that adopted by Zhao *et al.* (1989) in a recently published VLA survey of northern clusters. These authors accept radio sources with $R/R_C < 0\cdot5$ as cluster members and justify their choice by adopting the additional restriction that the source should be identified with a galaxy brighter than 17 mag. However, unless redshift measurements of these galaxies have been made and agree well with the cluster redshifts it is possible to incorrectly assign the source to the cluster. Further, our results show that the identification restriction may often result in ignoring sources that are cluster members—approximately 25 per cent of the strongest sources near cluster centres have no apparent optical counterpart (paper in preparation).

Having established a criterion for cluster membership we can now expand our data set to include 10 clusters for which the rms levels are >100 μJy/beam, but which are still complete to $S_{1\cdot5} = 20$ mJy and fully surveyed out to $R/R_C \geq 0\cdot40$; these are identified by daggers in Table 3. We can also include

the clusters (identified in Table 3 by section marks) that are complete to $S_{1\cdot5} = 20$ mJy and surveyed completely out to $R/R_C \geq 0\cdot20$; the resulting sample of 44 clusters can then be used to investigate how the numbers of sources vary for $R/R_C \leq 0\cdot2$. Fig. 73 shows the results of the source summations.

In Fig. 73*a*, the large excess of sources with $R/R_C < 0\cdot28$ is obvious. Indeed in Fig. 73*b* the number of sources with $R/R_C < 0\cdot10$ is ~20 times the expected background count.

**Table 4. Median parameters of most powerful source in cluster**

A cluster is one with $R/R_C < 0\cdot28$ and $S_{1\cdot5} > 20$ mJy

| Parameter | No. of clusters | Median | Range |
|---|---|---|---|
| Log$P_{1\cdot5}$ (WHz$^{-1}$) | 43 | 24·47 | 22·91–25·54 |
| Log($\Sigma P_{1\cdot5}$) (WHz$^{-1}$) | 43 | 24·50 | 22·91–25·80 |
| Largest linear size (kpc) | 34 | 81 | 16–1148 |
| Spectral index | 35 | −1·02 | −0·56 to −2·90 |

*(a) Intrinsic Parameters of Cluster Sources*

Table 4 lists the intrinsic properties of the most powerful sources in each cluster. All sources fulfil our criterion for cluster membership i.e. $S_{1\cdot5} > 20$ mJy, $R/R_C < 0\cdot28$. By selecting the most powerful emitter one can make a more meaningful comparison between the same parameter in different clusters and attempt to determine how this parameter is influenced by optical and X-ray properties. Power and linear size have been computed assuming a static Euclidean model with $H_0 = 75$ kms$^{-1}$ Mpc$^{-1}$. For each source, the largest linear size has been derived from the major axis of the best fitting elliptical Gaussian; in nine clusters the source was effectively unresolved by our C-Array beam (FHPW ~ 14″). The spectral index (defined by $S(\nu) \propto \nu^{\alpha}$) is derived from our VLA measurements at 1·5 and 4·9 GHz; however, in eight clusters the sources were not detected at 4·9 GHz due to their being attenuated by the primary beam pattern of the VLA antennae and their steep spectra.

We see from Table 4 that most of the sources in these 43 clusters have moderate values of $P_{1\cdot5}$, characteristic of the Faranoff-Riley (1974) (FR) class 1 radio galaxies; eight sources, however, have $P_{1\cdot5} > 10^{25}$ WHz$^{-1}$ and therefore belong to the luminous FR class 2 sources. We also list in Table 4 the summed radio powers of the sources in each cluster, from which it is clear that the radio emission is usually dominated by one galaxy.

The largest linear dimensions of the resolved radio sources are also of moderate value, although we should point out that the method of fitting a single deconvolved elliptical Gaussian sometimes underestimates the size, especially in the case of well resolved double sources. Even so, 14 of the 34 resolved sources have major axes >100 kpc to the 10 per cent brightness level and of these seven have major axes >200 kpc.

The spectral indices of these dominant radio sources are unusually steep; however, this is probably a result of our selection criteria, which included clusters showing the presence of steep spectrum sources. Only three of the 35 sources with VLA spectra have spectral indices > −0·80 (near the average

for a randomly selected sample) whereas twelve have spectra steeper than $-1\cdot10$. Of these, six sources have spectral indices steeper than $-1\cdot48$.

**Table 5. Significant regressions**

Here $L_{1\cdot5}$ is the major axis of deconvolved elliptical Gaussian (kpc); $P_{1\cdot5}$ the power emitted at 1·5 GHz ($WHz^{-1}$); $A_{1\cdot5}$ the area of source (deconvolved axes) to 10% brightness $(kpc)^2$; $A_{a,b}$ the area of components of double sources to 10% brightness $(kpc)^2$; $P_{a,b}$ the power of components of double sources ($WHz^{-1}$); $\alpha_a/\alpha_b$ the ratio of spectral indices for components of double sources; and $S_a/S_b$ the ratio of 1·5 GHz flux densities for components of double sources

| Parameters | No. of sources or components | Correlation coefficient | Regression equation | Confidence level (%) |
|---|---|---|---|---|
| (1) Sources in clusters | | | | |
| $\text{Log}L_{1\cdot5}$–$\text{Log}P_{1\cdot5}$ | 33 | 0·435 | $\text{Log}L_{1\cdot5} = -5\cdot410+0\cdot300\ \text{Log}P_{1\cdot5}$ | 98·5 |
| (2) Double sources in clusters | | | | |
| $\text{Log}L_{1\cdot5}$–$\text{Log}P_{1\cdot5}$ | 20 | 0·640 | $\text{Log}L_{1\cdot5} = -9\cdot773+0\cdot485\ \text{Log}P_{1\cdot5}$ | 99·8 |
| $\text{Log}A_{1\cdot5}$–$\text{Log}P_{1\cdot5}$ | 20 | 0·471 | $\text{Log}A_{1\cdot5} = -12\cdot759+0\cdot664\ \text{Log}P_{1\cdot5}$ | 96 |
| $\text{Log}A_{a,b}$–$\text{Log}P_{a,b}$ | 34 | 0·360 | $\text{Log}A_{a,b} = -7\cdot677+0\cdot454\ \text{Log}P_{a,b}$ | 96 |
| (3) Double sources outside clusters | | | | |
| $\alpha_a/\alpha_b - S_a/S_b$ | 14 | 0·888 | $\alpha_a/\alpha_b = 0\cdot741+0\cdot196S_a/S_b$ | >99·9 |
| (4) All double sources | | | | |
| $\alpha_a/\alpha_b - S_a/S_b$ | 28 | 0·714 | $\alpha_a/\alpha_b = 0\cdot857+0\cdot195S_a/S_b$ | >99·9 |

**Table 6. Significant ranking tests**

Here $\Sigma P_{1\cdot5}$ is the total power emitted at 1·5 GHz of cluster sources ($WHz^{-1}$) and $\alpha$ is the spectral index between 1·5 and 4·9 GHz

| Parameters | Rank categories 1 | Rank categories 2 | No. of clusters* | Median values 1 | Median values 2 | Confidence level (%) |
|---|---|---|---|---|---|---|
| (1) Sources in clusters | | | | | | |
| $\text{Log}(\Sigma P_{1\cdot5})$–Richness class | Richness = 0 | Richness = 1–4 | 17/26 | 24·34 | 24·66 | 96 |
| $\alpha$–BM class | BM = I, I–II | BM = II, II–III, III | 13/20 | −1·13 | −0·97 | 98 |

* Numbers of clusters in each rank category.

**Table 7. Ranking tests—sources in and out of clusters**

| Parameters | Number of sources In cluster | Number of sources Out of cluster | Median values In cluster | Median values Out of cluster | Confidence level |
|---|---|---|---|---|---|
| (1) All sources | | | | | |
| Spectral index $\alpha$ | 35 | 29 | −1·02 | −0·96 | NS† |
| Surface brightness* $B_{1\cdot5}$ | 33 | 25 | 0·73 | 1·33 | NS |
| (2) Double sources | | | | | |
| Component fluxes $S_a/S_b$ | 21 | 17 | 1·38 | 1·31 | NS |
| Component major axes $\theta_a/\theta_b$ | 19 | 13 | 1·67 | 1·29 | 95% |
| Component areas $A_a/A_b$ | 17 | 13 | 1·01 | 1·11 | NS |
| Component brightness* $B_a/B_b$ | 17 | 13 | 1·20 | 1·18 | NS |
| Component spectra $\alpha_a/\alpha_b$ | 15 | 14 | 1·03 | 1·02 | NS |

* Surface brightness derived from flux density/angular area, i.e. $mJy/(''arc)^2$.
† Not significant.

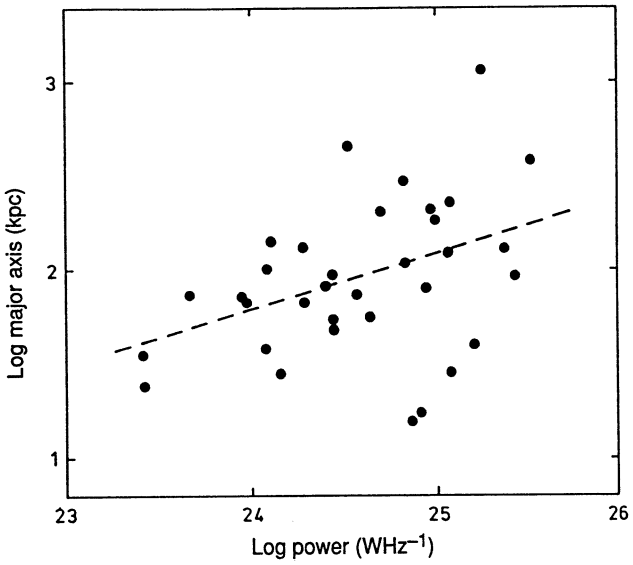


**Fig. 74.** Scatter plot of the largest linear dimension ($L_{1.5}$) against emitted power ($P_{1.5}$). The most powerful source in the cluster has been fitted by a deconvolved elliptical Gaussian. The regression line (see Table 5) is shown dashed.

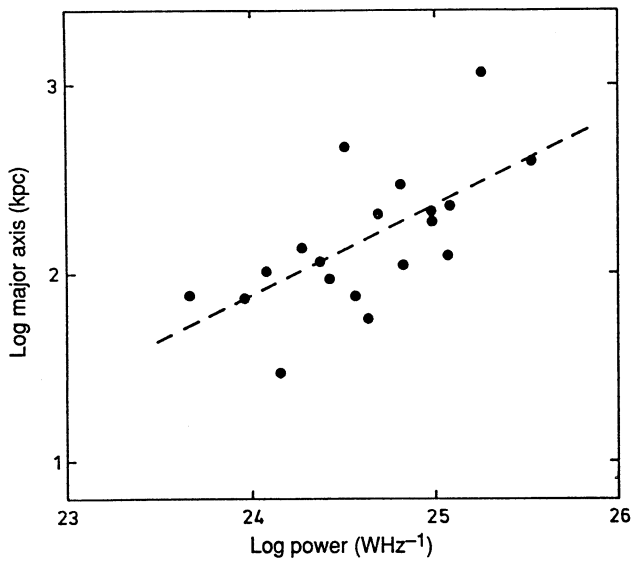


**Fig. 75.** Scatter plot of the largest linear dimension ($L_{1.5}$) against emitted power ($P_{1.5}$) for the cluster doubles. The strongest double in each cluster has been fitted by a deconvolved elliptical Gaussian; with one exception these are also the strongest sources (of whatever morphology) in the clusters and are included in Fig. 74. The regression line (see Table 5) is shown dashed.

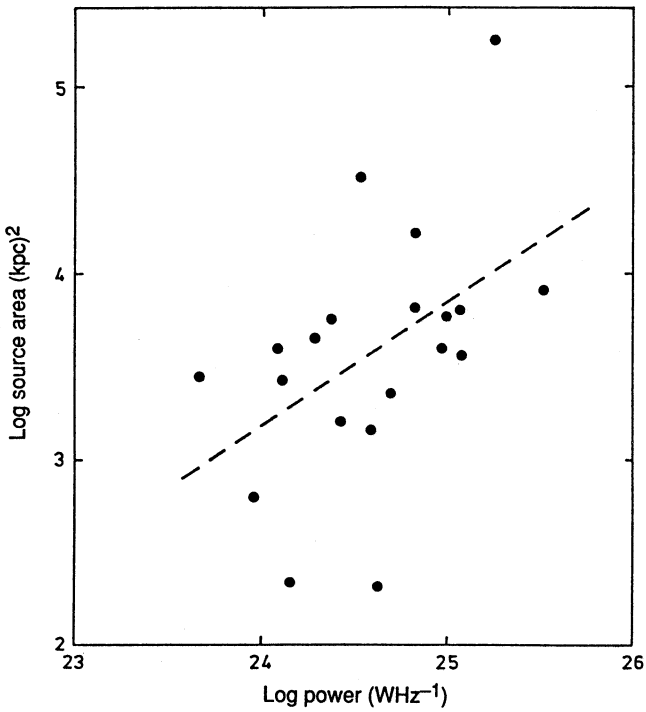


**Fig. 76.** Scatter plot of the source area ($A_{1.5}$) against emitted power ($P_{1.5}$) for the cluster doubles. The area to the 10% brightness level has been computed from the best fitting deconvolved elliptical Gaussian and refers to the most powerful double in each cluster. The regression line (see Table 5) is shown dashed.

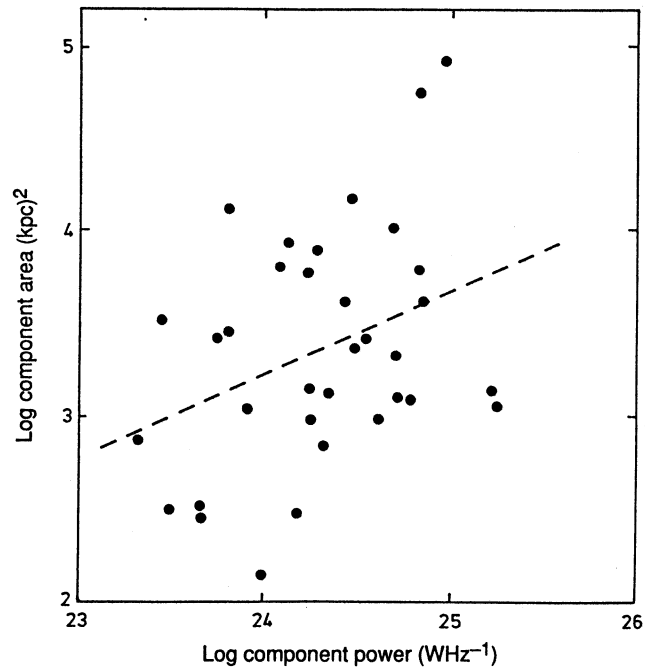


**Fig. 77.** Scatter plot of the source area ($A_{1.5}$) of each component of a cluster double against its corresponding emitted power ($P_{1.5}$). The component area to the 10% brightness level and component power have been computed from the best fitting deconvolved elliptical Gaussian. The doubles are the most powerful in each cluster and are included in Fig. 76. The regression line (see Table 5) is shown dashed.

*(b) Relationships Between Radio Parameters*

We should be cautious in interpreting relationships between the radio parameters of power, surface brightness, largest linear size, spectral index and distance from the cluster centre. Such relationships may not be generally applicable to all radio sources in clusters because our sample is biased towards steep spectrum sources. However it is a relatively unbiased sample of *steep spectrum* radio sources both in and outside clusters because our fields were selected from low resolution surveys of complete samples of Abell clusters. Hence a study of the correlations may be instructive from the point of view of steep spectrum radio galaxies.

Where possible we used both the standard regression analysis and the distribution-independent Kruskall-Wallis ranking test (Hughes and Grawoig 1971). If one of the variables in the relation under test was discontinuous (e.g. power versus richness class) then only the ranking test was possible.

We tested relationships between almost all combinations of the following variables (taken in pairs): emitted power, surface brightness, largest linear dimension, source area, angular distance from the cluster centre and spectral index. A separate study was made of classical doubles (in addition to their being included as single elliptical Gaussians with the remaining sources) by fitting deconvolved elliptical Gaussians to their components. For these sources we tested all combinations of: the ratios of component flux densities, major angular axes, angular areas, surface brightness and spectral indices.

Tables 5, 6 and 7 present our results. If a particular pair of variables does not appear in one or more of these tables then the relationship was not significant at the 95 per cent confidence level (in most cases well below). We now discuss the significant relationships.

*(c) Linear Size and Power*

The regressions of Log $L_{1\cdot5}$ on Log $P_{1\cdot5}$ are significant for the cluster sample as a whole and for the subset of cluster doubles; the relevant plots are shown in Figs 74 and 75 respectively. This relationship for the components of cluster doubles (not shown in Table 5) is not so clear being significant at only the 92 per cent confidence level. For the cluster doubles (both for the whole source and its components) the source area also increases with emitted power; the relevant plots are shown in Figs 76 and 77. The relationship for all cluster sources (not shown in Table 5) is not so strong with a confidence level of 93 per cent.

The implication of the regression equations for doubles in Table 5 is that $P_{1\cdot5} \propto A_{1\cdot5}^2$, so that the fundamental property of surface brightness ($B_{1\cdot5} \propto P_{1\cdot5}/A_{1\cdot5}$) increases approximately as the source area.

*(d) Spectral Indices and Flux Densities of Components of Double Sources*

The strong correlation between the ratios of component spectral indices and flux densities in Table 5 is unexpected, especially in view of the lack of correlation between the spectral indices and total emitted powers of the cluster sources including the cluster doubles. The correlation between $\alpha_a/\alpha_b$ and $S_a/S_b$ was strongest in the doubles outside clusters but the significance of

the result was not diminished by adding the components of cluster doubles. We suggest therefore that the correlation is a property of all double sources. A scatter plot is shown in Fig. 78, in which the ratios inside clusters are denoted by filled circles and the ratios outside clusters by crosses.

A referee has correctly pointed out that the use of ratios plotted on linear scales and subjected to regression analysis may bias the result in the direction of producing a spurious correlation. We have answered this objection by a contingency analysis with the result illustrated in Table 8. Here we have divided the double sources into two approximately equal groups with $S_a/S_b$ above and below 1·30; the expected numbers in each cell are given in parentheses alongside the actual numbers. We compute $\chi^2 = 8 \cdot 00$, which is significant at the 96% confidence level. Hence there is little doubt that the double sources with higher $S_a/S_b$ tend to possess higher values of $\alpha_a/\alpha_b$.

**Table 8. Number of double sources in contingency cells**

| $S_a/S_b$ | $\alpha_a/\alpha_b$ | |
|---|---|---|
| | <1·00 | >1·00 |
| <1·30 | 7(7) | 5(7) |
| >1·30 | 3(7) | 13(7) |

It is not clear why the more powerful component of a double source should, on average, possess the steeper spectrum. The reason is probably related to the fact that the more powerful component is also of higher surface brightness, which depends upon the relativistic electron energy spectrum and average magnetic field strength in the source.

*(e) Power and Richness Class*

The result of the ranking test in Table 6 shows that the summed power of cluster sources ($\Sigma P_{1 \cdot 5}$) tends to increase with cluster richness. The power of the dominant radio galaxy ($P_{1 \cdot 5}$) also tends to increase with cluster richness but with a lower confidence level of 93 per cent. The ranking tests are rather crude because there are not enough clusters to assign more than two categories of cluster richness. However, the sources in the richer clusters ($R = 1$–$4$) emit 2–3 times the power of sources in the poorest cluster ($R = 0$). Slee *et al.* (1983), from a survey of cluster sources with a larger range of spectral indices, found no correlation between source power and richness. It may be that the correlation is confined to the steeper spectrum sources favoured in the present analysis.

*(f) Spectral Index and Optical Morphology*

Bautz and Morgan (1970) introduced a simple classification of the optical morphology of a cluster by assigning Roman numerals I, I–II, II, II–III, III, depending upon whether the cluster is dominated by a single bright elliptical at the cluster centre in I or contains many equally bright galaxies in III. In this sample, the ranking test result in Table 6 indicates that the spectral index of the source in a BM I/I–II cluster is likely to be higher than in the later

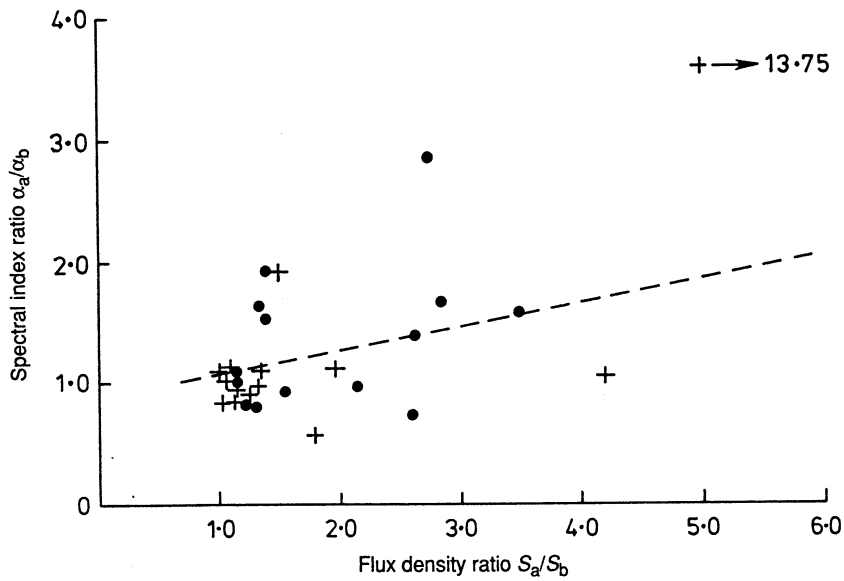


**Fig. 78.** Spectral index ratio plotted against flux density ratio for the components of classical double sources. Component 'a' is the one with the higher 1·5 GHz flux density. The filled circles refer to doubles inside clusters, and the crosses to doubles outside clusters. The regression line has a slope of 0·195 (see Table 5).

morphological classes. Therefore, despite the fact that this sample is biased towards steep spectrum sources, the steepest of them are found in clusters with one or two central dominant galaxies. A similar result was noted by Slee *et al.* (1983) using sources with a considerably wider range of spectral indices.

*(g) Sources Inside and Outside Clusters*

Table 7 lists the results of ranking tests on pairs of variables that do not depend on a knowledge of source distance, a variable which is often not available for the sources outside clusters. The quantities listed do, however, contain information on the intrinsic radio parameters of spectral index, surface brightness and, for the double sources, the ratios of emitted power, linear size, surface brightness and spectral index of the components.

It is clear that all except one of these parameters are not significantly different for these steep spectrum samples of sources inside and outside clusters. The exception, the ratios of component linear sizes when combined with the negligible difference in their ratios of areas, implies that the more powerful components of doubles inside clusters tend to be longer but narrower than their counterparts outside clusters. The lack of a difference in spectral index between sources in and out of clusters does not agree with the result of Slee *et al.* (1983), who found that the mean spectral index of a large group of cluster sources was significantly higher than the mean spectral index of a similar number of identified sources outside clusters. Most of the disagreement may be ascribed to our selection of VLA fields centred on sources with spectra significantly steeper than the average for extragalactic sources. Some 23 fields of the total of 58 VLA fields were deliberately centred on steep spectrum

sources at angular distances of $0 \cdot 28 < R/R_C < 1 \cdot 0$ from the nearest cluster centre; this was done as a control measure to help identify differences in the morphology of extended sources with steep spectra in and out of clusters.

*(h) The Non-significant Regressions and Ranking Tests*

The following are comments on some of the more important negative results, especially on those for which significance was claimed by Slee *et al.* (1983).

(1) Largest linear size ($L_{1 \cdot 5}$), spectral index ($\alpha$) versus cluster richness. Our negative results for these two pairs of variables agree with those of Slee *et al.* (1983) for a more general sample of cluster sources.

(2) Largest linear size ($L_{1 \cdot 5}$), power ($P_{1 \cdot 5}$), spectral index ($\alpha$) versus angular distance ($R/R_C$) from the cluster centre. The lack of correlation between $L_{1 \cdot 5}$ and $R/R_C$ in the present steep spectrum sample agrees with Slee *et al.* (1983) for a more general sample; Slee *et al.* did find, however, that both $P_{1 \cdot 5}$ and were higher for sources with $R/R_C < 0 \cdot 10$. The disagreement over the spectral index variation is understandable in view of the steep spectrum bias of the present sample.

(3) Power ($P_{1 \cdot 5}$), largest linear size ($L_{1 \cdot 5}$) versus BM class. Our finding of no correlation agrees with the results of Slee *et al.* (1983).

## 6. Conclusions

We have surveyed 58 rich clusters of galaxies with the VLA using scaled arrays in the B/C and/or C/D configurations at $1 \cdot 5$ GHz and $4 \cdot 9$ GHz. The fields were centred on steep spectrum sources in or near clusters that were surveyed with lower resolution telescopes. The angular resolutions were $\sim 4''$ in the B/C configurations and $\sim 14''$ in the C/D configurations.

A source list (Table 2) has been constructed from these maps containing sources with $S_{1 \cdot 5}$ down to ~1 mJy and $S_{4 \cdot 9}$ down to $\sim 0 \cdot 5$ mJy. The positions are accurate to $\sim 1''$ in either coordinate. Spectral indices are given for many of the sources within $5'$ of the map phase centre. The resulting $512 \times 512$ pixel maps have angular dimensions at $1 \cdot 5$ GHz of $38' \times 38'$ in the C-array or $13' \times 13'$ in the B-array and have been cleaned to a rms noise level of $\sim 80$ $\mu$Jy/beam. The total area of sky surveyed at $1 \cdot 5$ GHz is $3 \cdot 5 \times 10^{-3}$ sr out to the half-power points of the primary antenna beam. All our $1 \cdot 5$ GHz maps and some of the $4 \cdot 9$ GHz maps are shown in Figs 1–71.

We have established two samples of sources, one complete to $S_{1 \cdot 5} \geq 2 \cdot 5$ mJy and the other to $S_{1 \cdot 5} > 20$ mJy and have used them to establish a criterion for radio source membership of clusters (Figs 72 and 73). We found that sources with $S_{1 \cdot 5} > 20$ mJy have a high probability of cluster membership if their angular distance from the cluster centre is $< 0 \cdot 28 R_C$. Sources with $S_{1 \cdot 5} < 20$ mJy are mostly background objects.

Statistical relationships have been explored between pairs of radio parameters and between radio and optical properties. This was performed for all cluster sources and separately for a subset of classical double sources in clusters (Tables 5 and 6). Another analysis compared radio parameters of sources inside and outside clusters (Table 7). The significant correlations are:

(1) largest linear dimension and source area increases with power;
(2) power increases with cluster richness;
(3) spectral index is highest in clusters with a central dominant galaxy;
(4) the more powerful component of a cluster double is longer but thinner than its counterpart in a double outside a cluster;
(5) the component of a double with the higher flux density also has the higher spectral index.

The data contain much more information than we are able to publish in this paper. We are preparing papers on the morphology, spectral index distributions, linear polarisation and identification of the strong sources on which the maps were centred. In addition, we shall attempt to identify optically all the sources in Table 2 and follow up with redshift measurements on the more positive identifications. Some preliminary analyses of a few of the steepest spectrum central sources have been published by Slee and Reynolds (1984).

## References

Abell, G. O. (1958). *Astrophys. J. Suppl.* **3**, 211.
Bautz, L. P., and Morgan, W. W. (1970). *Astrophys. J.* **162**, L140.
Condon, J. J., and Mitchell, K. J. (1984). *Astron. J.* **89**, 610.
Faranoff, B. L., and Riley, J. M. (1974). *Mon. Not. R. Astron. Soc.* **167**, 31P.
Hughes, A., and Grawoig, G. (1971). 'Statistics: a Foundation for Analysis' (Addison–Wesley: Cambridge, Mass.).
Mills, B. Y., and Hoskins, D. G. (1977). *Aust. J. Phys.* **30**, 509.
Oort, M. J. A., and Windhorst, R. A. (1985). *Astron. Astrophys.* **145**, 405.
Slee, O. B., and Siegman, B. C. (1983). *Proc. Astron. Soc. Aust.* **5**, 114.
Slee, O. B., Wilson, I. R. G., and Siegman, B. C. (1983). *Aust. J. Phys.* **36**, 101.
Slee, O. B., and Reynolds, J. E. (1984). *Proc. Astron. Soc. Aust.* **5**, 516.
Struble, M. F., and Rood, H. J. (1987*a*). *Astrophys. J. Suppl. Ser.* **63**, 555.
Struble, M. F., and Rood, H. J. (1987*b*). *Astrophys. J. Suppl. Ser.* **63**, 543.
Zhao, J. H., Burns, J. O., and Owen, F. N. (1989). *Astron. J.* **98**, 64.

Manuscript received 3 October, accepted 15 November 1989